



Experimental Study of Various Techniques to Protect Ice-Rich Cut Slopes

Construction Report

Lin Li, M.S.

Xiong Xhang, Ph.D., P.E.

Dept. of Civil and Environmental Engineering

Mingchu Zhang

School of Natural Resources and Agricultural Sciences (SNRAS)

University of Alaska Fairbanks

Robert McHattie

GZR Engineering

July 2013

Prepared By:

Alaska University Transportation Center
Duckering Building Room 245
P.O. Box 755900
Fairbanks, AK 99775-5900

Alaska Department of Transportation
Research, Development, and Technology
Transfer
2301 Peger Road
Fairbanks, AK 99709-5399

INE/AUTC 13.07

FHWA-AK-RD-13-13

REPORT DOCUMENTATION PAGE

Form approved OMB No.

Public reporting for this collection of information is estimated to average 1 hour per response, including the time for reviewing instructions, searching existing data sources, gathering and maintaining the data needed, and completing and reviewing the collection of information. Send comments regarding this burden estimate or any other aspect of this collection of information, including suggestion for reducing this burden to Washington Headquarters Services, Directorate for Information Operations and Reports, 1215 Jefferson Davis Highway, Suite 1204, Arlington, VA 22202-4302, and to the Office of Management and Budget, Paperwork Reduction Project (0704-1833), Washington, DC 20503

1. AGENCY USE ONLY (LEAVE BLANK) FHWA-AK-RD-13-13		2. REPORT DATE July 2013	3. REPORT TYPE AND DATES COVERED Final Report; Aug 24, 2011 – Dec 31, 2012	
4. TITLE AND SUBTITLE Experimental Study of Various Techniques to Protect Ice-Rich Cut Slopes			5. FUNDING NUMBERS AUTC #510010 T2-11-05 Federal # HPR-4000(112)	
6. AUTHOR(S) L. Li, M.S., University of Alaska Fairbanks Xiong Zhang, Ph.D., P.E., Univeristy of Alaska Fairbanks Mingchu Zhang, School of Natural Resources and Agricultural Sciences Robert McHattie, GZR Engineering			8. PERFORMING ORGANIZATION REPORT NUMBER INE/AUTC 13.07	
7. PERFORMING ORGANIZATION NAME(S) AND ADDRESS(ES) Alaska University Transportation Center Institute of Northern Engineering College of Engineers and Mines PO Box 755900 Fairbanks, AK 99775-5900			10. SPONSORING/MONITORING AGENCY REPORT NUMBER FHWA-AK-RD-13-13	
9. SPONSORING/MONITORING AGENCY NAME(S) AND ADDRESS(ES) Research and Innovative Technology Administration (RITA), U.S. Dept. of Transportation (USDOT) 1200 New Jersey Ave, SE, Washington, DC 20590 Alaska Department of Transportation: Research, Development, and Technology Transfer 2301 Peger Road, Fairbanks, AK 99709-5399 TransCanada Alaska Company, LCC 450-1 Street SW, Calgary, Alberta, Canada, T2P 5H1			11. SUPPLEMENTARY NOTES	
12a. DISTRIBUTION / AVAILABILITY STATEMENT No restrictions.			12b. DISTRIBUTION CODE	
13. ABSTRACT (Maximum 200 words) Permafrost underlies most areas of Alaska. Cuts are usually required to achieve design grades in these ice-rich permafrost areas. However, excavation and exposure of a cut slope will destroy the existing thermal balance and result in degradation of the ice-rich permafrost. Uncontrolled erosion and runoff as well as slope failures on a cut slope resulted from thawed ice-rich permafrost cause environmental distress, project delays, change orders, and claims. The problem had been documented for more than fifty years and still exists. Solutions that are environmentally acceptable, legal, and economically viable are still rare at present, while new and strict environmental laws continue the increasing trend to make long accepted Alaska Department of Transportation and Public Facilities (AKDOT&PF) methods for dealing with ice-rich permafrost either undesirable or completely unacceptable. It is proposed in this research to study several potential thermal erosion mitigation techniques that address the regulatory concerns raised by the current practices and will be particularly effective in controlling erosion from the cut face in the first thaw season. Several test sections will be constructed in the experimental study and monitored to evaluate the effectiveness of different mitigation techniques. Recommendations and guidelines for design, construction, and maintenance will be provided to insure proper application of successfully tested mitigation approaches on future construction projects that require cuts in ice-rich permafrost.				
14. KEYWORDS : Permafrost (Rbspfp), Frozen soils (Rbspfh), Embankments (Pdxe), Slope stability (Jbgpx)			15. NUMBER OF PAGES	
			16. PRICE CODE N/A	
17. SECURITY CLASSIFICATION OF REPORT Unclassified	18. SECURITY CLASSIFICATION OF THIS PAGE Unclassified	19. SECURITY CLASSIFICATION OF ABSTRACT Unclassified	20. LIMITATION OF ABSTRACT N/A	

Notice

This document is disseminated under the sponsorship of the U.S. Department of Transportation in the interest of information exchange. The U.S. Government assumes no liability for the use of the information contained in this document.

The U.S. Government does not endorse products or manufacturers. Trademarks or manufacturers' names appear in this report only because they are considered essential to the objective of the document.

Quality Assurance Statement

The Federal Highway Administration (FHWA) provides high-quality information to serve Government, industry, and the public in a manner that promotes public understanding. Standards and policies are used to ensure and maximize the quality, objectivity, utility, and integrity of its information. FHWA periodically reviews quality issues and adjusts its programs and processes to ensure continuous quality improvement.

Author's Disclaimer

Opinions and conclusions expressed or implied in the report are those of the author. They are not necessarily those of the Alaska DOT&PF or funding agencies.

SI* (MODERN METRIC) CONVERSION FACTORS

APPROXIMATE CONVERSIONS TO SI UNITS

Symbol	When You Know	Multiply By	To Find	Symbol
LENGTH				
in	inches	25.4	millimeters	mm
ft	feet	0.305	meters	m
yd	yards	0.914	meters	m
mi	miles	1.61	kilometers	km
AREA				
in ²	square inches	645.2	square millimeters	mm ²
ft ²	square feet	0.093	square meters	m ²
yd ²	square yard	0.836	square meters	m ²
ac	acres	0.405	hectares	ha
mi ²	square miles	2.59	square kilometers	km ²
VOLUME				
fl oz	fluid ounces	29.57	milliliters	mL
gal	gallons	3.785	liters	L
ft ³	cubic feet	0.028	cubic meters	m ³
yd ³	cubic yards	0.765	cubic meters	m ³
NOTE: volumes greater than 1000 L shall be shown in m ³				
MASS				
oz	ounces	28.35	grams	g
lb	pounds	0.454	kilograms	kg
T	short tons (2000 lb)	0.907	megagrams (or "metric ton")	Mg (or "t")
TEMPERATURE (exact degrees)				
°F	Fahrenheit	5 (F-32)/9 or (F-32)/1.8	Celsius	°C
ILLUMINATION				
fc	foot-candles	10.76	lux	lx
fl	foot-Lamberts	3.426	candela/m ²	cd/m ²
FORCE and PRESSURE or STRESS				
lbf	poundforce	4.45	newtons	N
lbf/in ²	poundforce per square inch	6.89	kilopascals	kPa
APPROXIMATE CONVERSIONS FROM SI UNITS				
Symbol	When You Know	Multiply By	To Find	Symbol
LENGTH				
mm	millimeters	0.039	inches	in
m	meters	3.28	feet	ft
m	meters	1.09	yards	yd
km	kilometers	0.621	miles	mi
AREA				
mm ²	square millimeters	0.0016	square inches	in ²
m ²	square meters	10.764	square feet	ft ²
m ²	square meters	1.195	square yards	yd ²
ha	hectares	2.47	acres	ac
km ²	square kilometers	0.386	square miles	mi ²
VOLUME				
mL	milliliters	0.034	fluid ounces	fl oz
L	liters	0.264	gallons	gal
m ³	cubic meters	35.314	cubic feet	ft ³
m ³	cubic meters	1.307	cubic yards	yd ³
MASS				
g	grams	0.035	ounces	oz
kg	kilograms	2.202	pounds	lb
Mg (or "t")	megagrams (or "metric ton")	1.103	short tons (2000 lb)	T
TEMPERATURE (exact degrees)				
°C	Celsius	1.8C+32	Fahrenheit	°F
ILLUMINATION				
lx	lux	0.0929	foot-candles	fc
cd/m ²	candela/m ²	0.2919	foot-Lamberts	fl
FORCE and PRESSURE or STRESS				
N	newtons	0.225	poundforce	lbf
kPa	kilopascals	0.145	poundforce per square inch	lbf/in ²

*SI is the symbol for the International System of Units. Appropriate rounding should be made to comply with Section 4 of ASTM E380.
(Revised March 2003)

EXPERIMENTAL STUDY OF VARIOUS TECHNIQUES TO PROTECT ICE-RICH CUT SLOPES

Final Project Report

By

Lin Li, M.S., Research Assistant

Department of Civil and Environmental Engineering

University of Alaska Fairbanks

Robert McHattie,

Consultant, GZR Engineering

Xiong Zhang, Ph.D., P.E.

Associate Professor

Department of Civil and Environmental Engineering

University of Alaska Fairbanks

and

Mingchu Zhang, Co-PI

School of Natural Resources and Agricultural Sciences (SNRAS)

University of Alaska Fairbanks

AUTC Project No. 510010

Project Title: Experimental Study of Various Techniques to Protect Ice-Rich Cut Slopes

Performed in cooperation with the

Alaska Department of Transportation & Public Facilities

and

Alaska University Transportation Center

February 2014

University of Alaska Fairbanks

Fairbanks, AK 99775-5900

Report Documentation Page

Acknowledgment of Sponsorship and Disclaimer Page

Metric Conversion

ACKNOWLEDGMENTS

The authors wholeheartedly thank those people who helped in this research project. Alaska University Transportation Center, Alaska Department of Transportation and Public Facilities (AKDOT&PF), and TransCanada Corporation jointly provided funding for this study. Geobruigg North America, LLC donated the Tecco-mesh used in the one of the test sections. Polar Supply Company provided the erosion control blankets for two of the test sections. Alaska Foundation Technology Inc. provided special services for drilling and installing the grouted anchors and duckbills. Great Northwest Inc. was the contractor responsible for general construction of the test sections. The AKDOT&PF Construction Section coordinated and monitored work on the project. Special thanks are extended to the following people: Billy Connor, Jeff Curry, James Sweeney, Jack Beattie, Jim Oswell, Steve Hickman, Tim Shevlin, Errol Master, Justin Morgan, and John Chamberlain. The authors would also like to thank Joel Bailey, Chuang Lin, and Peng Li for their contributions to the field work.

EXECUTIVE SUMMARY

Permafrost underlies most areas of Alaska. Cuts are usually required to achieve design grades in these ice-rich permafrost areas. However, excavation and exposure of a cut slope will destroy the existing thermal balance and result in degradation of the ice-rich permafrost. Uncontrolled erosion and runoff as well as slope failures on a cut slope resulted from thawed ice-rich permafrost cause environmental distress, project delays, change orders, and claims. The problem had been documented for more than fifty years and still exists. Solutions that are environmentally acceptable, legal, and economically viable are still rare at present, while new and strict environmental laws continue the increasing trend to make long accepted Alaska Department of Transportation and Public Facilities (AKDOT&PF) methods for dealing with ice-rich permafrost either undesirable or completely unacceptable.

This research project studied three potential thermal erosion mitigation techniques (1 ft wood chips, coconut blanket, and coconut blanket + Tecco-mesh) that address the regulatory concerns raised by the current practices and will be particularly effective in controlling erosion from the cut face in the first thaw season. Four test sections (Section A: 1 ft wood chips, Section B: coconut blanket, Section C: coconut blanket + Tecco-mesh, and Section D: 1 ft crushed rock) were constructed at the Dalton Highway 9 Mile Hill. Temperature and moisture sensors were installed to monitor four sections for evaluating the effectiveness of different mitigation techniques. Also, a weather station was built to record the climatic information at the Experimental Feature.

During the first thaw season, it was found that the performance of the slope protection method was highly dependent on the ice content of the slope. Same coconut blanket was used to cover the slope surface of Sections B and C. About one and a half months after the construction, the performance of the slope protection was drastically different. No erosion was found on Section B. However, Section C failed due to thermal erosion. This difference in performance was considered mainly due to the presence of the massive ground ice in Section C.

For Section A, which was protected by 1 ft wood chips, no significant erosion was identified in this section until the end of September, 2013. Also, it was found that the temperature in this section was lower than the temperatures in Sections B and C, which indicated that wood chips worked better than coconut blanket.

The Tecco-mesh did not protect the ice-rich slope that contained massive ice inclusions. Once the ice-rich permafrost in the slope thawed, a large quantity of the fully saturated silty soil behaved like mud and flowed out from under the very robust and intact tent of strongly suspended Tecco-mesh. The Tecco-mesh itself did not fail, but it did nothing to hold the saturated silty soil in place. It is stressed here that there were absolutely no problems with the Tecco-mesh material itself per se. This was simply an experimental application of Tecco-mesh for which it was not suited. Also, the anchored Tecco-mesh survived intact during the soil thawing process that was occurring beneath it.

Crushed rock was used to protect Section D. Due to the presence of massive ground ice detected during construction, obvious thermal erosion was also found in this section even though 1 ft crushed rock was used. However, temperatures in this section were generally lower than that in Section C. Also, erosion in Section D was less compared with Section C and was not problematic—even though Section D also contained much massive ice. The crushed rock treatment worked much better than the Section C treatment (coconut blanket + Tecco-mesh).

A photogrammetric method was adopted to monitor the changing topography of the ice-rich cut slope. This method was proved to be reliable and cost-effective. To apply this photogrammetric method for such a purpose, stable control points were required to build the coordinate system. By comparing the exact locations of the slope surface at different times within a given period, the total volume of the erosion or surface accumulation during that period could be measured. Also, erosion measurement results from this study were consistent with previous research-related observations.

This report represents but one year's observations. Consequently, no long termed performance can be drawn. In order to maximize the value of the experiment, a follow-on project has been established to continue monitoring the performance of the slope protection techniques

constructed under this project through the summer of 2014. The final report should be available by December 2014.

TABLE OF CONTENTS

ACKNOWLEDGMENTS	5
EXECUTIVE SUMMARY	6
LIST OF FIGURES	10
LIST OF TABLES	Error! Bookmark not defined.
CHAPTER 1. INTRODUCTION	14
CHAPTER 2. LITERATURE REVIEW	20
CHAPTER 3. DESIGN OF EXPERIMENTAL FEATURE.....	28
CHAPTER 4. CONSTRUCTION OF EXPERIMENTAL SECTIONS	39
CHAPTER 5. CONSTRUCTION OF DATA ACQUISITION STATION	57
CHAPTER 6. PERFORMANCE PROBLEMS SOON AFTER CONSTRUCTION	65
CHAPTER 7. RESULTS AND ANALYSIS.....	73
CHAPTER 8. CONCLUSIONS AND RECOMMENDATIONS	107
REFERENCES	112
APPENDIX.....	113

LIST OF FIGURES

Figure 1.1 Idealized development of stability in ice-rich cut (after Berg and Aiken, 1976)	15
Figure 1.2 Dalton Highway.....	16
Figure 1.3 Location of ice-rich cut slope (from Google Maps®).....	17
Figure 1.4 Ice-rich cut slope site area prior to construction (looking north)	17
Figure 2.1 Ice-rich cut slope (Mageau and Rooney, 1984).....	21
Figure 2.2 Four test sections and control section at Hess Creek, Alaska (after APSC 1974)	23
Figure 2.3 Dalton Highway cut in ice-rich permafrost (Vinson and McHattie 2009).....	24
Figure 2.4 Erosion control blanket (from http://www.thelandstewards.com/blankets.htm).....	26
Figure 2.5 Tecco-mesh field examples (Tecco slope stabilization system product manual, 2010)	27
Figure 3.1 Experimental Feature layout with three experimental and one control section	29
Figure 3.2 Profile of Section A.....	30
Figure 3.3 Profile view showing temperature sensor locations in Section A	30
Figure 3.4 Profile of Section B	31
Figure 3.5 Layout of Section B.....	32
Figure 3.6 Enlargements of Duckbill Earth Anchor and Pins	32
Figure 3.7 Profile for Section C.....	33
Figure 3.8 Section C, anchor and sensor locations	34
Figure 3.9 Detail of Section C anchor	34
Figure 3.10 Nail and anchor detail with boundary rope	35
Figure 3.11 Plan view - connection of mesh sheets in Section C.....	35
Figure 3.12 Connection details	36
Figure 3.13 Profile of Section D.....	37
Figure 3.14 Layout for temperature sensor locations	37
Figure 3.15 Layout for temperature sensor locations	38
Figure 4.1 Cut slope at Dalton Highway 9-mile construction project location	39
Figure 4.2 Layout on the cut slope.....	40
Figure 4.3 Drilling on the cut slope	41

Figure 4.4 Drilling at the upper part of the slope.....	41
Figure 4.5 Installation for sensor housing.....	42
Figure 4.6 Instrumentation hole with sensor housing installed	43
Figure 4.7 Cut slope erosion during construction.....	44
Figure 4.8 Ice in the cut slope.....	44
Figure 4.9 Ice exposed in the cut slope.....	45
Figure 4.10 Cut slope protected from erosion during drilling	45
Figure 4.11 Cable end of installed Duckbill earth anchor	46
Figure 4.12 Installation of hollow rebar anchor.....	47
Figure 4.13 Re-smoothing the cut slope surface.....	48
Figure 4.14 Seeded cut slope	48
Figure 4.15 Placement of coconut erosion control matting	49
Figure 4.16 Placement of coconut erosion control matting	50
Figure 4.17 Section B showing Duckbill anchor plates after construction.....	51
Figure 4.18 Enlargement of a circle wire top pin	51
Figure 4.19 Placement of Tecco-mesh.....	52
Figure 4.20 Cutting away excess Tecco-mesh.....	53
Figure 4.21 Connecting adjacent Tecco-mesh strips	53
Figure 4.22 Section C appearance after construction	54
Figure 4.23 Close-up view of Tecco-mesh at an anchoring point	54
Figure 4.24 Construction of Section D	55
Figure 4.25 Spreading wood chips along top portion of cut slope	56
Figure 4.26 Appearance of Experimental Feature very soon after completion	56
Figure 5.1 Backfilling with sand after insertion of temperature sensor string.....	57
Figure 5.2 Installation of moisture sensor at top of temperature sensor string.....	58
Figure 5.3 Temperature and moisture sensor location.....	59
Figure 5.4 Data collection station.....	60
Figure 5.5 Data collection station after completion.....	61
Figure 5.6 CR1000 data logger and AM16/32B multiplexing equipment.....	61
Figure 5.7 Air Temp/Relative Humidity sensor	62
Figure 5.8 Wind sensor	62
Figure 5.9 Radiation sensor	63
Figure 5.10 Precipitation sensor	63

Figure 5.11 Two cameras installed for slope monitoring	64
Figure 6.1 Panorama view of Experimental Feature showing failure in Tecco-mesh section	66
Figure 6.2 Close view of failure within the Tecco-mesh section	66
Figure 6.3 Close views showing exposure of soil anchor grout (left) and portion of massive ice feature under Tecco-mesh (right)	67
Figure 6.4 Surface protection matting in areas showing no grass growth are not in direct contact with ground surface	68
Figure 6.5 Section C without Tecco-mesh and coconut blanket	70
Figure 6.6 Massive ice in Section C	70
Figure 6.7 Covering Section C with crushed rock	71
Figure 6.8 Cut slope after construction on Section C	71
Figure 6.9 Start of thaw related damage at top of Experimental Feature cut slope	72
Figure 7.1 Air temperatures at the Experimental Feature site	74
Figure 7.2 Temperature variations for three different days	74
Figure 7.3 Precipitation at the Experimental Feature site	75
Figure 7.4 Relative humidity at the Experimental Feature site	75
Figure 7.5 Wind direction frequencies at Experimental Feature site	76
Figure 7.6 Wind speed at Experimental Feature site	77
Figure 7.7 Incident solar radiation received at Experimental Feature site	77
Figure 7.8 Incident solar radiation at Experimental Feature site on three different days	78
Figure 7.9 Battery output voltage at Experimental Feature site	78
Figure 7.10 Temperature variations in Section A	80
Figure 7.11 Temperature variations in Section B	82
Figure 7.12 Temperature variations in Section C	84
Figure 7.13 Temperature variations in Section D	86
Figure 7.14 Temperature contours at different times in Section A	88
Figure 7.15 Temperature contour at different times in Section B	89
Figure 7.16 Temperature contour at different times in Section C	90
Figure 7.17 Temperature contour at different times in Section D	91
Figure 7.18 Volumetric moisture content variations in Section A	93
Figure 7.19 Volumetric moisture content variations in Section B	93
Figure 7.20 Volumetric moisture content variations in Section C	94

Figure 7.21 Volumetric moisture content variations in Section D	94
Figure 7.22 Erosion on Section A.....	96
Figure 7.23 Section A after construction on April 26 th , 2013.....	96
Figure 7.24 Section A with more wood chips on April 30 th , 2013.....	97
Figure 7.25 Section A with more wood chips on September 27 th , 2013	97
Figure 7.26 Erosion on Section B.....	98
Figure 7.27 Section B on June 17 th , 2013.....	99
Figure 7.28 Section B on July 15 th , 2013.....	99
Figure 7.29 Section B on August 8 th , 2013.....	100
Figure 7.30 Section B on September 27 th , 2013	100
Figure 7.31 Erosion on Section C.....	101
Figure 7.32 Section C on April 30 th , 2013.....	102
Figure 7.33 Section C on June 13 th , 2013.....	102
Figure 7.34 Section C on June 17 th , 2013.....	103
Figure 7.35 Section C on September 27 th , 2013	103
Figure 7.36 Erosion on Section D.....	104
Figure 7.37 Section D on April 30 th , 2013.....	105
Figure 7.38 Section C on June 13 th , 2013.....	105
Figure 7.39 Section C on June 17 th , 2013.....	106
Figure 7.40 Section C on September 27 th , 2013	106
Figure A.1 Camera and lens.....	114
Figure A.2 Principle of Photogrammetry.....	115
Table A.1 Camera calibration parameters	116
Figure A.3 Typical image captured for erosion monitoring.....	117
Figure A.4 Coordinate system for erosion measurement.....	118
Figure A.5 Camera stations at different view angles.....	119
Figure A.6 Point cloud for erosion monitoring.....	120
Figure A.7 Mesh generated for Section A for volume calculation.....	120
Figure A.8 Mesh generated for Section B	121
Figure A.9 Mesh generated for Section C	121
Figure A.10 Mesh generated for Section D	122
Figure A.11 Volume calculation for a single mesh cell.....	123

CHAPTER 1. INTRODUCTION

General

The Alaska Department of Transportation & Public Facilities (AKDOT&PF) and other users (such as pipeline companies) need to make construction cuts in ice-rich permafrost. In general, the technique used in the past was to make, for example, an over-wide ditch and cut the ice-rich permafrost vertically at the back of the ditch. Over a period of years, the vertical, ice-rich permafrost face thaws. The thaw progresses rapidly into the vertical face mainly due to the fact that the natural, thermally protective vegetation has been removed, causing the bank to collapse and the vegetation mat to slump down from above on top of the thawing soil-ice mass (as shown in Figure 1.1). Eventually the cut becomes an undulating slope covered with vegetation that is relatively stable. In the interim, meltwater carrying soil and organics from within the slump mass flows onto the bench and potentially into protected areas such as wetlands, streams, lakes, etc. Over the last several decades, regulatory agencies have refined and developed more stringent environmental regulations that prohibit such discharges. At present, thermal erosion mitigation techniques that are both environmentally acceptable and economically viable require much in the way of development and testing. Consequently, there is a significant need for research in this direction that justifies the work documented in this report.

The first thaw season after construction of the soil cut represents the most critical period as thawing and soil erosion will be most active in this period. Long term, natural processes such as revegetation lessen the eroded soil volume. Hence, mitigation techniques that are effective in the first thaw season are of primary importance. This research studied three potential thermal erosion mitigation techniques designed to address the regular concerns raised by the current practices and be effective in controlling erosion from the cut face in the first thaw season.

This report covered design and construction of the Experimental Feature and provides initial performance results based on data collected during the first thawing season after construction.

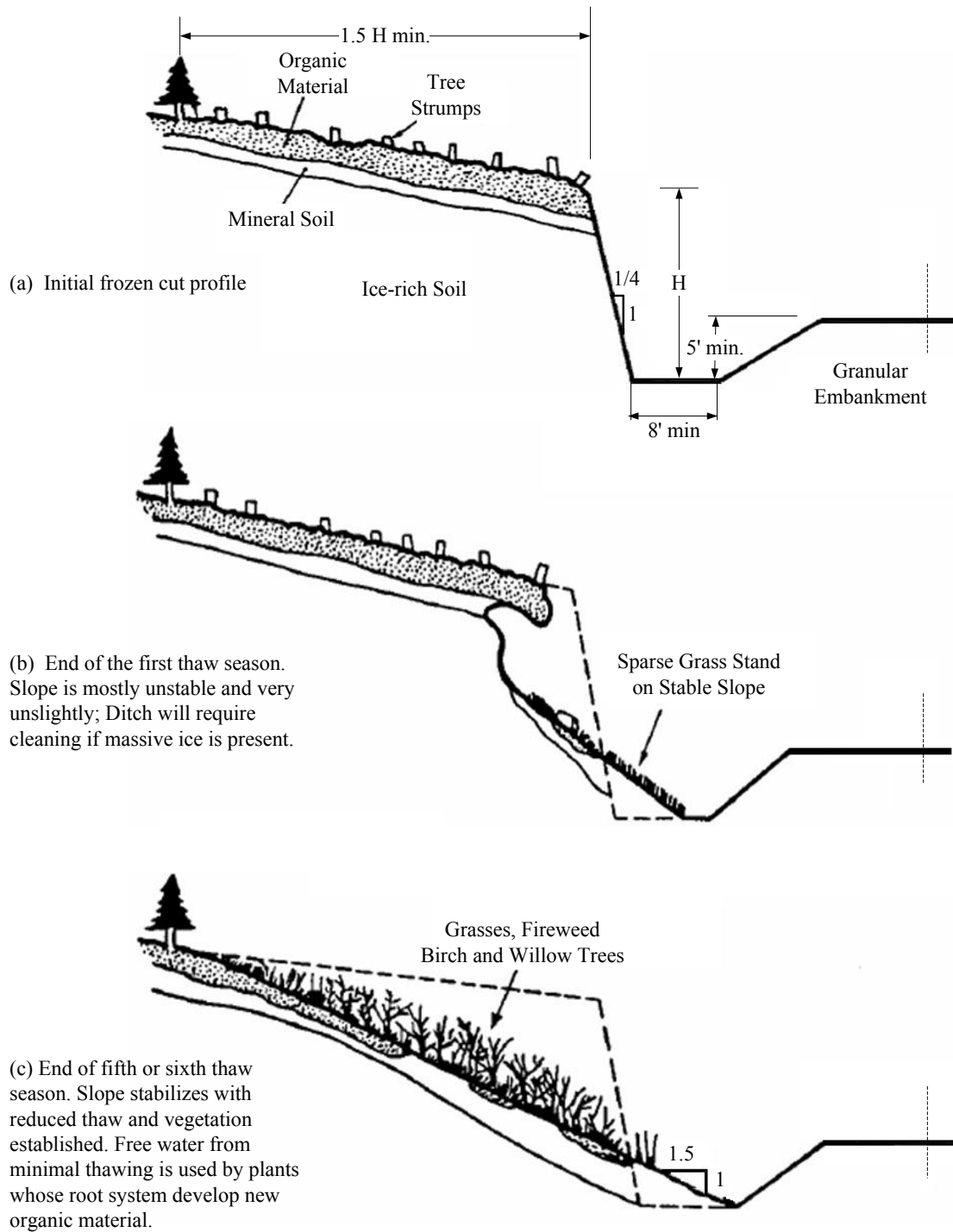


Figure 1.1 Idealized development of stability in ice-rich cut (after Berg and Aiken, 1976)

The following map (Figure 1.2) shows the Dalton Highway location of the Experimental Feature. The Experimental Feature as shown in Figure 1.3 can be seen using the Google Maps® program. The Experimental Feature area, which is shown in Figure 1.4, is located at approximately latitude of 65.553584 and longitude of -148.905602 (near mile post 10 of the Dalton Highway).

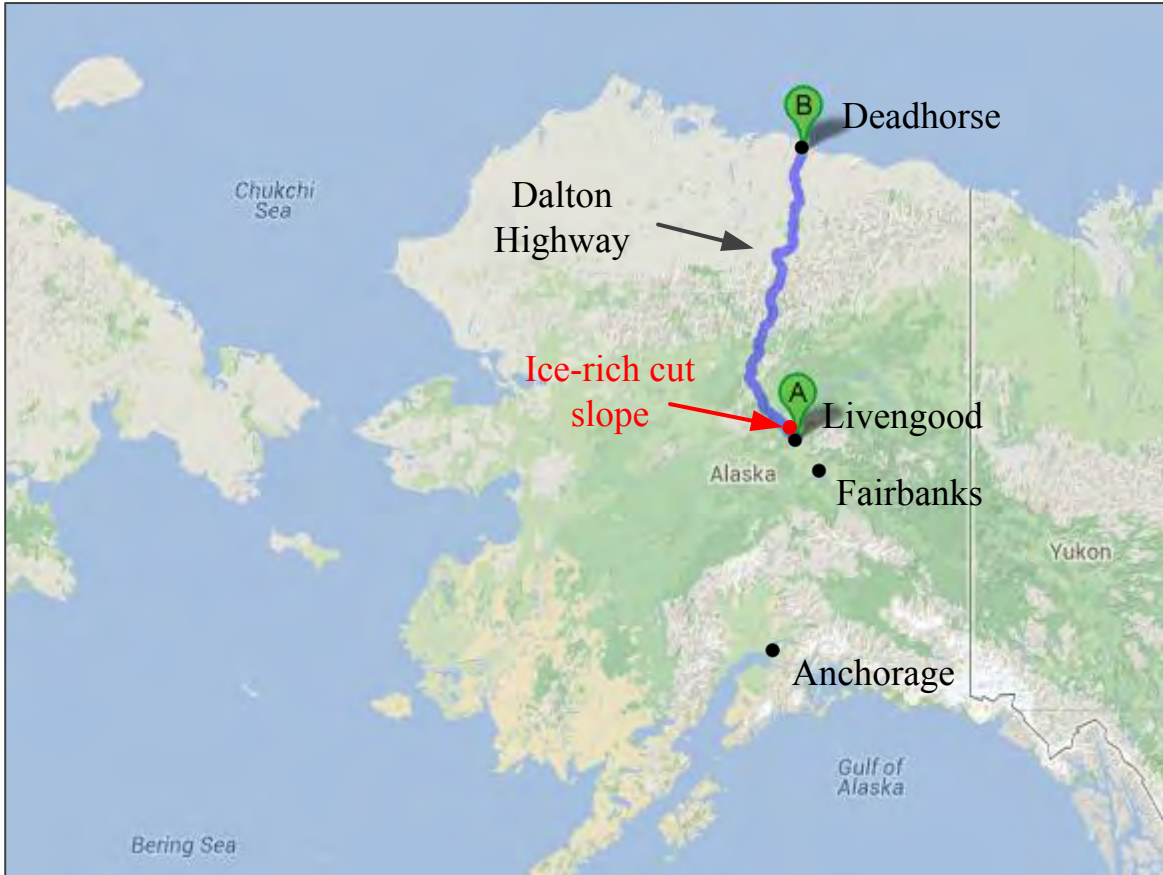


Figure 1.2 Dalton Highway



Figure 1.3 Location of ice-rich cut slope (from Google Maps®)



Figure 1.4 Ice-rich cut slope site area prior to construction (looking north)

The test sections incorporated the following design approaches:

- Biodegradable Erosion Control Blanket with Hydro-seeding - this mitigation technique involved hydro-seeding the cut slope, then applying a well-anchored erosion control blanket. The

purpose of the hydro-seeding is to establish vegetation that, with time, will provide the necessary erosion control on the slope. The layer of erosion control blanket placed over the slope functions as a short term erosion control measure while the vegetation was establishing. The biodegradable erosion control blanket will be used so that it will eventually degrade to a mulch or compost consistency as the surface vegetation is established.

- Anchored Tecco-mesh with Biodegradable Erosion Control Blanket and Hydro-seeding - this is a much heavier duty version of the above-mentioned biodegradable erosion control blanket with hydro-seeding. A very well anchored, non-biodegradable layer of steel Tecco-mesh was applied over a layer of biodegradable erosion control blanket on the ice-rich cut slope and then hydro-seeded. The purpose is to improve the slope stability during thawing. It will be compared with the previous technique to determine if the much more robust slope stabilization is necessary.

- Wood Chip Slope Treatment - for this mitigation technique a relatively thin layer of wood chip material is placed on the cut slope face. The thickness of the wood chip layer is approximately 1 ft. Past experience with wood chips as both a thermal and erosion control mitigation has been well documented. Wood chips proved to be extremely effective in reducing the velocity of water (both water released from thawing ice-rich soils as well as precipitation) percolating through the wood chips. An additional attractive feature of this surface treatment is that as the subgrade deforms in response to the thaw of underlying material, the wood chips will tend to conform exactly to the deforming ground surface. This property insures that the wood chips remain in good contact with the mineral soil, thus protecting it by preventing piping and direct erosion along the surface of the thawing ground.

General Research Objectives and Research Approach

The objective of the research is to experimentally investigate the feasibility of using three promising erosion mitigation techniques intended to protect cuts in ice-rich permafrost. Four test sections were constructed at the Dalton Highway 9 Mile Hill: 1) control section; 2) wood chip layer (1 ft thick); 3) biodegradable erosion control blanket with hydro-seeding; 4) Anchored Tecco-mesh with biodegradable erosion control blanket and hydro-seeding. Assessment of the experimental sections began during the spring of 2013. This initial stage of monitoring will

continue through the 2013 thaw season, a portion of which is presented in this report. As data collection and analyses progresses, additional recommendations and guidelines for design, construction, and maintenance were provided. Continued monitoring insures appropriate application of the tested mitigation methods on future construction projects that require cuts in ice-rich permafrost. Construction problems, contractor personnel requirements, special equipment needs, and initial results were discussed in the report.

To meet the general objectives of this study, the following major tasks were completed:

- Task 1: Literature survey
- Task 2: Identification of an ice-rich permafrost site and obtain permits for construction and agreement, soil sampling, and laboratory testing
- Task 3: Construction of test sections with implementation of various mitigation techniques
- Task 4: Field monitoring of performance of test sections
- Task 5: Draft of Final Report and Recommendations

CHAPTER 2. LITERATURE REVIEW

General

In this chapter, a literature review was performed on protection methods for ice-rich soils in cold regions. For ice-rich cut slopes, the protection usually involves erosion control and protection from slope failure. Generally, the majority of erosion on ice-rich cut slopes comes from running water due to melt of ice and snow. This kind of erosion was commonly referred as thermal erosion. This thermal erosion can be divided into two stages which are snow and ground ice melt stages. When atmosphere (ambient) temperature rose up to above freezing point, snow started to melt. The runoff of snow melt can certainly cause significant erosion of the slope. During the second stage, when temperature is high enough to melt ice wedges and other forms of ground ice, significant thaw-settlement and runoff erosion often occurs. Runoff from individual precipitation events was not found to be a significant source of thermal erosion. Thus, erosion due to precipitation was not discussed in this study.

Ice-rich Cut Slope Protection

In Alaska, problems associated with excavation of cut slopes in ice-rich permafrost were reported as early as the 1920s during development of the Fairbanks mining district and military construction of the Alaska Highway in the early 1940s. Unfortunately, there was very limited technical documentation of ground conditions and slope performance. In general, the technique used in the past was to make a wide, relatively level, “bench” area and cut the ice-rich permafrost vertically some distance from the bench. Over a period of years, the ice-rich permafrost thaws where the vegetation has been removed. The bank collapses and the vegetation mat slumps down from above on top of the thawing soil-ice mass. Eventually the cut becomes an undulating slope covered with vegetation that becomes relatively stable. Due to the difficulties associated with thermal degradation of ice-rich soils, subsequent emphasis has been given to minimize cuts in ice-rich frozen soil and evaluation and documentation of frozen soil cut slope performance in Alaska has been limited (Mageau and Rooney, 1984). In 1969, major near-vertical cuts were made in ice-rich silts on the initial 56-mile Livengood to the Yukon River segment of the Dalton Highway. Performance of these near-vertical cut slopes was monitored by

Alyeska Pipeline Service Company (APSC). The overall natural restabilization and revegetation of the thermally degraded slopes was considered satisfactory at a time when worries about environmental impacts were attuned to localized observable consequences. Of course this view has become obsolete as far reaching, comprehensive, and rigorously enforced State and Federal regulations became the present reality. Figure 2.1 shows two pictures of a near vertical ice-rich cut slope, indicating the condition immediately after the slope was cut (top photo) and after a new thermal equilibrium was established (bottom photo).



Figure 2.1 Ice-rich cut slope (Mageau and Rooney, 1984)

In 1973 a test site was constructed by APSC near Hess Creek on the Dalton Highway to evaluate the effect of four different surface treatments in reducing thermal erosion on slopes cut at about 1.5: 1 (horizontal to vertical) into ice-rich silt (APSC, 1974 and 1975). The test sections, originally monitored during the 1973 and 1974 summer seasons, are shown in Figure 2.2. The findings were summarized in Vinson and McHattie (2009). All test sections were sprayed with the same grass seed mixture after construction. For Section I, during the second summer large thaw induced depressions developed under the insulation and large downslope movements of the thawed soil occurred. The slope movements destroyed 70% of the insulation. Thaw depths averaged 0.7 m (2.3 ft) in 1974. Sections II experienced failure during the first summer, especially near the toe, with much of the failed material flowing into the ditch. By the end of the second summer 50% of the slope was covered with the excelsior blanket, a vertical scarp had formed at the top of the slope, and the overall appearance was similar to Section I. Thaw depths averaged 0.8 m (2.6 ft) in 1974. Section III, which was originally burlap (East) or nylon (West) painted with high reflectivity titanium dioxide paint, became soaked and distorted with mudflows during construction. Two layers of excelsior blanket were placed over this material. Section III failed repeatedly in 1973. Mass movements in this test section were greater than the other four sections during 1973. Thaw depths in 1974 were 0.9 m (3 ft) at the toe and greater than 1.5 m (5 ft) at the top of the slope. The Section IV insulation layer was treated with straw mulch and seed to stimulate vegetation growth. The sand filter layer was intended to intercept meltwater and reduce excess pore water during periods of rapid thawing. Very little evidence of soil movement, sloughing, or meltwater release was observed in this section thru 1974. Thaw depths were 0.6 to 0.9 m (2 to 3 ft) in 1974. Test section V (control) experienced considerable caving and sloughing in 1973. The material was not transported far from the slope, as was the case for Sections I and II. By the end of the summer (1973) a vertical scarp developed at the top of the slope. No caving, sloughing, or erosion was observed in 1974 and sparse vegetation appeared on the slope surface. Thaw depths were 0.9 to 1.2 m (3 to 4 ft) in 1974. Longer term performance of the test sections was evaluated during two field investigations conducted during the 1983 summer season. They noted that all the slopes were stable. However, significant slope deterioration caused by large volume reduction and downslope movement occurred on the majority of the test sections. Revegetation was well established on slopes which had experienced

significant slope displacement and consequent flattening of the slope. Revegetation on steeper, less deformed slopes was not well established or non-existent.

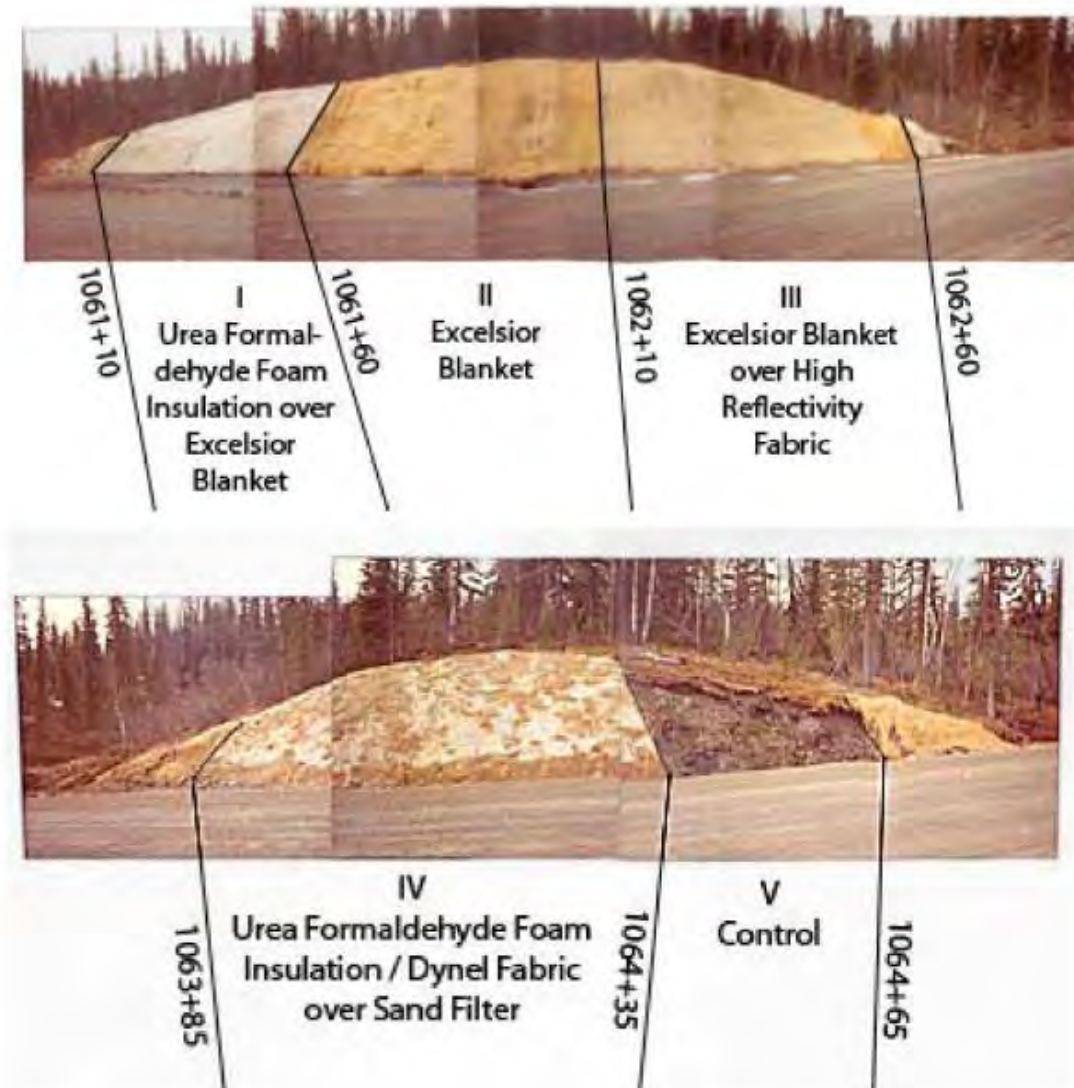


Figure 2.2 Four test sections and control section at Hess Creek, Alaska (after APSC 1974)

A recent example (Vinson and McHattie 2009) related to thermal erosion of cut slopes in ice-rich permafrost is on the Dalton Highway, Milepost 37 to 49. The cut volume, originally considered as bedrock and weathered bedrock, turned out to be highly weathered ice-rich bedrock. The cut design, though appropriate for the weathered bedrock, was inappropriate for the unexpected ice-rich mineral soils. Uncontrolled erosion, thawed slurry runoff, and slope failure resulted in significant environmental concern.

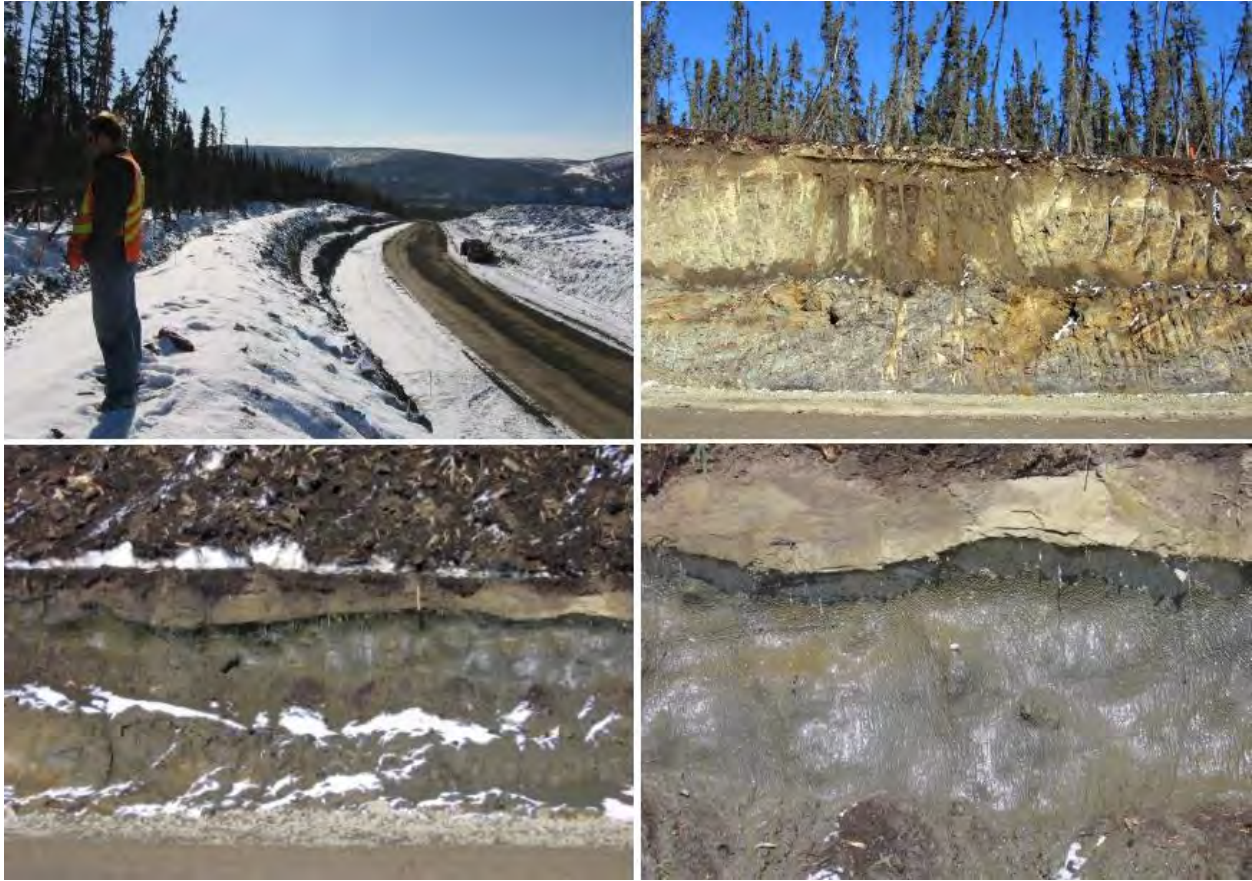


Figure 2.3 Dalton Highway cut in ice-rich permafrost (Vinson and McHattie 2009)

McHattie and Vinson (2008) and Vinson and McHattie (2009) summarized the best management practices for ice-rich permafrost exposed during construction operations. It was concluded that solutions that are environmentally acceptable and economically viable must be developed and evaluated because new and strict environmental laws and regulations make the historical AKDOT&PF methods for dealing with ice-rich permafrost either undesirable or unacceptable. In addition to the near vertical cut method presented before, another AKDOT&PF technique has included cutting the ice-rich permafrost slope at about 1.5H:1V and placing a free-draining gravel blanket on the slope surface. The horizontal width of one successful gravel blanket was about 8 ft — the width being an expedient to allow rapid construction using a belly-dump truck. The 1.5H:1V blanket side slope matched the cut slope. The gravel blanket performs several functions, i.e., as insulation, as a filter, and as a retaining structure, which reduces thermal erosion of the soil and runoff. In addition, the blanket can accommodate large thaw settlement and deformation by conforming to the changing shape of the underlying cut slope surface as

thawing progresses. The disadvantage of this option is that the gravel surface limits growth of vegetation, and at locations where gravel is not readily available, the cost for constructing such a blanket can be prohibitively high. The use of wood chips as a thermal mitigation technique to reduce the rate of permafrost thawing on selected slopes along the Norman Wells pipeline is well documented (Naviq Consulting Inc and AMEC Earth & Environmental, 2007). Less well documented is the secondary benefit of the erosion control aspects of the wood chips.

While the problem of environmentally acceptable and economic erosion mitigation remains unsolved, it is expected that the need for such mitigation will occur more and more in the future, as during the construction of proposed natural gas pipelines. It is hoped that techniques evaluated during this research project will provide some of the needed cost-effective and environmentally friendly solutions to the problem.

Slope Protection

The major factors affecting soil erosion are soil characteristics, climate, runoff intensity and duration, vegetation or other surface cover, and topography. Also, the quantity and size of the soil particles that are loosened and removed increased with the velocity of the runoff. Soil erosion is evident in many situations and the environmental impact can be significant. In China, usually, crushed stone was used as shade and insulation to keep the ground ice in cut slopes from melting.

To prevent soil erosion from non-frozen slopes, commonly available erosion control materials are easy to use and quite affordable. Erosion control blankets are generally a machine produced mat of organic, biodegradable mulch such as straw, curled wood fiber (excelsior), coconut fiber or a combination thereof, evenly distributed on or between photodegradable polypropylene or biodegradable natural fiber netting. Erosion control blankets can be provided immediate soil surface stabilization as shown in Figure 2.4. Even if herbaceous vegetation does not grow, the blankets will provide excellent protection for at least one season. After the vegetation grows the Erosion Control Blanket degrades over time until only the vegetation is left in place. The vegetation, once established, provides permanent erosion control. Erosion control blankets also

protect seeds from predators, reduce desiccation, and evaporation by insulating the soil and seed environment.



Figure 2.4 Erosion control blanket (from <http://www.thelandstewards.com/blankets.htm>)

Tecco-mesh represents an extremely heavy duty version of a slope protection blanket and was one of the materials evaluated during this research project. Tecco-mesh is a high-tensile mesh slope stabilization system, usually considered appropriate for stabilizing steep soil, sediment and rock slopes. Tecco-mesh can be pretensioned on the slope at a defined force using soil or rock nails and spike plates as shown in Figure 2.5. Generally, no maintenance is required provided that the slope stabilization system is correctly installed, fastened and pretensioned, and has not been damaged through external influences.



Figure 2.5 Tecco-mesh field examples (Tecco slope stabilization system product manual, 2010)

CHAPTER 3. DESIGN OF EXPERIMENTAL FEATURE

General

This chapter describes the design of the test section treatments and the sensor instrumentation. The slope at the site was cut at a gradient of 1.5H:1V in October, 2012. In order to evaluate different methods to permanently protect the stability of cut slopes in ice-rich permafrost soils, the cut slope was divided into four sections (Sections A, B, C, and D) with different treatment methods. These included three special protection designs using wood chips, coconut erosion control blanket, and coconut erosion control blanket plus Tecco-mesh. The fourth treatment method involved use of a blanket of crushed rock and will provide a control section for the Experimental Feature. The crushed rock blanket was the AKDOT&PF designer's standard treatment, used throughout the project, intended for protecting ice-rich cut slopes. Construction for different slope protection methods was performed during the period April 17th through April 27th, 2013, and instrumentation installation was completed April 30th, 2013.

Designs for the different protection methods used on the cut slope are summarized in Figure 3.1. Section A which is at the left side as well as the upper part of the slope was covered with wood chips. Section B was protected by one layer of coconut erosion control blanket. Section C was protected by one layer of coconut erosion control blanket as well as Tecco-mesh. Section D, i.e., the control section which is located at the right side of the slope (the end nearest Fairbanks), was protected by two feet of crushed rock.

Detailed designs for these sections are presented on following pages of this report. Various types of sensors such as for recording temperature, moisture, precipitation, radiation, wind speed, and air temperature were used to monitor locations above, on, and under the Experimental Feature's cut slope face. The following pages contain much information about the design and installation of the instrumentation.



Figure 3.1 Experimental Feature layout with three experimental and one control section

Test Section A

This section is protected by 1 ft of wood chips. The profile for this section is shown in Figure 3.2. This section, which is 30 ft (slope length) × 35 ft (centerline length), extends from station 520 + 10 to 520 + 45. Three holes (2 inches in diameter) at station 520 + 30 located near the top, middle, and bottom of the treated slope were drilled for placement of temperature sensors as shown in Figure 3.3. The top and bottom sensor holes are 10 ft in depth and the middle hole is 20 ft deep. The diameter and depth of these holes and sensor placement locations are the same for the other three sections. Holes for the sensors were drilled perpendicular to the surface of the cut slope. Temperature sensors were installed at various depths in the holes according to Figure 3.3. Also, some moisture measurement sensors were installed at the surface of the slope with the surface temperature sensors.

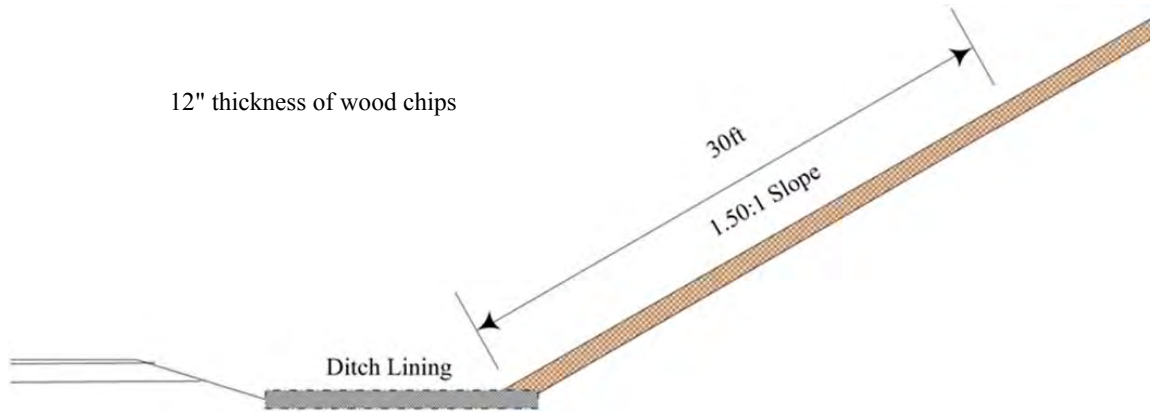


Figure 3.2 Profile of Section A

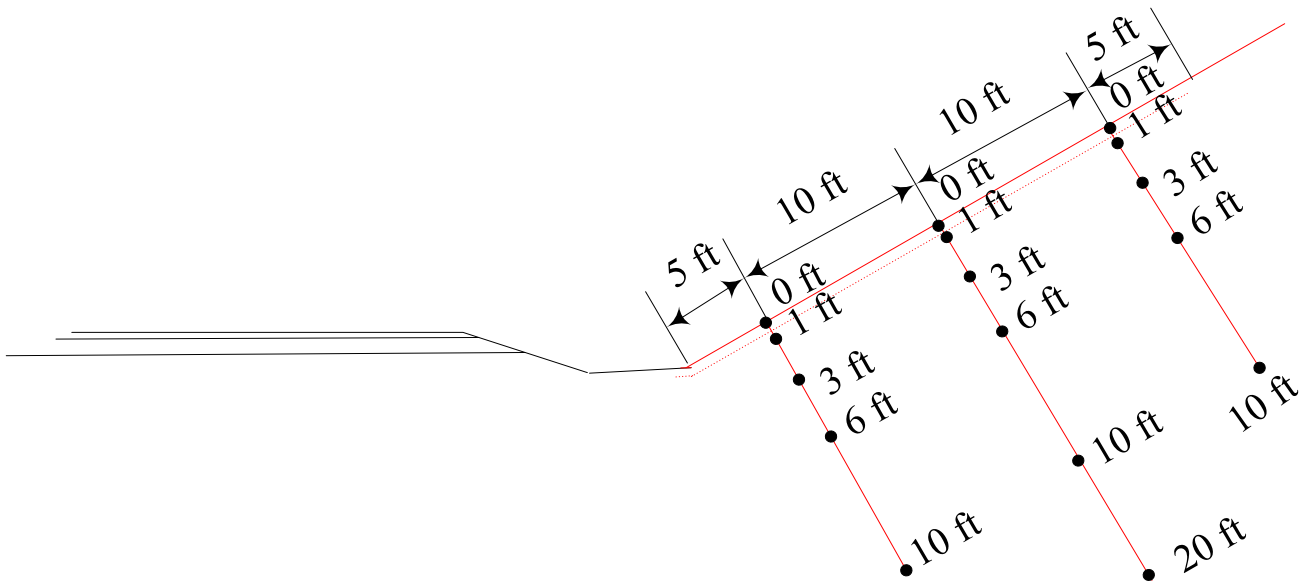


Figure 3.3 Profile view showing temperature sensor locations in Section A

Test Section B

This section is protected by one layer of coconut erosion control blanket. The profile for this section is shown in Figure 3.4. This 30 ft by 50 ft section extends between stations 519 + 60 and 520 + 10 as shown in Figure 3.4. Similar to Section A, three holes at station 519 + 85, located at the top, middle, and bottom, were drilled for placement of temperature sensors. Also, three moisture measurement sensors were installed at the surface of the slope along with the surface temperature sensors. In addition to the coconut matting, a heavy application of mulch seeding

was included as part of the design for this section. To hold the coconut mat in place, 32 holes (each with a diameter of 2 inches and depth of 8 ft) were drilled to allow placement of modified duckbill earth anchors. The duckbill anchors were modified in such a way that it is possible to easily readjust tension on them after construction to insure that good contact between the coconut matting and the ground surface is maintained.

The duckbill anchors were installed along the cut slope according to a spacing of 7.5 feet and 6 feet in the vertical and horizontal directions respectively as shown in Figure 3.6. Also, circle top wire pins were installed with a spacing of 1.5 ft and 1.2 ft in vertical and horizontal directions, as shown in Figure 3.7. The wire pins were added to the design in an attempt to insure initial maximum contact between the coconut matting and the cut slope surface. This additional anchoring measure was intended to promote vegetation growth as soon as possible after construction.

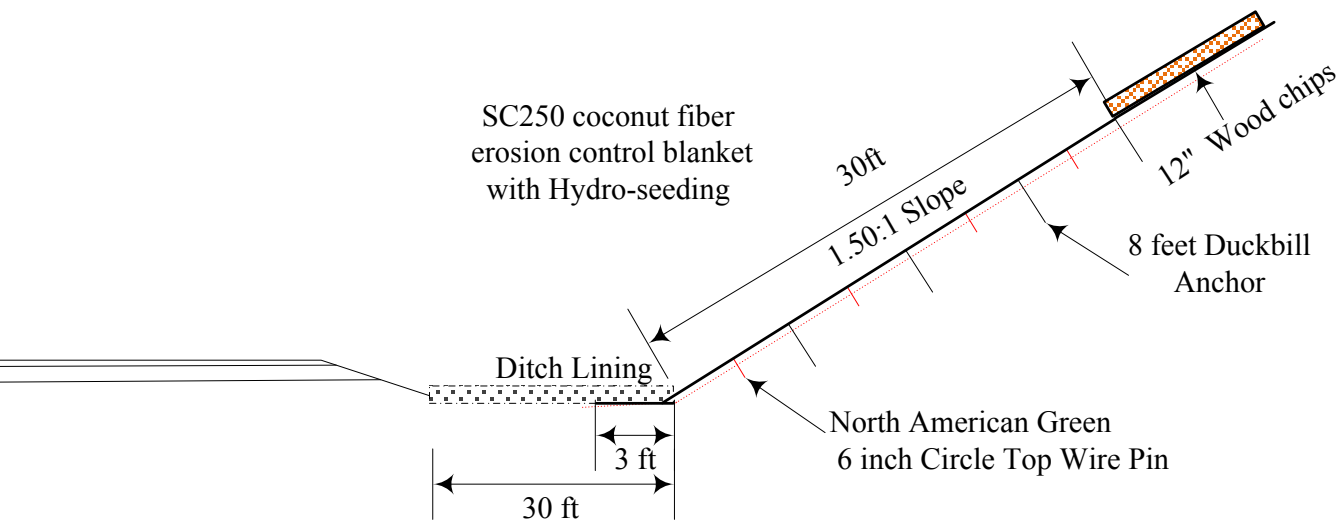


Figure 3.4 Profile of Section B

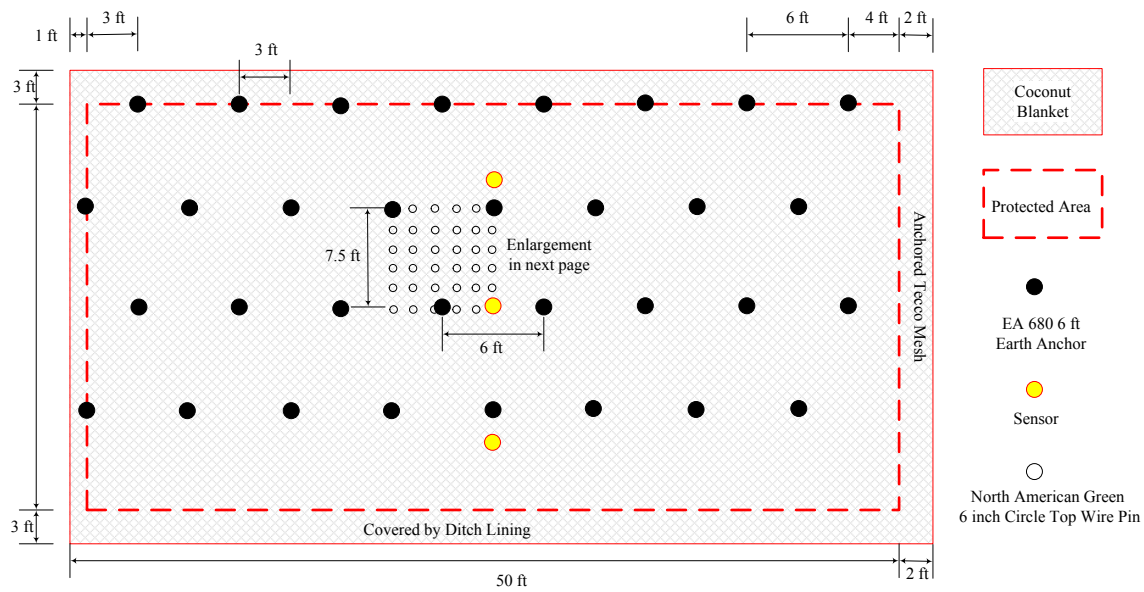


Figure 3.5 Layout of Section B

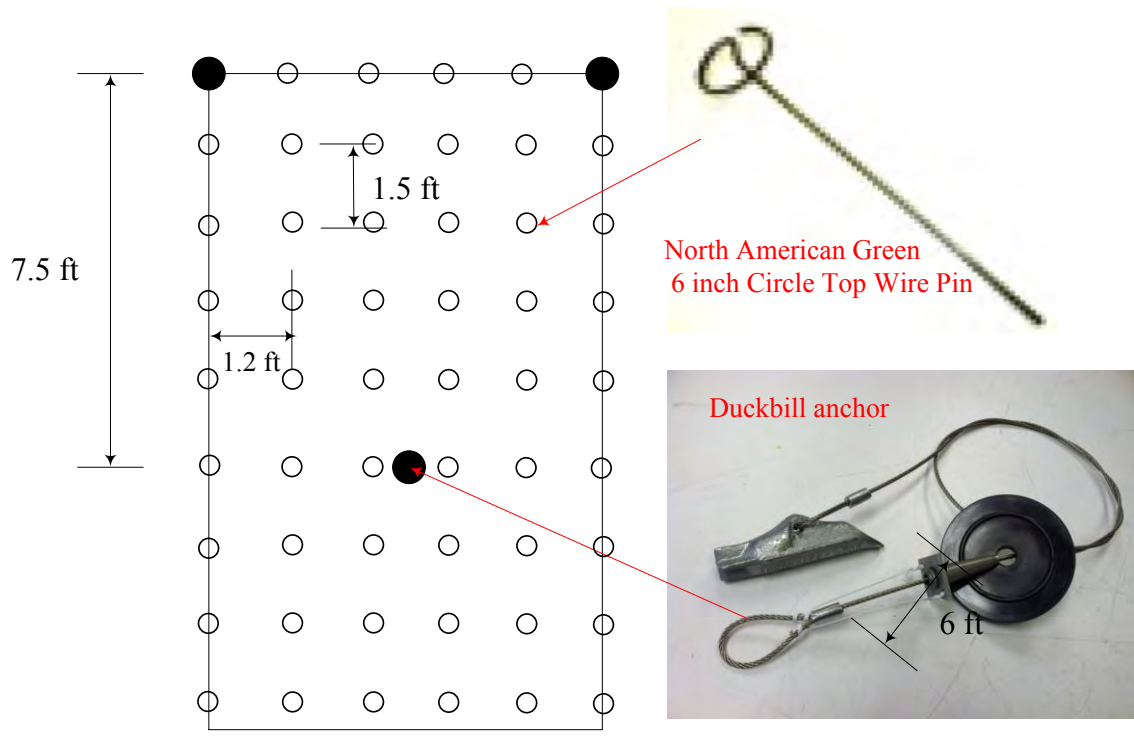


Figure 3.6 Enlargements of Duckbill Earth Anchor and Pins

Test Section C

This section is protected by one layer of coconut erosion control blanket as well as Tecco-mesh. The profile for this section is shown in Figure 3.7. This section is identical in size to Section B (30 ft × 50 ft) and extends from station 519 + 10 to 519 + 60 as shown in Figure 3.8. Similar to Section A, three holes at station 519 + 35 located at the top, middle, and bottom were drilled for temperature sensors. Three moisture measurement sensors were installed at the surface of the slope with the temperature sensors. As with Section B, mulch seeding was done in this section. In this section, larger earth anchors were used to hold the Tecco-mesh in place instead of the smaller duck bill type used to anchor the coconut matting in Section B. The Tecco-mesh was affixed to the cut slope using hollow-core steel rebar anchors. Thirty two 3-inch diameter holes were drilled for anchor installation on the slope with spacings of 7.5 feet and 6 feet in the vertical and horizontal directions as shown in Figure 3.8. The holes for the anchors are 9 feet deep. Details of the Tecco-mesh installation can be found in Figures 3.9 through 3.12.

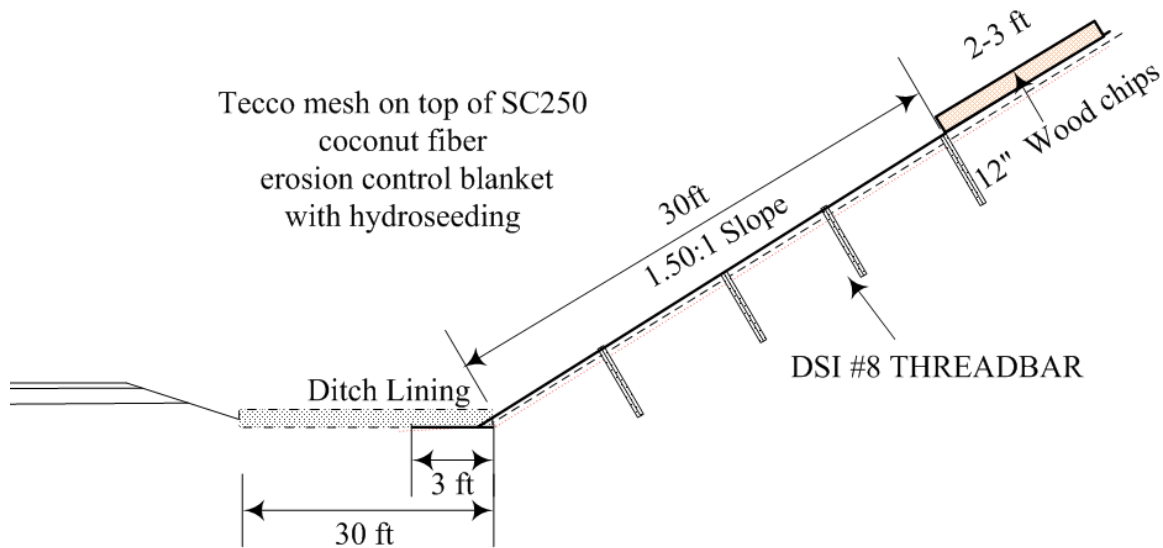


Figure 3.7 Profile for Section C

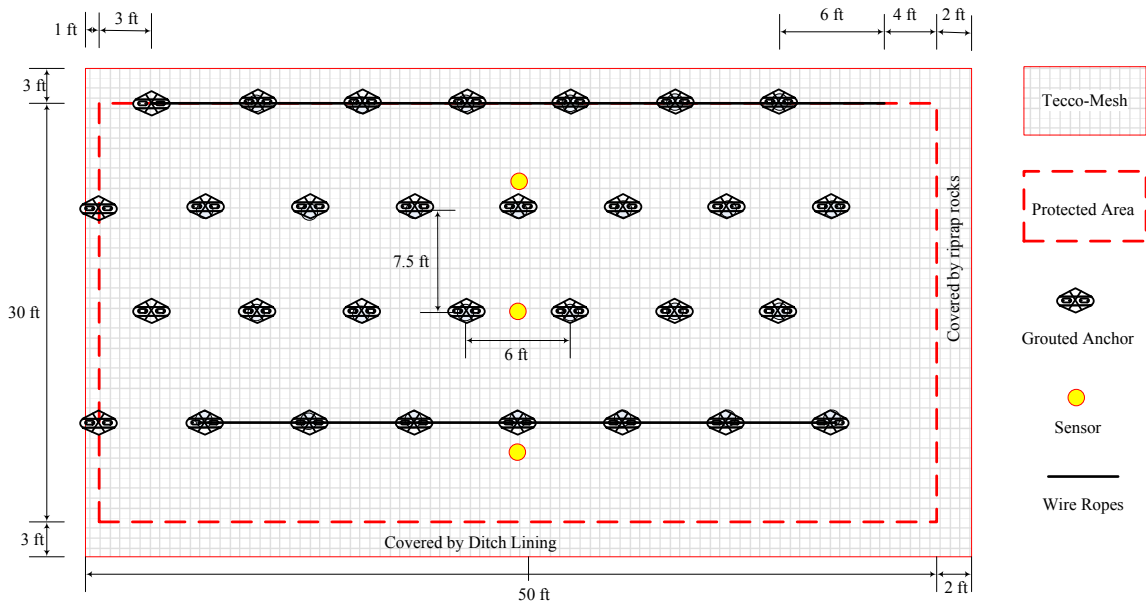


Figure 3.8 Section C, anchor and sensor locations

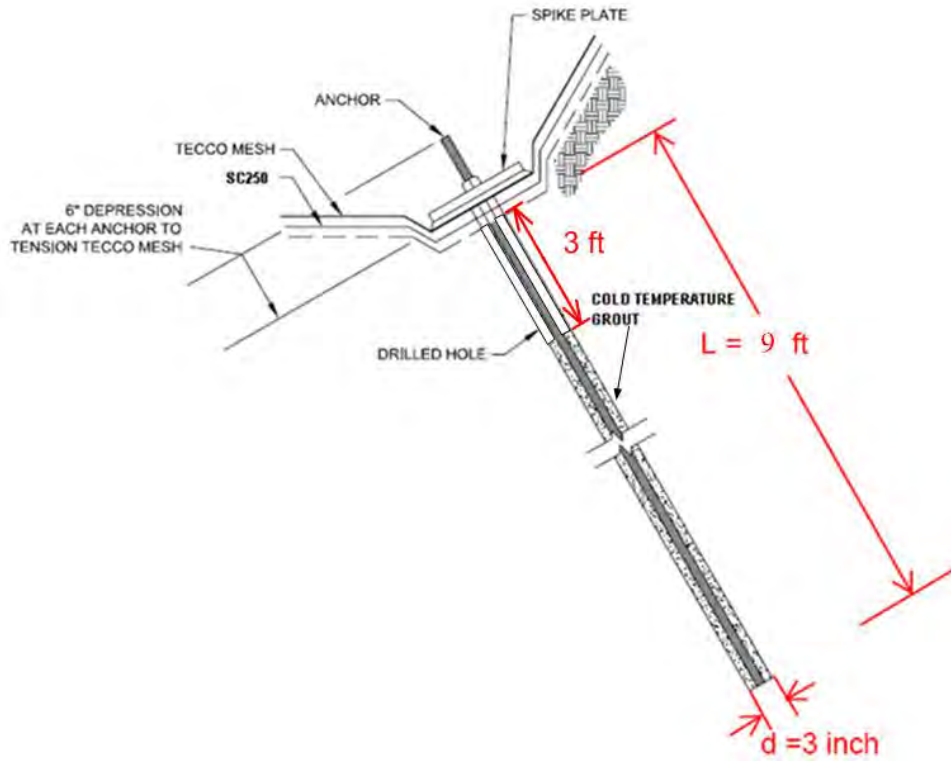


Figure 3.9 Detail of Section C anchor

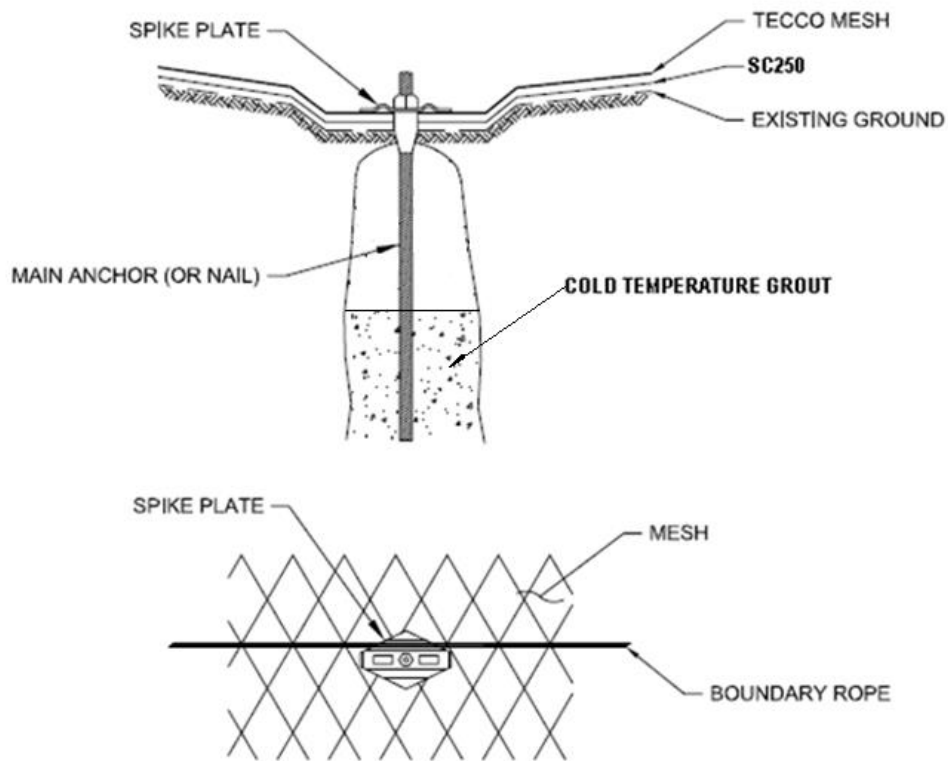


Figure 3.10 Nail and anchor detail with boundary rope

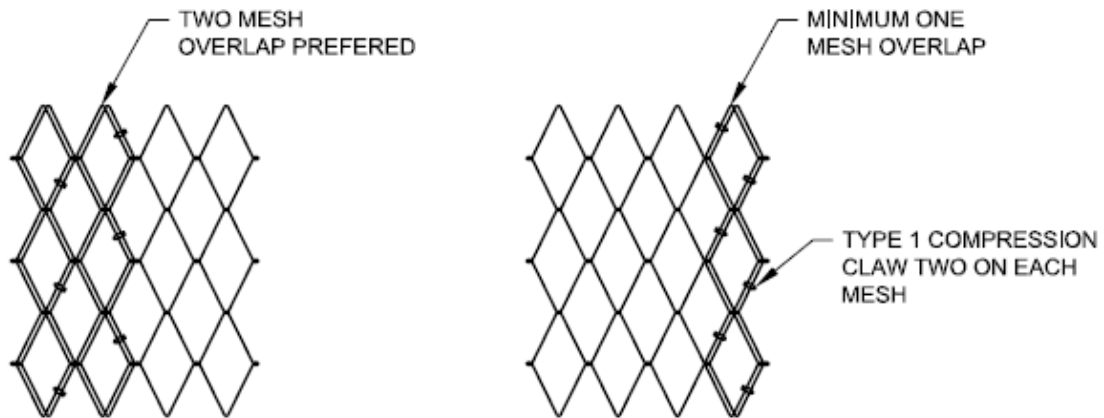


Figure 3.11 Plan view - connection of mesh sheets in Section C

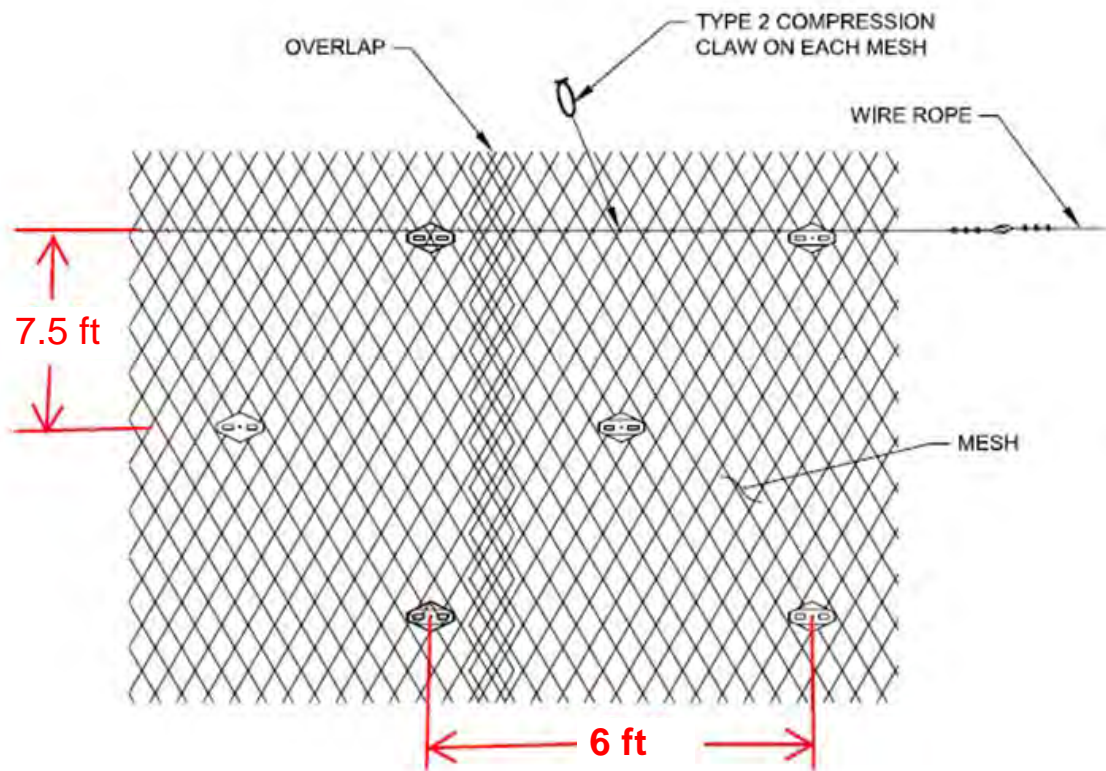


Figure 3.12 Connection details

Test Section D

This is the control section. It is protected by the standard project-design crushed rock blanket intended to protect ice-rich soil cut slopes. The standard design crushed rock blanket is 2 feet thick. The profile for the control section's standard rock blanket is shown in Figure 3.13. This section, identical in size to Section A, is 30 ft × 35 ft, extends between stations 518 + 75 and 519 + 10. Three holes at station 518 + 90, located at the top, middle, and bottom, were drilled for temperature sensors as shown in Figures 3.14 and 3.15. As for the other subsurface sensors, the holes were drilled perpendicular to the surface of the cut slope. Temperature sensors were installed at the depths indicated in Figure 3.3. Moisture measurement sensors were installed at the surface of the slope with the temperature sensors.

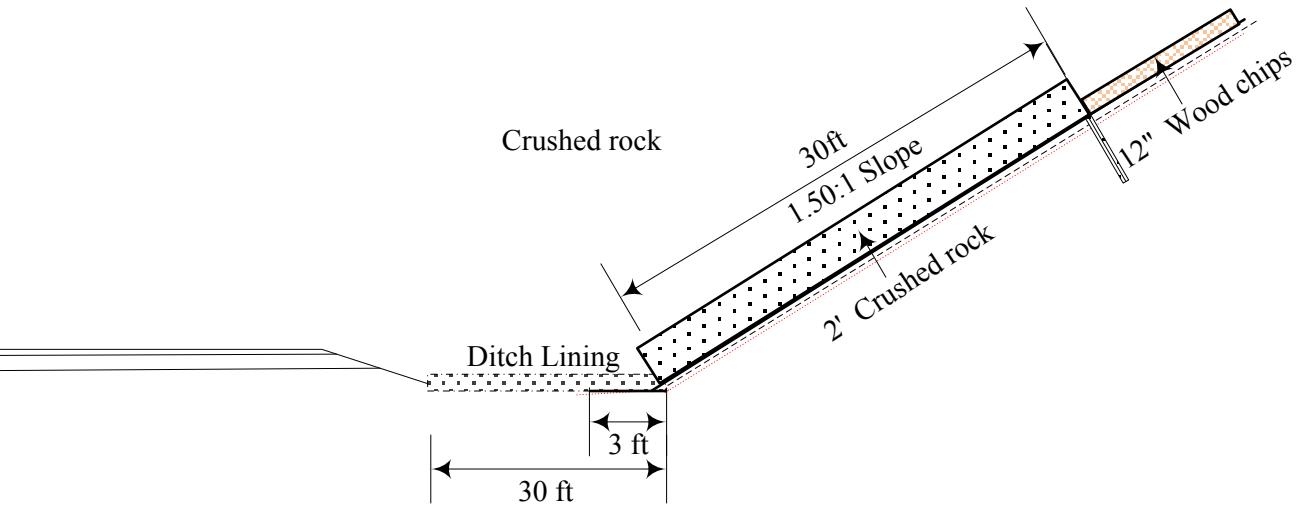


Figure 3.13 Profile of Section D

The layout for the temperature sensors for four sections is presented in Figures 2.14 and 2.15. The data collection station was installed at the top of Section D which is the control section. Other sensors were installed at the data collection station and the top of the cut slope. These will be discussed later in this report.

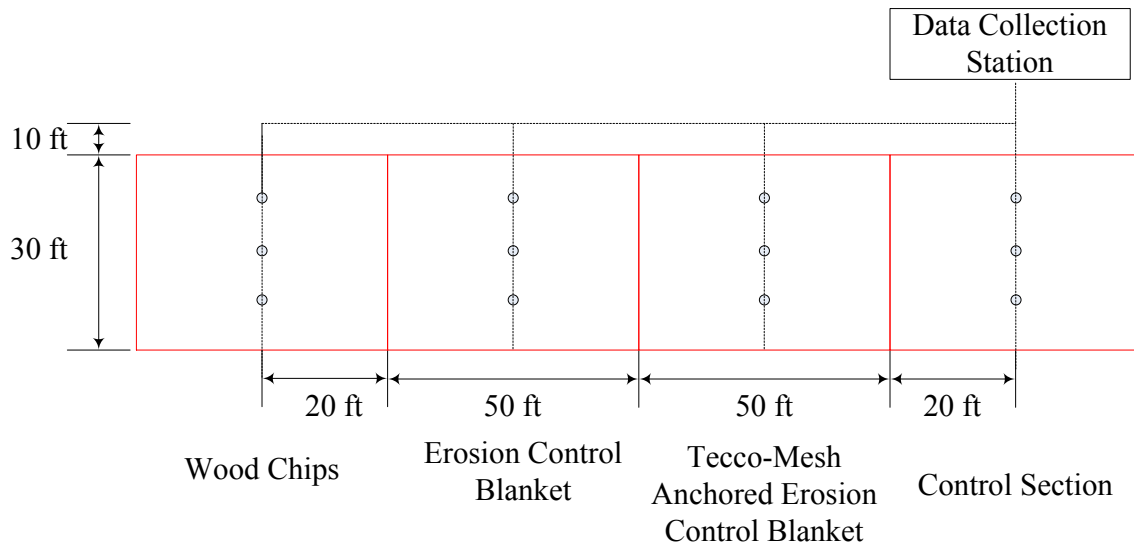


Figure 3.14 Layout for temperature sensor locations

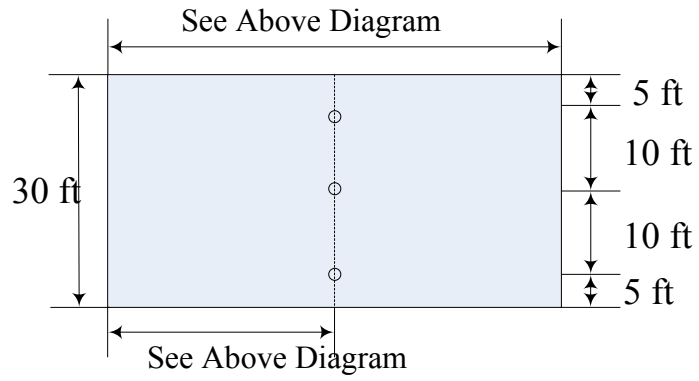


Figure 3.15 Layout for temperature sensor locations

CHAPTER 4. CONSTRUCTION OF EXPERIMENTAL SECTIONS

This chapter describes the construction process for the experimental cut slope treatments and instrumentation. Construction of all experimental sections within the Experimental Feature was performed during the period April 17 through April 27, 2013. Instrumentation was completed April 30, 2013.

On April 17, 2013, the snow on the cut slope at the Experimental Feature site was removed. Figure 4.1 shows the cut slope before placement of the various surface treatments. Sensors for obtaining data on temperature, moisture, precipitation, radiation, wind speed, and air temperature were installed as part of the construction process. These are now being used to monitor environmental conditions at the Experimental Feature site.



Figure 4.1 Cut slope at Dalton Highway 9-mile construction project location

Before placement of the individual surface treatments began on the cut slope on April 17, 2013, a layout of each section was drawn on the slope as shown in Figure 4.2 according to the designs indicated Chapter 3. Holes for anchors and temperature sensors were marked with different

colors. After this, drilling on the slope was performed. Holes were drilled with diameters of either 2 inches or 3 inches depending on purpose and location (2 inches for duckbill holes and 3 inches for rebar anchor holes). Figure 4.3 shows a close up of drilling activity on the slope. During construction, the slope was initially exposed to the air without any insulating protection. The afternoon temperatures rose to above freezing, and the slope began to thaw and became wet as shown in portions of Figure 4.2. The slope was a fairly steep workplace and, especially in the afternoon, became slippery. Therefore, it was sometimes necessary to tie the drilling machine to an excavator at the top of the cut slope (Figure 4.4).



Figure 4.2 Layout on the cut slope



Figure 4.3 Drilling on the cut slope



Figure 4.4 Drilling at the upper part of the slope

For those holes used for temperature sensor installations, PVC pipes were placed into the holes to protect the holes from intrusion of thawed material from the cut slope surface as shown in Figure 4.5. Figure 4.6 shows an instrumentation hole after the PVC pipe has been installed. It

was obvious that mud released from the surrounding cut slope face would have filled the instrumentation holes if the PVC housings had not been used.



Figure 4.5 Installation for sensor housing



Figure 4.6 Instrumentation hole with sensor housing installed

Due to high afternoon temperatures, thawing at the cut slope surface created visibly obvious areas of erosion. Compared with the slope before construction as shown in Figure 4.1, significant erosion can be seen on the slope especially within Sections C and D as shown in Figure 4.7. Close-ups of this erosion are shown in Figures 4.8 and 4.9. To protect the slope from erosion during construction, insulating tarps (normally used aid concrete curing during cold weather) were used to cover the entire cut slope as shown in Figure 4.10. Nails were used to affix the tarp sections to the cut slope surface.



Figure 4.7 Cut slope erosion during construction



Figure 4.8 Ice in the cut slope



Figure 4.9 Ice exposed in the cut slope



Figure 4.10 Cut slope protected from erosion during drilling

After holes were drilled, the duckbill earth anchors and the large hollow steel rebar anchors were installed in the holes. Figure 4.11 shows the cable end of a duckbill earth anchor (with its adjustable cinch mechanism) after the anchor has been placed in the slope. After the hollow rebar anchors were placed in the holes, each was grouted in place. A close-up photo of one of the grouted anchors is shown in Figure 4.12.



Figure 4.11 Cable end of installed Duckbill earth anchor



Figure 4.12 Installation of hollow rebar anchor

As mentioned previously, significant erosion was observed after the drilling process on the slope as shown in Figure 4.7. The eroded, uneven slope surface quickly became unsuitable for placement of the coconut erosion control matting and the Tecco-mesh. It was necessary that both of these treatments be placed on a smooth ground surface to prevent air circulation between treatment matting and the cut slope surface. Such air circulation would reduce the thermally protective effects of both treatment types. Therefore, prior to placement of the coconut (Section B) and Tecco-mesh (Section C) slope coverings, the bucket of a large backhoe excavator was used to smooth out the uneven surface of the cut slope. This operation is shown in Figure 4.13. Then Sections B and C were seeded. Figure 4.14 shows a small area of the cut slope after seeding.



Figure 4.13 Re-smoothing the cut slope surface

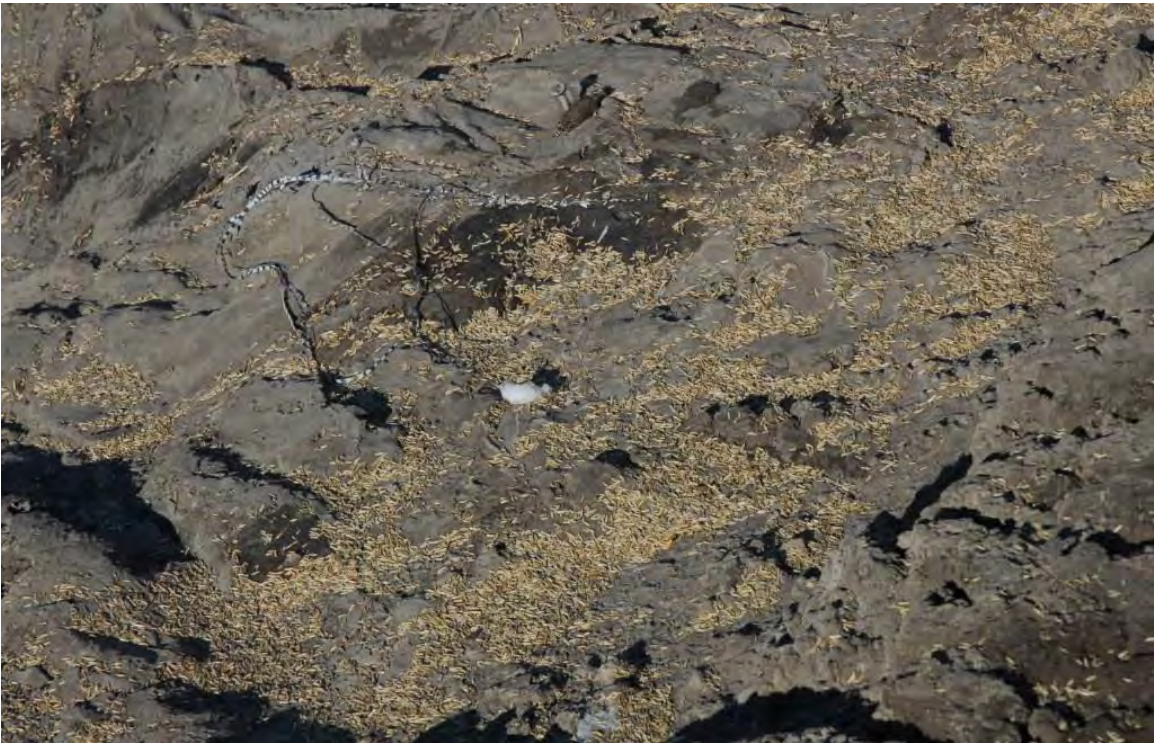


Figure 4.14 Seeded cut slope

The coconut erosion control blankets were placed after seeding. Coconut matting rolls were hauled to the top of Sections B and C, and then unrolled down the cut slope as shown in Figures 4.15 and 4.16. The overlap for adjacent mat strips was about 1 foot. All soil anchors used on the cut slope penetrated through the coconut matting.



Figure 4.15 Placement of coconut erosion control matting



Figure 4.16 Placement of coconut erosion control matting

After placement of the coconut erosion control blankets in Sections B and C, the Duckbill earth anchors were locked into place in Section B by pulling upward on the anchor's cable. Because of the Duckbill anchor design, an upward pull on the anchor's cable (after the anchor has been placed in its hole) causes the anchor head to rotate and then dig into the undisturbed soil at the anchor head location. After the Duckbill anchors were set, the round plates, located high on the anchor cable (the special cinching mechanisms), were pushed firmly downward, thus cinching the anchor cables to the ground surface to tightly hold the coconut blankets in place which is shown in Figure 4.17. After the Duckbill anchor plates had been cinched in place within Section B, circle top wire pins were inserted through the Section B coconut matting and into the cut slope surface. Due to the initially hard-frozen nature of the slope surface, these pins could not simply be hammered into the soil. A portable drill was used to create a pilot hole for each pin which facilitated placement of the pin. Figure 4.18 shows a pin which has been placed into the slope.

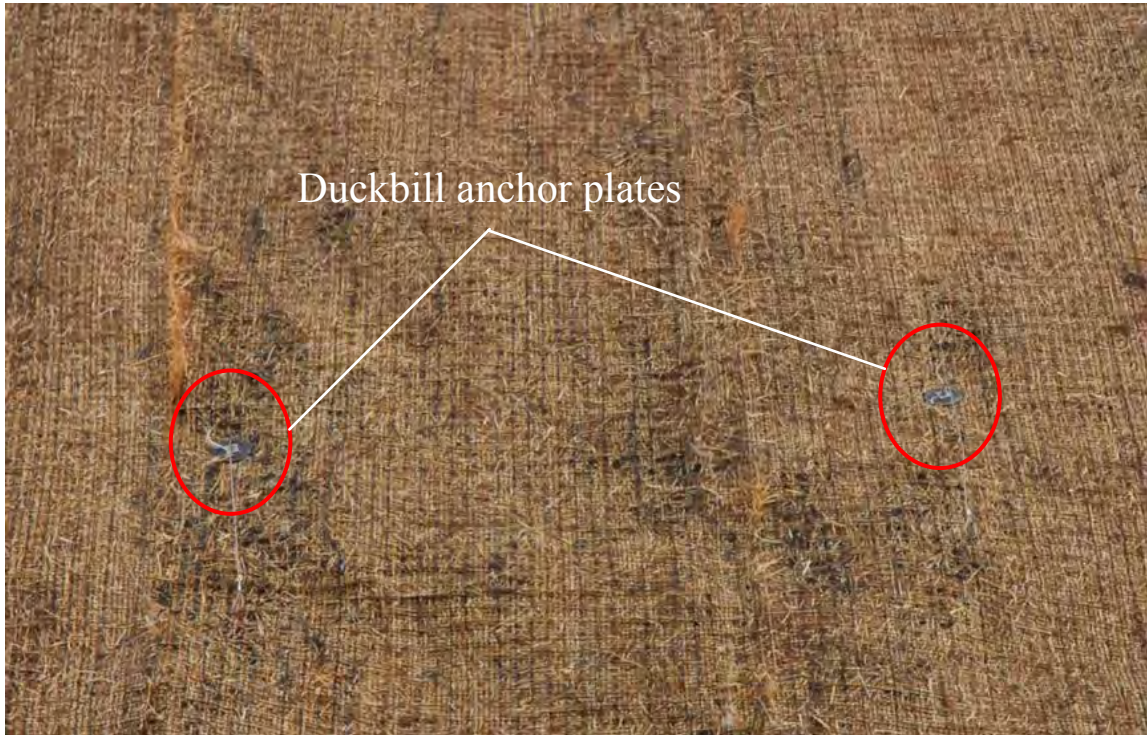


Figure 4.17 Section B showing Duckbill anchor plates after construction

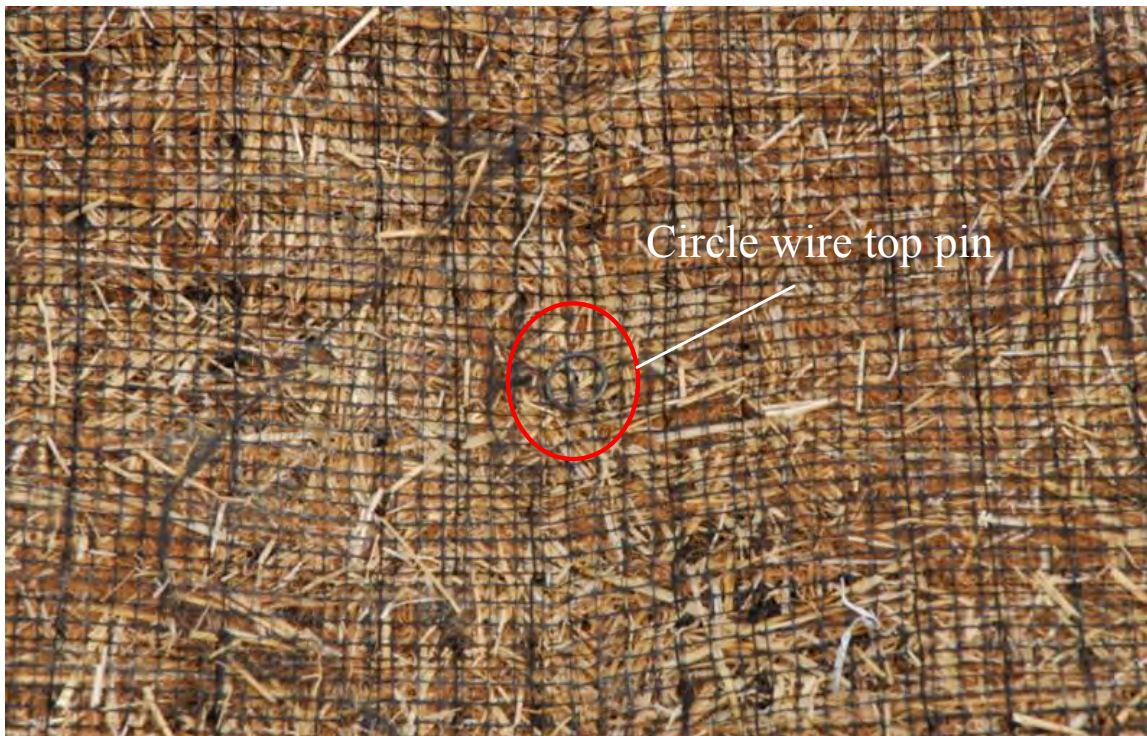


Figure 4.18 Enlargement of a circle wire top pin

For Section C, after the placement of the coconut blanket, Tecco-mesh was installed as a second layer. Similar to the installation of the coconut mat, Tecco-mesh was hoisted to the top of section C and then unrolled down the cut slope as shown in Figure 4.19. Extra Tecco-mesh was trimmed off at the bottom of the slope as shown in Figure 4.20. Adjacent Tecco-mesh strips were connected along their adjoining lengths using connection clips as shown in Figure 4.21. A Tecco-mesh connection clip is shown in the upper right corner of Figure 4.21. After the Tecco-mesh had been installed in Section C, spike plates were put in place to hold the Tecco-mesh tightly to the cut slope surface. The plates were held in place, across the cut slope surface, with hex nuts as shown in Figure 4.22. A close-up view of the anchor plate and nut is shown in Figure 4.23.

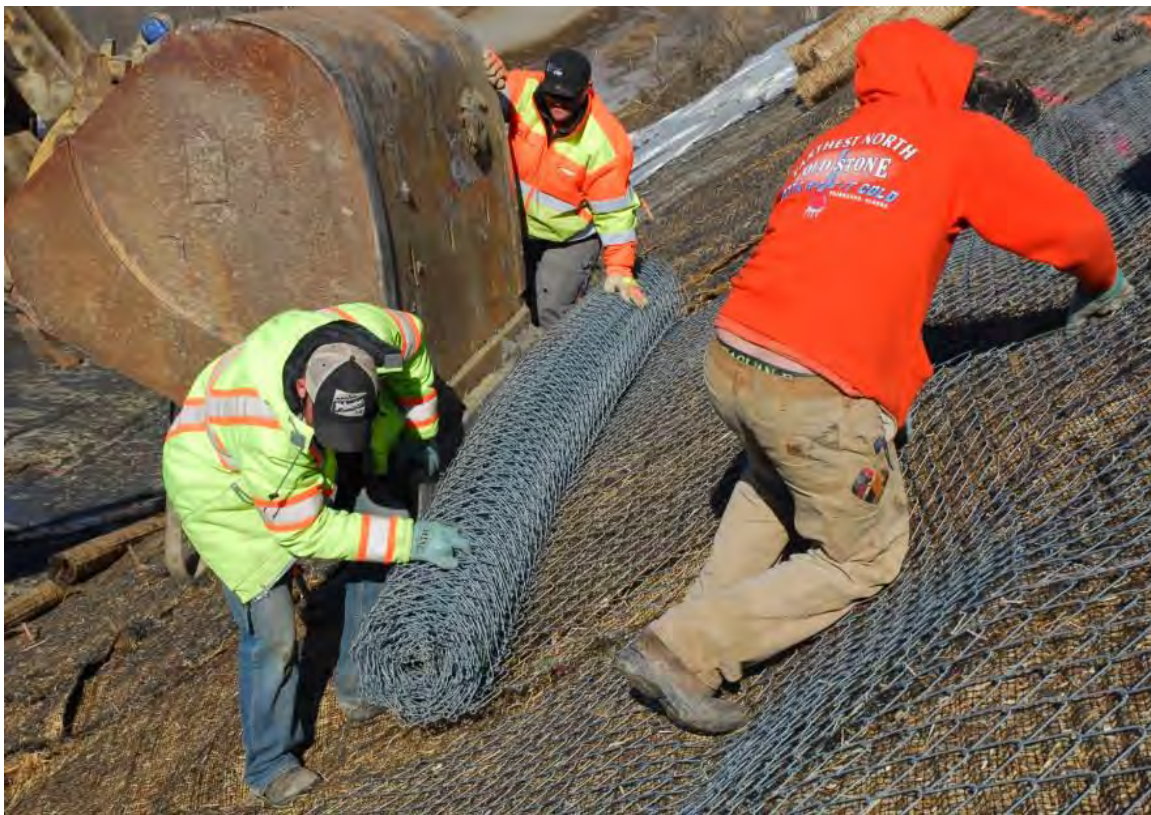


Figure 4.19 Placement of Tecco-mesh



Figure 4.20 Cutting away excess Tecco-mesh



Figure 4.21 Connecting adjacent Tecco-mesh strips



Figure 4.22 Section C appearance after construction



Figure 4.23 Close-up view of Tecco-mesh at an anchoring point

After construction for Sections B and C, crushed rock was hauled to the test site. A backhoe excavator was used to cover Section D with two feet of crushed rock as shown in Figure 4.24.

Finally, wood chips were hauled to the top of the slope and then spread along the upper part of the cut slope and on Section A as shown in Figure 4.25. An enlargement showing wood chips used at the experimental site is in the upper right corner of Figure 4.25. Figure 4.26 is a panorama of the cut slope Experimental Feature shortly after construction.



Figure 4.24 Construction of Section D



Figure 4.25 Spreading wood chips along top portion of cut slope



Figure 4.26 Appearance of Experimental Feature very soon after completion

CHAPTER 5. CONSTRUCTION OF DATA ACQUISITION STATION

On April 24, 2013, the Experimental Feature's temperature sensors were installed. For Sections A and D, the PVC tubes were found to be frozen into the ground, and it was therefore necessary that those tubes be left in place. It was possible, however, to remove the PVC tubes from the middle two Sections (B and C), before the sensors were installed. Dry sand was used to fill the holes after the sensor installation as shown in Figure 5.1. A moisture sensor was installed, at the ground surface at the top of each string of temperature sensors (see Figures 5.2 and 5.3). After installation, cables for these sensors were bundled together and the cable bundles were extended across the cut slope to their termination location at the data collection station.



Figure 5.1 Backfilling with sand after insertion of temperature sensor string



Figure 5.2 Installation of moisture sensor at top of temperature sensor string

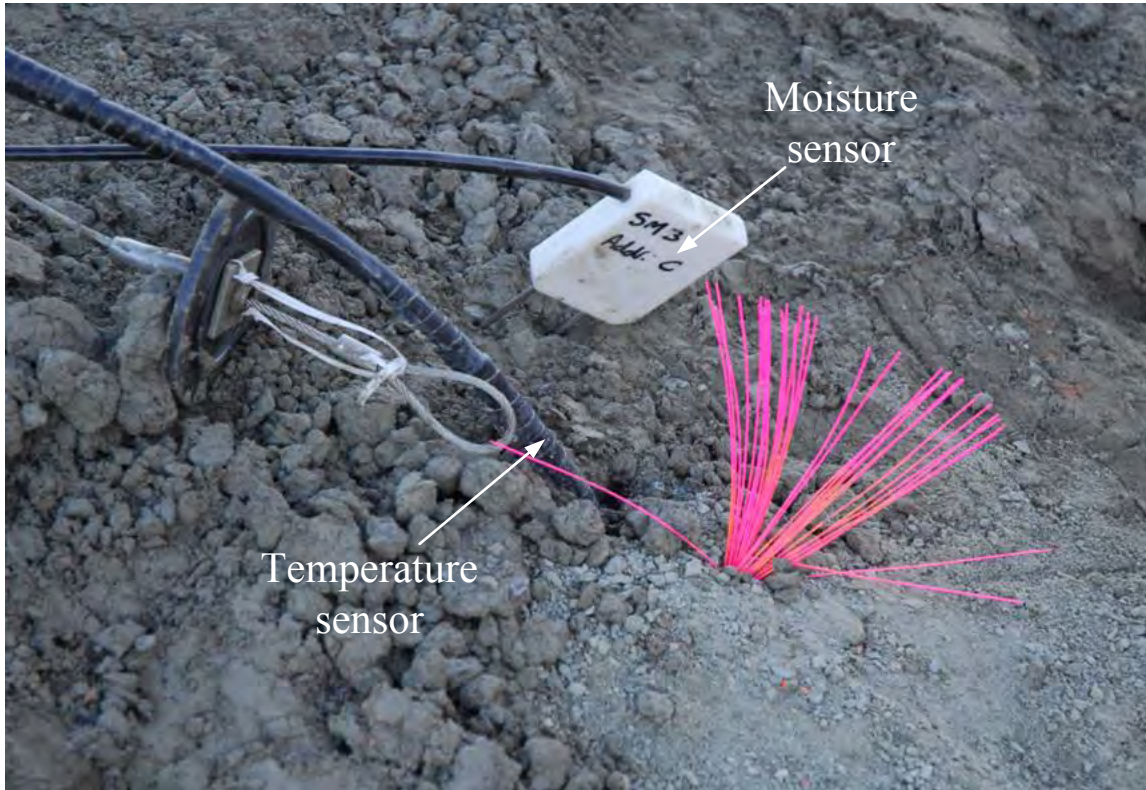


Figure 5.3 Temperature and moisture sensor location

Aluminum conduits were used to protect cable running along the surface of the ground from damage. The aluminum conduits were grouped together and routed to the data collection station located above Section D. The data station is shown in Figure 5.4. Figure 5.5 is a picture of the data station after completion. The Campbell Scientific data collection box was mounted on a tripod as shown in Figure 5.4. The sensor cables were attached to a Campbell Scientific CR1000 data logger through two AM16/32B relay multiplexers. The data logger was set to record temperatures and moisture contents from all sensors at 15 minute intervals. Figure 5.6 shows the interior of the data logger box after the data logger and multiplexer attachments have been made. In addition to the individual temperature and moisture sensors located at discrete points on or under the cut slope face, an HMP45C Air Temp/Relative Humidity sensor was installed (above the data logger box) to monitor air temperature and air relative humidity generally representative of the Experimental Feature area. The HMP45C sensor is shown in Figure 5.7. Radiation, wind, and precipitation sensors were also installed near the data logger box to collect other

environmental data generally representative of the Experimental Feature site. These sensors are shown in Figures 5.8 to 5.10.



Figure 5.4 Data collection station

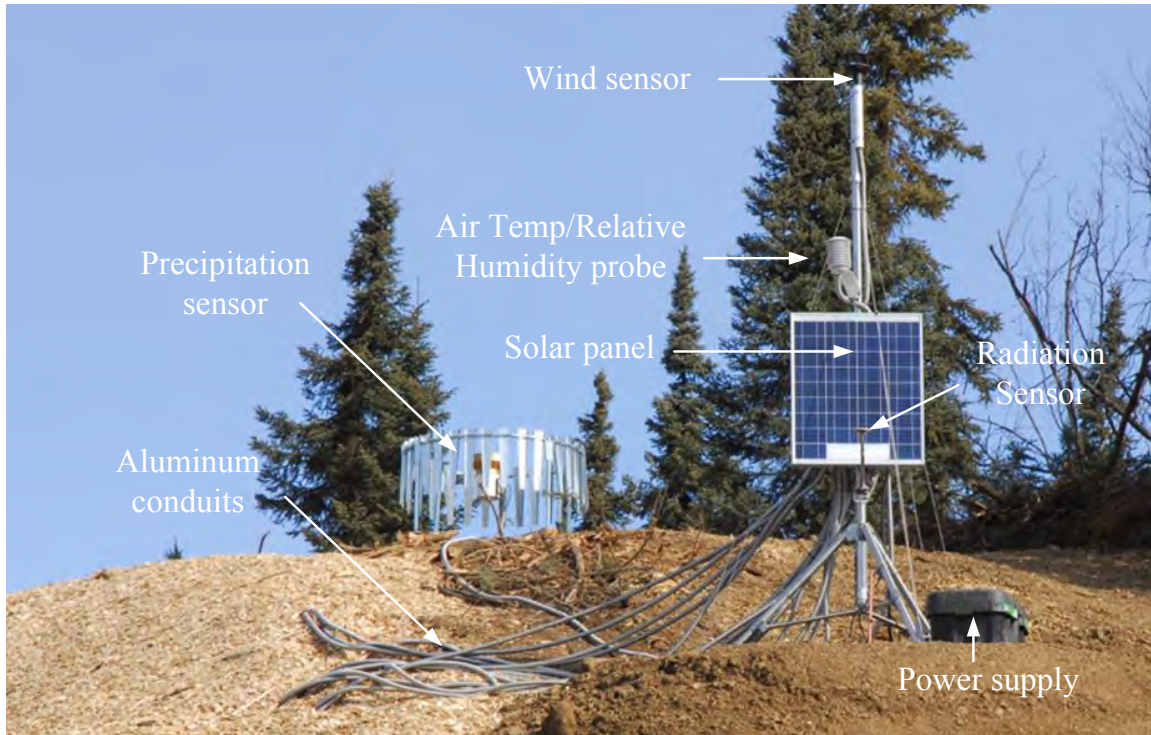


Figure 5.5 Data collection station after completion

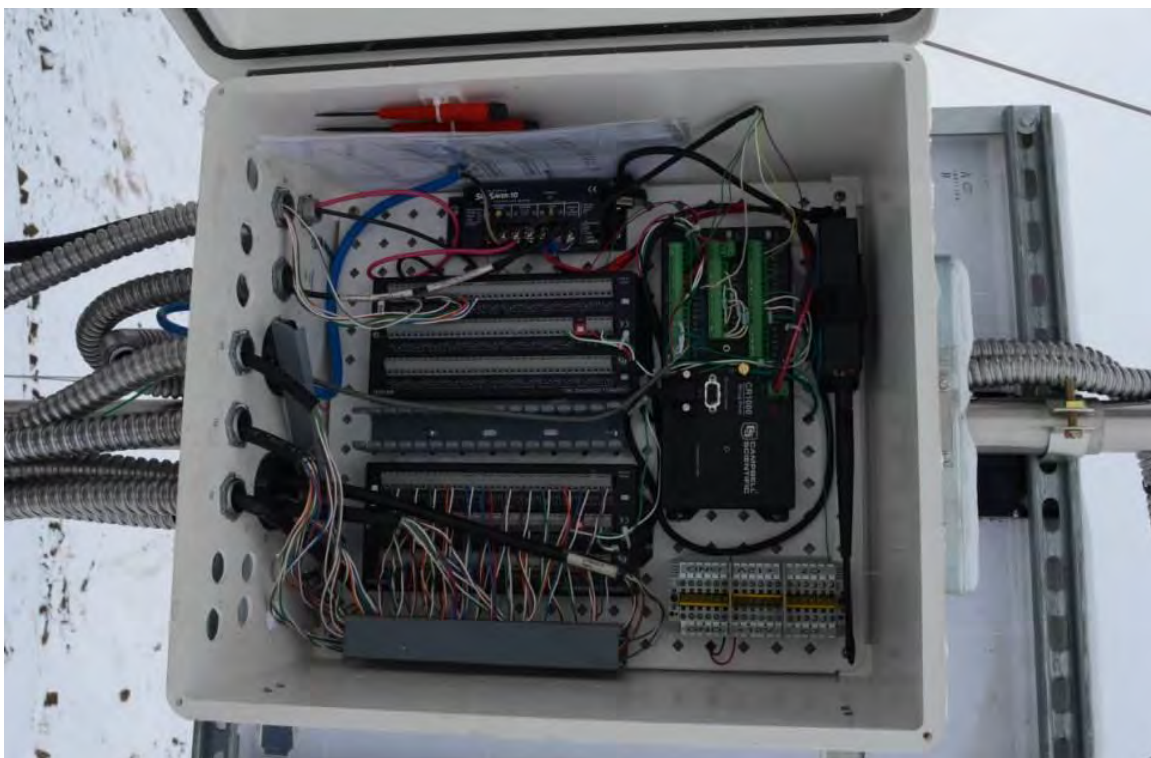


Figure 5.6 CR1000 data logger and AM16/32B multiplexing equipment



Figure 5.7 Air Temp/Relative Humidity sensor



Figure 5.8 Wind sensor



Figure 5.9 Radiation sensor



Figure 5.10 Precipitation sensor

Beside these, as shown in Figure 5.11, two cameras mounted on a tripod were installed at the other side of the road two monitoring the ice-rich slope change with time on September 27th, 2013. Each camera covered about half of the slope. The two cameras were set to capture two pictures of the slope per day.



Figure 5.11 Two cameras installed for slope monitoring

CHAPTER 6. PERFORMANCE PROBLEMS SOON AFTER CONSTRUCTION

Researchers discovered substantial problems within the Tecco-mesh experimental section of the Experimental Feature by the first week of June 2013. Based on problems that were obvious in photos and observations by L. Li (project team member) on Friday June 7th, R. McHattie (project team member) visited the site on Sunday June 9th, 2013. During this visit, Friday's observations were confirmed and more photos/observations were obtained. As a result of discussions resulting from the observations and photos, the project team and AKDOT&PF Construction personnel concurred that remedial action was necessary to prevent the rapid occurrence of further damage at the Experimental Feature site.

The panorama photo labeled Figure 6.1 shows the entire face of the Experimental Feature and the circled failure areas within the Tecco-mesh section. Observation at the site found that there had been an obvious loss of original cut slope soil volume from the slope face. This loss of volume could be seen easily thru the Tecco-mesh — an observation that was confirmed by probing and peering through the Tecco-mesh at many locations along the mesh surface.

The obvious loss of volume from the cut face can be seen through the Tecco-mesh in Figure 6.2, especially where massive ice is exposed near the upper right corner of the photo. What was initially exposed during construction as a planar area of ice-rich material on the surface of the cut slope prior to Tecco-mesh placement, eventually became recognizable (after thawing) as an irregular massive ice feature that unfortunately extended across much of the Tecco-mesh section. By June 9th the massive ice feature could be easily recognized through the Tecco-mesh at a number of locations (labeled and clearly visible in Figure 6.3).

Much surface volume had been lost beneath the Tecco-mesh due to thaw and runoff. This condition extended beneath the roll of coconut matting (in Section B) closest to the Tecco-mesh section, but less soil volume had been lost there. By far the worst soil volume loss was within the central portion of the Tecco-mesh section itself. It appeared that most of the volume loss had been through runoff of silt and water into the ditch with little if any due to thaw-consolidation. As of June 9th, the soil/ice material visible across much of the Tecco-mesh section existed as an

irregular thawing surface with an intact Tecco-mesh covering (a sort of tent) suspended one to several feet above the present soil/ice surface. At that time, none of the Tecco-mesh and only small areas of the coconut matting within Section C had failed.



Figure 6.1 Panorama view of Experimental Feature showing failure in Tecco-mesh section



Figure 6.2 Close view of failure within the Tecco-mesh section

The significant loss of material from the original cut slope is evident in the left side of Figure 6.3 where the anchor grout is exposed. The nominal plan depth from cut slope face to top-of-grout was 3 feet. The lighter gray material labeled in the right side of Figure 6.3 is some of the massive ground ice that caused serious problems with the Tecco-mesh experimental section.



Figure 6.3 Close views showing exposure of soil anchor grout (left) and portion of massive ice feature under Tecco-mesh (right)

In Figure 6.4, the areas where the ground surface is not in contact with the Tecco-mesh or the adjoining coconut matting are those areas where no grass had yet appeared. As Figure 6.4 shows by the appearance of grass, only the very top portion of the Tecco-mesh section still has soil-Tecco-mesh contact.



Figure 6.4 Surface protection matting in areas showing no grass growth are not in direct contact with ground surface

Based on the June 7th, June 9th appearance of the test section, the Tecco-mesh, although intact, did not appear to be serving any useful function relevant to retarding thaw or preventing further loss of cut slope material into the ditch. It may have been possible to perform some adjustments on the Tecco-mesh anchors to bring the mesh closer to the existing cut slope surface. However, it was apparent that such adjustments would not have offered much improvement given the large volume of cut slope material that had already been lost. Obvious evidence of the foregoing and a realization that continued deterioration/runoff would almost certainly produce a noticeable environmental issue, required a fairly substantial change in the Experimental Feature plan. The following recommendations were agreed upon by the research team, the AKDOT&PF, and the contractor—and executed by the contractor:

June 2013 Recommendations to Modify the Design of the Experimental Feature:

- Detach the Tecco-mesh and underlying coconut matting from its anchors within the Tecco-mesh section, and remove the mesh and matting from the slope surface.
- Extend the rock blanket material (control section material) across that section. During this process, leave as many of the Tecco-mesh anchors in place as possible. It was thought that thaw-related problems would initially continue given the very high ice content of some of the cut slope material, and that the rock blanket would conform to slope surface as it receded. The rock blanket would provide some degree of insulation and serve as a filter to keep silt from running into the ditch. Initial failure of the project's standard design thickness of blanket material, due to loss of massive ice volume, would require placement of additional blanket material.
- Cinch down all duckbill anchors in the coconut matting test section. This was particularly necessary in the portion of that section closest to the Tecco-mesh section.

According to the recommendations listed above, on June 17th 2013, Tecco-mesh and the coconut erosion control blankets at Section C were removed which is shown in Figure 6.5. The great loss of volume in Section C can be seen especially where massive ice is exposed as shown in Figure 6.6. Crushed rock was hauled to the test site. Then, an excavator was used to cover Section C with crushed rock (see Figure 6.7). The hollow rebar anchors were left intact during these repairs to serve as survey and photogrammetric reference points. Figure 6.8 shows the cut slope after completion of repairs on June 17th 2013.



Figure 6.5 Section C without Tecco-mesh and coconut blanket



Figure 6.6 Massive ice in Section C



Figure 6.7 Covering Section C with crushed rock



Figure 6.8 Cut slope after construction on Section C

Dr. Zhang (Mingchu Zhang, project Co-P.I.) visited the Experimental Feature site on Friday June 21st. During his inspection of the site he noticed that an area of significant size, along the top of the Experimental Feature cut slope, had been cleared of natural vegetation. Figure 6.9 presents a close up (left) and total view (right) of the cleared area on the date of his visit.

Dr. Zhang was concerned that thermal degradation might progress downward from surface of the cleared area and eventually influence the thermal regime of soils behind the experimental cut slope face. He recommended: 1) that the wood chips first be removed from the surface of the cleared area, 2) that the entire area then be graded to drain, 3) that the entire area then be covered with an erosion control blanket, i.e., using remnants of the Experimental Feature's coconut matting or functionally similar erosion control matting, and 4) finally, that the mat-covered area be heavily seeded to encourage a quick, lush growth of vegetation. This recommended treatment will eliminate water ponding along the top of the cut slope. Even more importantly, the natural cooling system (via evapotranspiration and shading) provided by a thick growth of vegetation will much reduce the thermal degradation of underlying soils.

This recommended work remains to be done at the time of this report's preparation (February 2014).



Figure 6.9 Start of thaw related damage at top of Experimental Feature cut slope

CHAPTER 7. RESULTS AND ANALYSIS

As presented in the previous chapter, a weather station was built at the test site. Air temperature, wind speed, wind direction, precipitation, solar radiation, and humidity information was recorded throughout the measurement period. Besides this, moisture and temperature information on and beneath the slope face were also monitored by the installed TDR and temperature sensors. The recorded weather information as well as the moisture and temperature information is presented in this chapter. Analysis regarding these recorded results was also performed and is presented. Erosion volume estimates for each section were obtained using a special survey method based on sophisticated analyses of sets of photographs of the slope surface.

Site Climatic Conditions

Figure 7.1 shows air temperatures, based on hourly data, at the Dalton Highway 9 Mile Experimental Feature in the two and a half months after the sensor's installation. The air temperature climbed up to above 0 °C at the middle of May and remained at above 0 °C until July at which time the field data collection ended. The air temperature generally varied between 5 and 30 °C. Before the middle of May, there was also a certain time period with temperatures above 0 °C. Diurnal temperature variations, based on hourly data, for three selected dates are presented in Figure 7.2. It was found that hourly temperatures varied with a range from 10 to 15 °C over a 24 hour period. The maximum and minimum of these diurnal temperatures were found to vary between the different days. On May 1st, 2013, the highest and lowest temperatures were found to be 7:00 pm and 9:00 am, respectively. However, on July 14th, 2013, the highest and lowest temperatures were found to be 4:00 pm and 7:00 am, respectively. The average air temperature at the test section raised nearly 30 °C between the first of May and mid-July. Precipitation information presented in Figure 7.3, based on hourly data, shows that rainfall was found on days with low average air temperature when referred to Figure 7.1. Relative humidity information during field data collection period was presented in Figure 7.4. Relative humidity, based on hourly data, varied from 15% to 95%. There were some time periods that the relative humidity was higher than 90% in some days. These periods were considered as rainfall events at the test section.

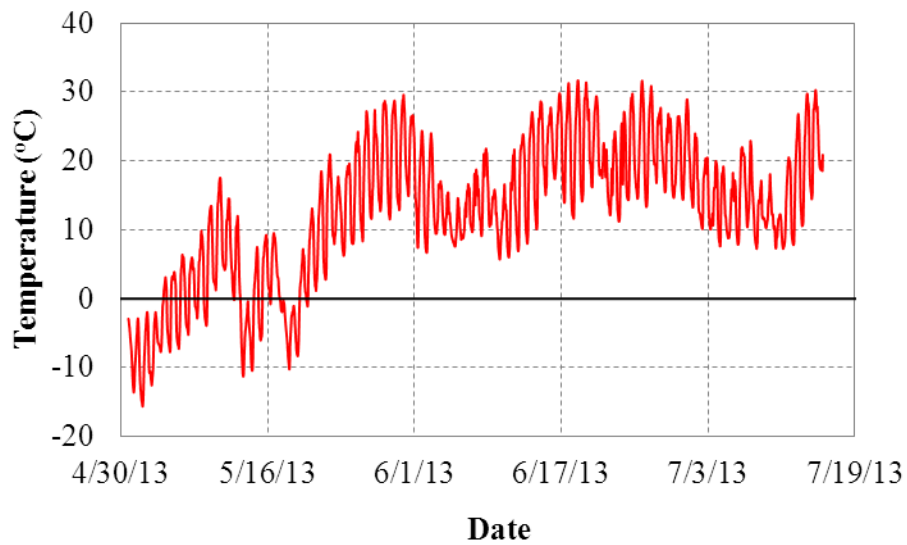


Figure 7.1 Air temperatures at the Experimental Feature site

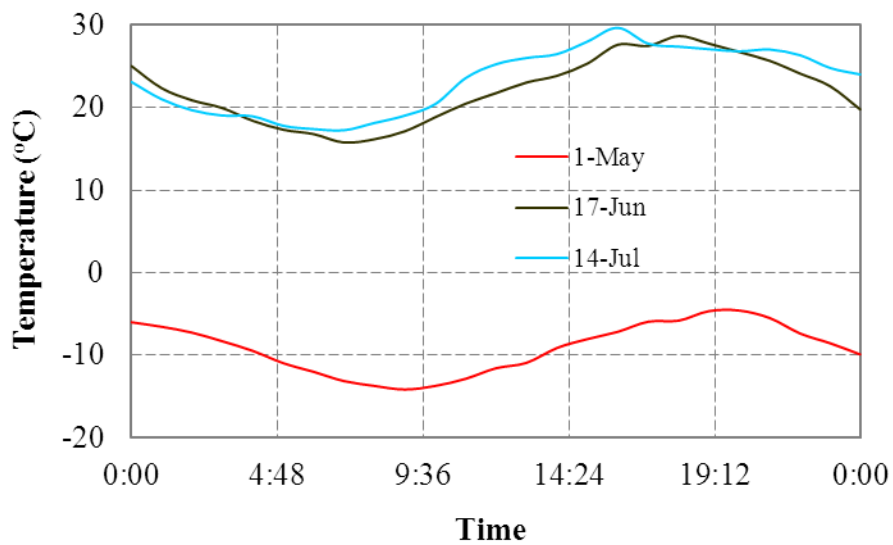


Figure 7.2 Temperature variations for three different days

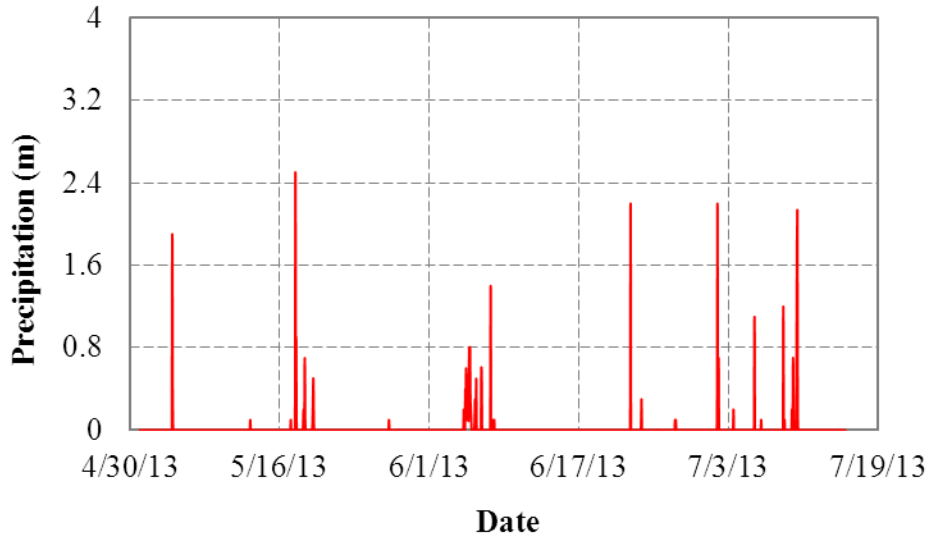


Figure 7.3 Precipitation at the Experimental Feature site

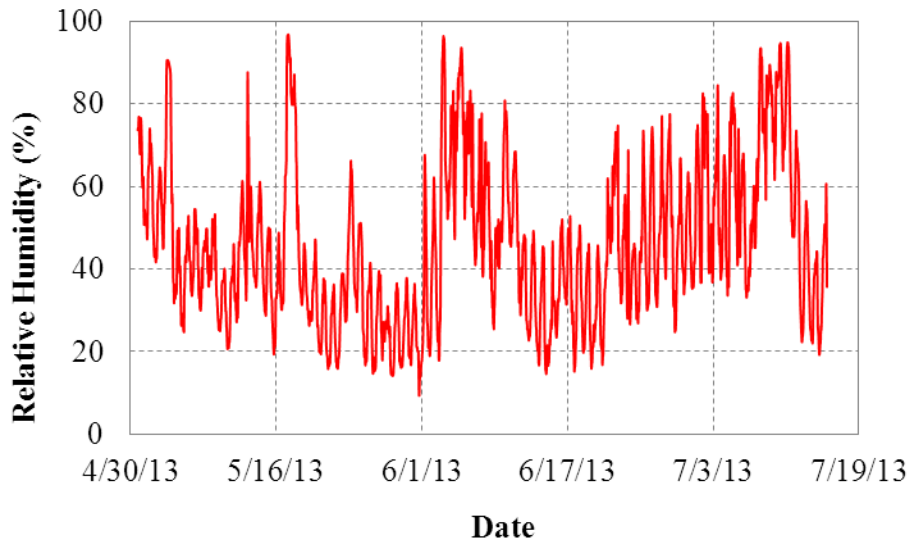


Figure 7.4 Relative humidity at the Experimental Feature site

Beside air temperature, relative humidity, and precipitation monitoring, wind speed, wind direction, and solar radiation at the Experimental Feature were also recorded by the installed weather station. Wind direction frequency distribution at the test site during the recorded time period is presented in Figure 7.5. About 30% of the time, the wind was found to be from northwest direction. Basically, wind direction from the other directions distributed evenly. Wind

speed throughout the recorded time period did not vary by much with an average of about 2.5 m/s as can be seen in Figure 7.6. On some days, the wind speed was higher than 6 m/s. Incident solar radiation at the test site was also monitored and recorded, on an hourly basis, as presented in Figure 7.7. Due the presence of rainfall on some of the days, the solar radiation detected is much lower than days without rainfall as shown in Figure 7.7. However, for non-rainy days, the variation in solar radiation at the test site is very low. The 24-hour solar radiation variation for three selected days is presented in Figure 7.8. The highest incident radiation was found to be at around 2:30 pm. Also as shown in Figure 7.8, solar radiation in May is slightly lower than in June and July. The voltage of the power supply battery for the sensors during the recording time period is presented in Figure 7.9. The voltage output, based on hourly data, was stable and well above the required 12 volts. Voltage averaged about 13.5 V, indicating that in terms of voltage requirements, the sensor readings should be reliable.

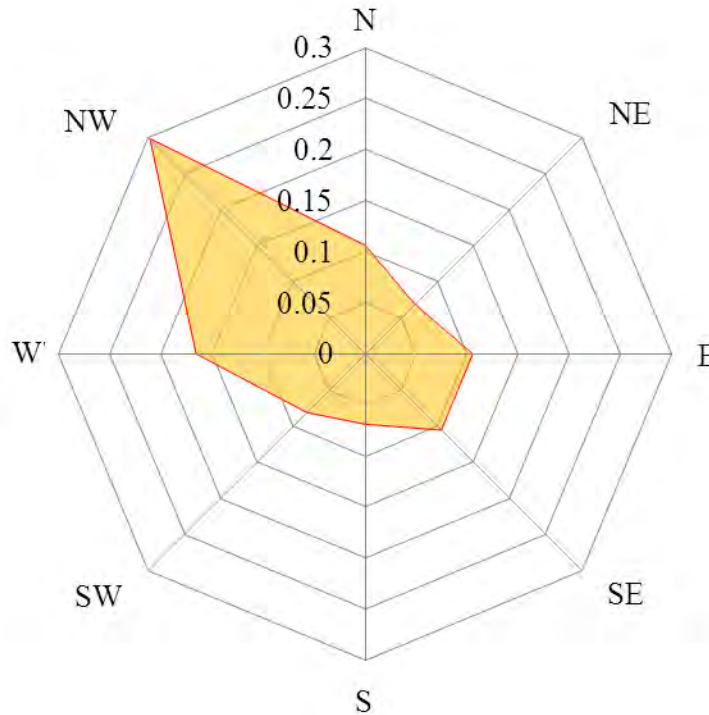


Figure 7.5 Wind direction frequencies at Experimental Feature site

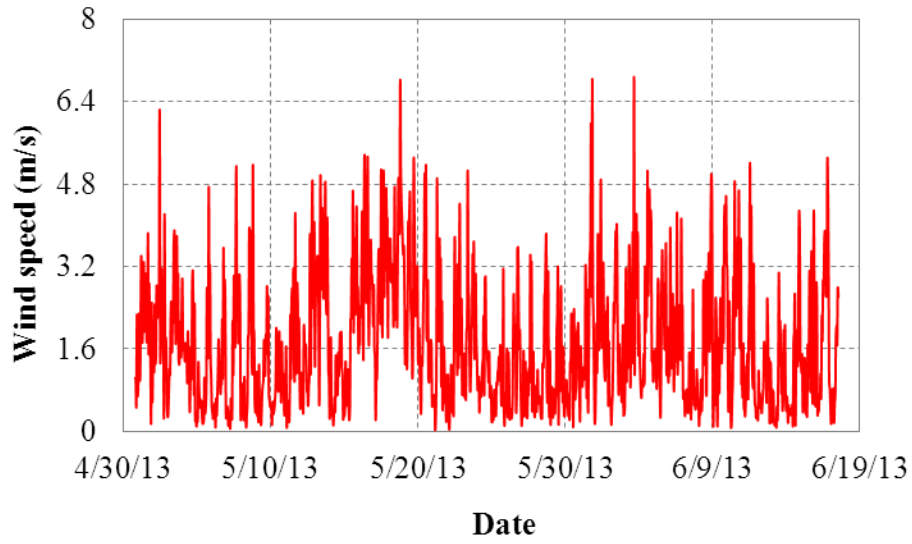


Figure 7.6 Wind speed at Experimental Feature site

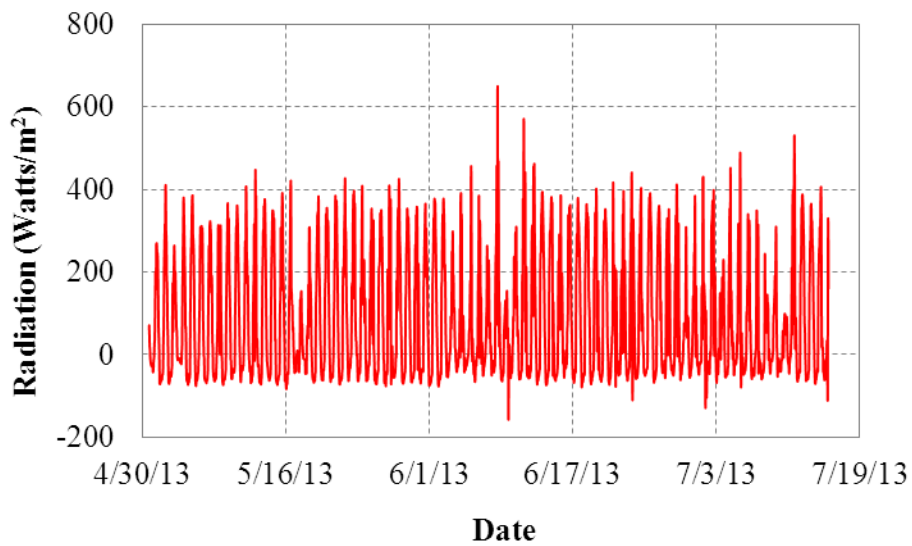


Figure 7.7 Incident solar radiation received at Experimental Feature site

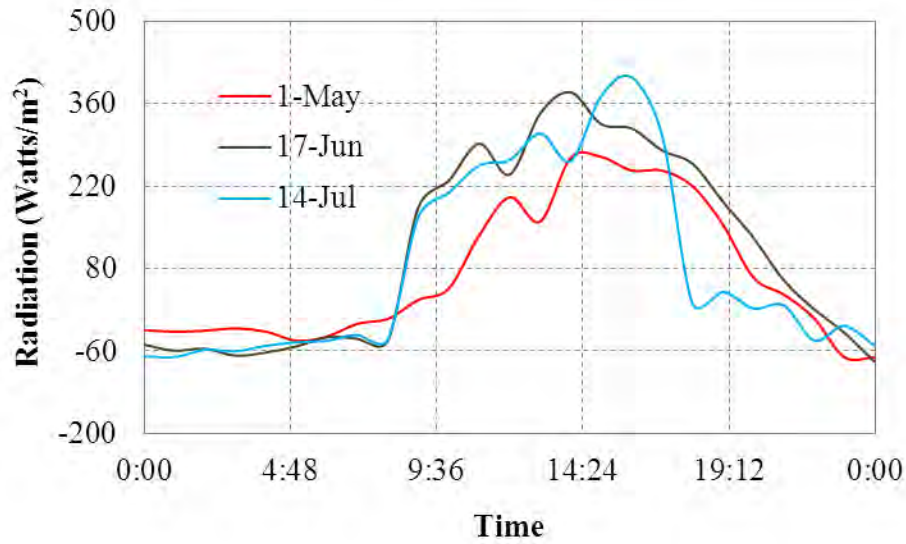


Figure 7.8 Incident solar radiation at Experimental Feature site on three different days

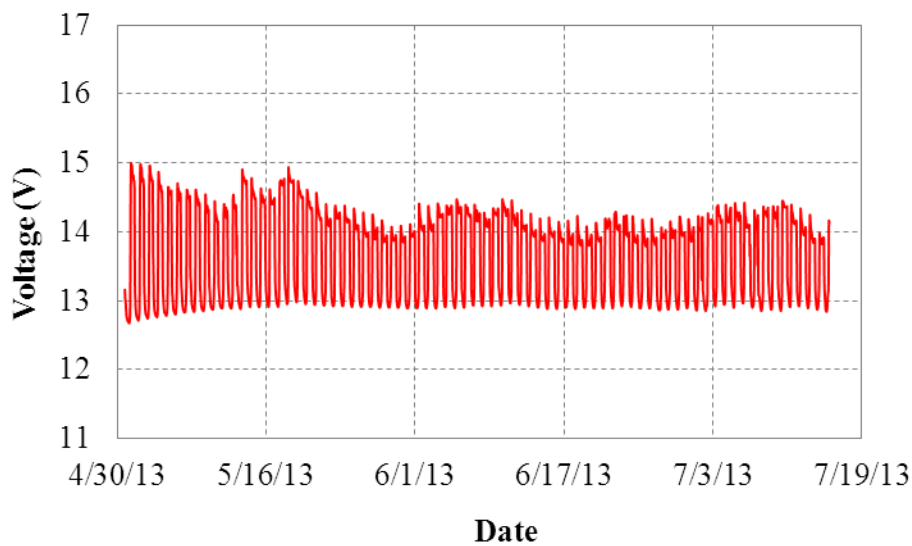
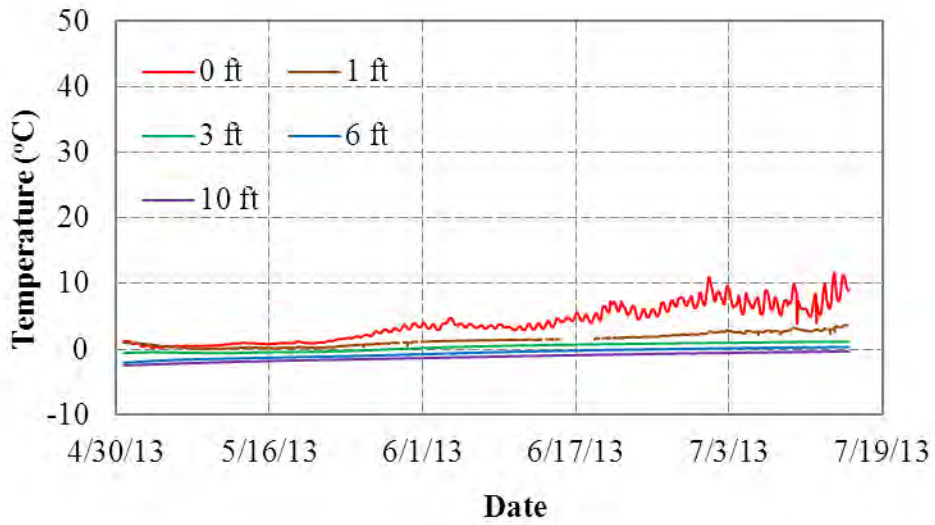


Figure 7.9 Battery output voltage at Experimental Feature site

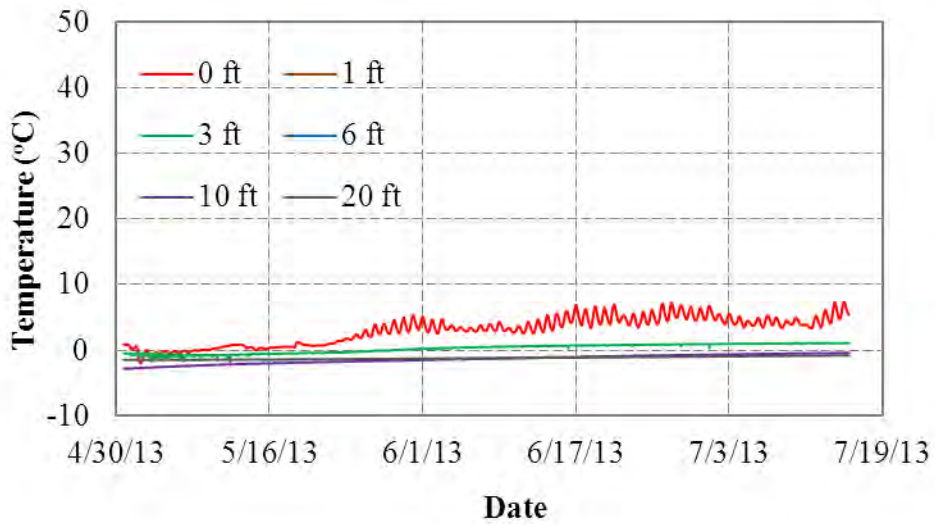
Temperature Changes in the Test Section

Figure 7.10 shows the temperature changes at the bottom, middle, and top of the Section A slope (wood chips) at different depths (0, 1, 3, 6, 10, and 20 ft). Temperature variations at different depths are presented in different colors. As indicated in Chapter 3, the maximum sensor depth, perpendicular to the slope face, is 10 ft for the sensor strings at the top and bottom of the slope

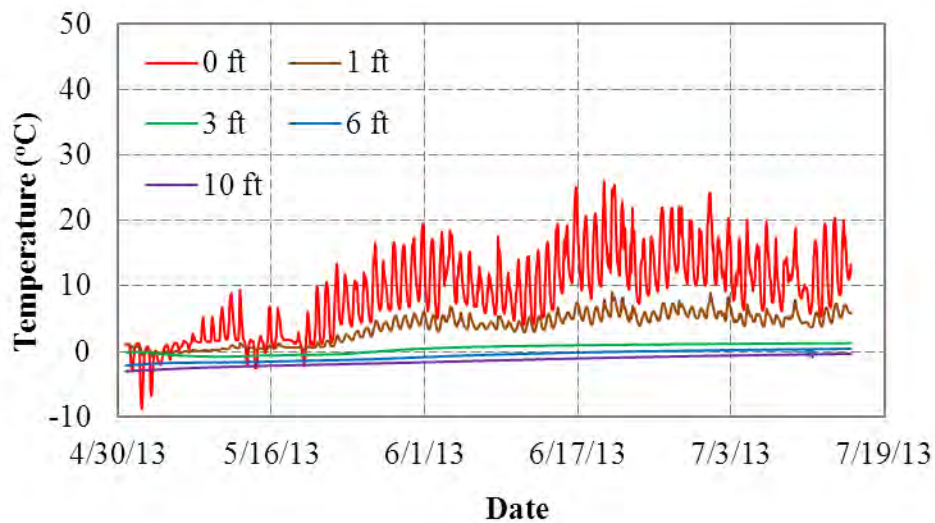
face for all four sections. The maximum depth for the sensor string at the middle of the slope for all sections is 20 ft. At the middle of Section A, no temperature data was obtained from sensors at depths of 1 and 6 feet due to malfunctioning.



(a) Bottom



(b) Middle

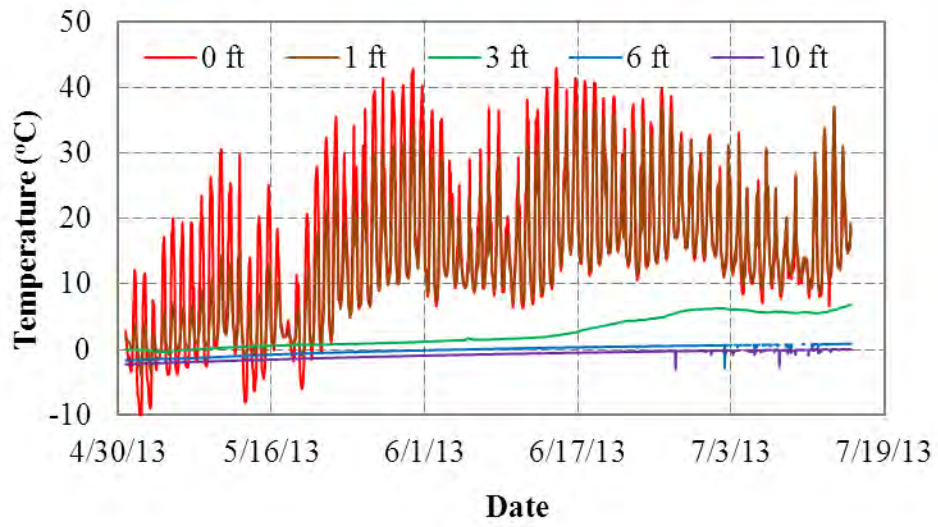


(c) Top

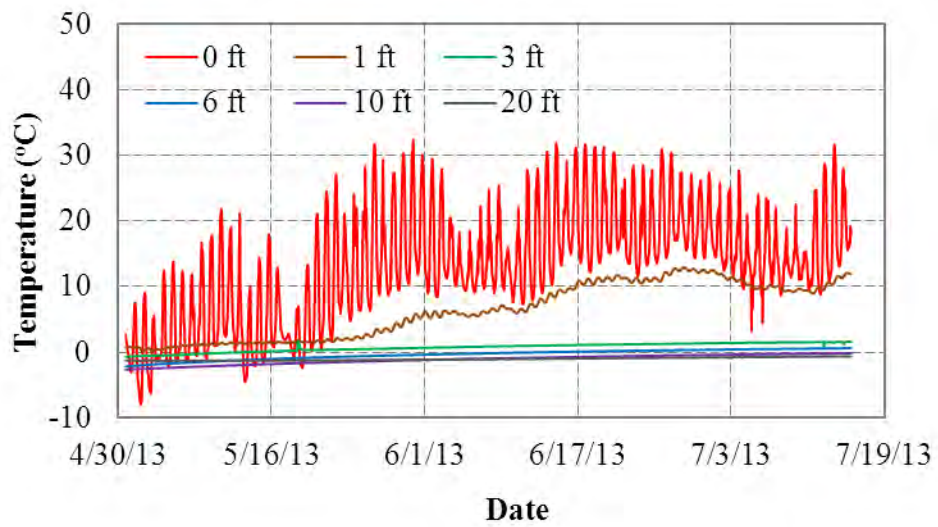
Figure 7.10 Temperature variations in Section A

Figure 7.10 indicates that temperatures increased throughout the monitoring period at all depths within Section A. Close to the slope face, temperature variations were controlled by daily air temperature variations even though one foot of wood chips covered the slope surface. Soil temperatures at deeper locations were lower and varied less with time. Temperatures at various depths, according to the sensor string at the upper part of the slope, were higher than temperatures measured by the strings further down the slope. This is because the wood chips were not evenly distributed on this section. The lower part of the slope (Figure 7.10a) was covered with more wood chips than that at the top (Figure 7.10c), and the chips worked as an insulation which protected the slope from air temperature changes. At the start of the monitoring period (the first week after construction), temperatures close the ground surface slightly decreased because the new cut slope surface was exposed to low ambient air temperatures early on. Seasonally warming air temperatures soon produced warming soil temperatures on and under the slope surface.

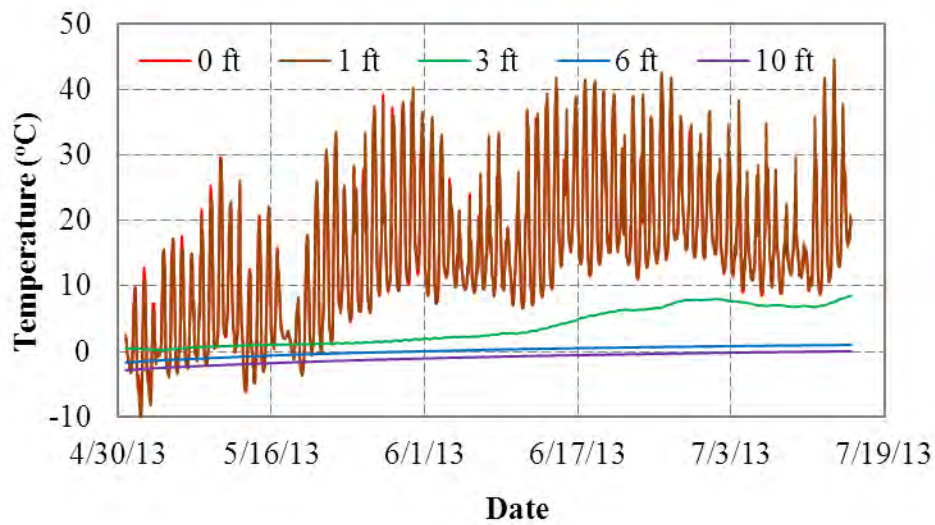
Figure 7.11 shows the temperature changes at the bottom, middle, and top of Section B (coconut blanket) at different depths (0, 1, 3, 6, 10, and 20 ft). As for Section A, temperature variations at different depths are presented in different colors.



(a) bottom



(b) middle



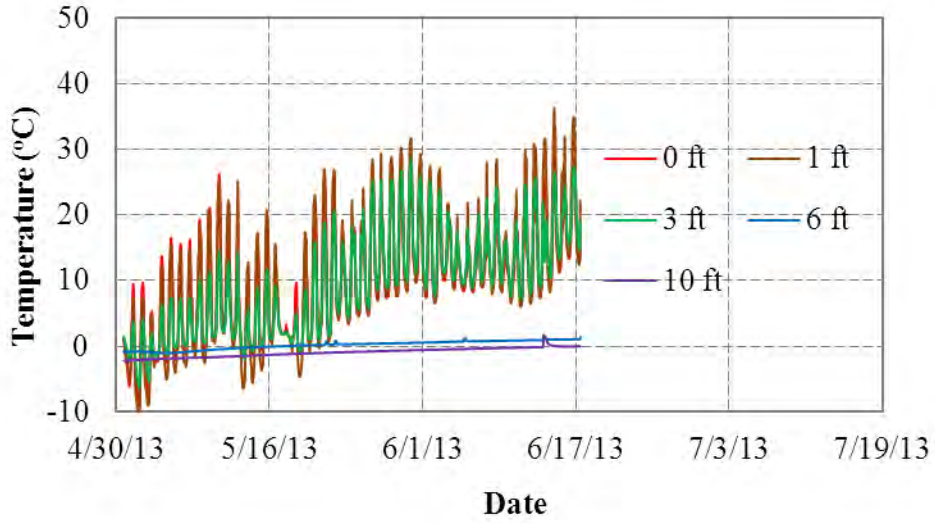
(c) top

Figure 7.11 Temperature variations in Section B

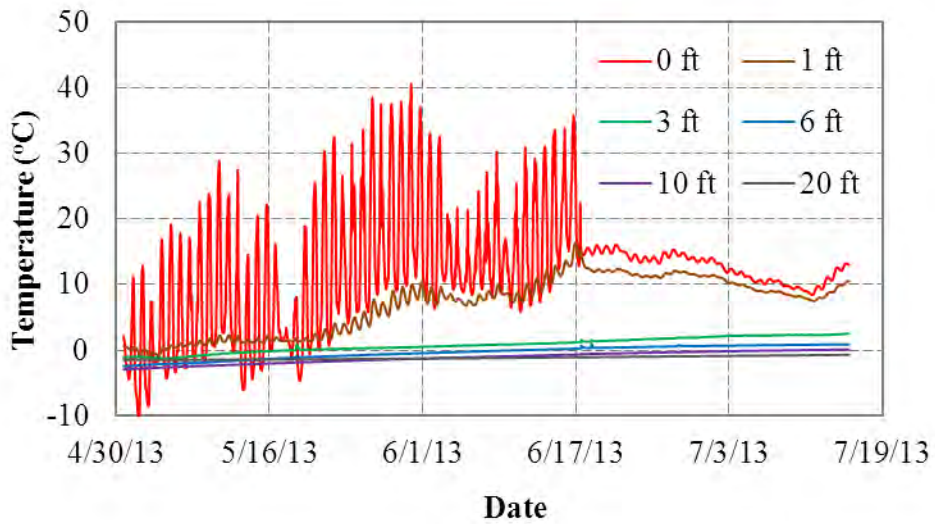
Similar to the temperature variation in Section A, due to the air temperature increase, temperatures increased throughout the monitoring period at different depths as can be seen in Figure 7.11. At the slope surface, the temperature changes closely followed the air temperature variation. Also, the temperature variations for the bottom, middle, and top of the section were consistent with one another due to the thickness uniformity of the coconut blanket except the temperatures at the middle with depth of 1 and 3 feet. At one foot below the slope surface in this section, especially for the temperatures at the top and bottom of this slope, the soil temperature changes closely followed the daily air temperature variation. Compared to the layer of wood chips, the coconut blanket (as expected) offered essentially no insulative benefit. Three feet below the slope surface of this section, soil temperature changes smoothly followed the long term increase in air temperature — in a much damped response compared to the soil at a one foot depth.

Figure 7.12 shows the temperature changes at the bottom, middle, and top of Section C (Tecco-mesh + coconut blanket) at different depths (0, 1, 3, 6, 10, and 20 ft). Temperature variations at different depths are presented in different colors. Due to thaw-related slope failures in this section, the Tecco-mesh and coconut blanket were removed and replaced by crushed rock on June 17th, 2013. The crushed rock layer used for this purpose was of variable thickness due to

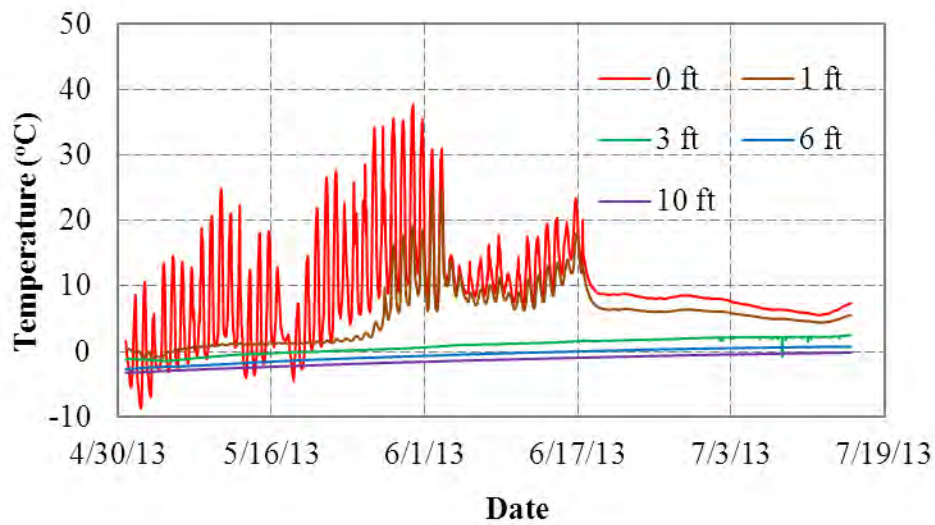
the uneven surface of the damaged slope. The thickness of the rock blanket ranged from about one to three feet. All temperature sensors located at the bottom of Section C stopped working after the June 17th repair work.



(a) Bottom



(b) Middle

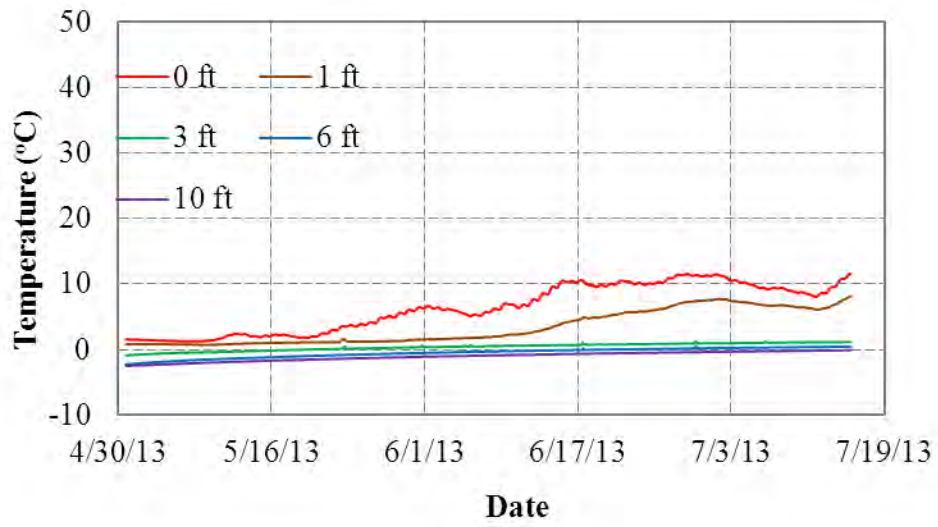


(c) Top

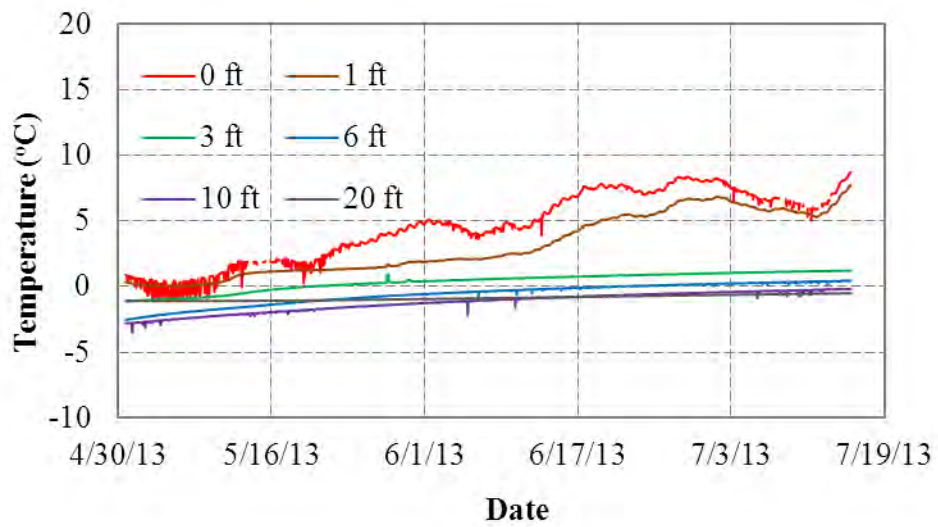
Figure 7.12 Temperature variations in Section C

Before the major repair work on June 17th, 2013, temperature variations within Section C were generally similar to those of Sections A and B as seen in Figure 7.12. Due to the air temperature increase, soil temperatures increased throughout the monitoring period at different depths. At the slope surface and one foot below, temperatures followed the daily air temperature variation. Compared to the wood chip section (Section A), the coconut blanket together with the Teccomesh offered essentially no insulative benefit as expected. After the replacement of the Teccomesh and coconut blanket with a rock blanket, temperature sensors at the original slope surface and originally one foot below indicated that a period of cooling occurred. No such period of cooling was seen in Sections A or B.

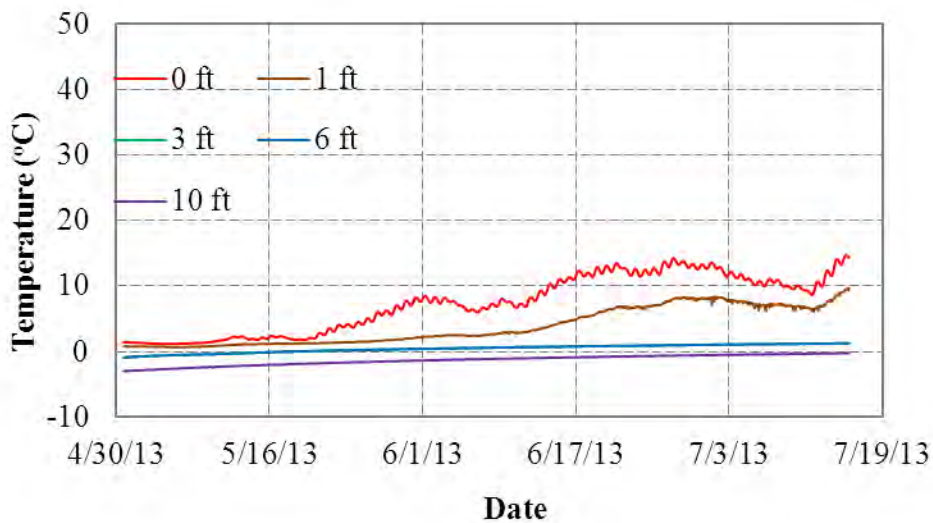
Figure 7.13 shows the temperature changes at the bottom, middle, and top of Section D (crushed rock) at different depths (0, 1, 3, 6, 10, and 20 ft). At the top of Section D, no temperature data was obtained from the sensor at 3 feet due to malfunctioning. Due to erosion in Section D, associated with repairs and placement of crushed rock in Section C, more crushed rock was also placed in Section D.



(a) Bottom



(b) Middle



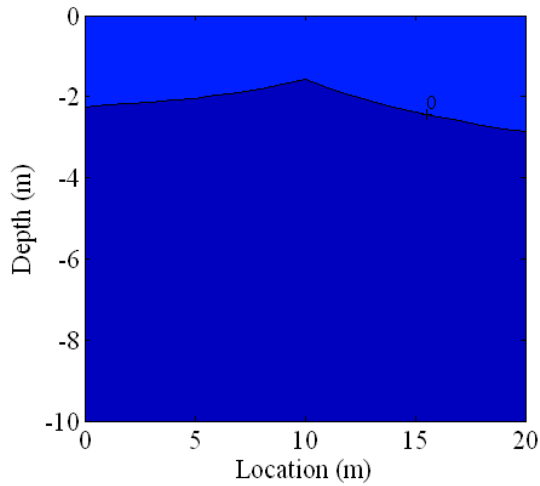
(c) Top

Figure 7.13 Temperature variations in Section D

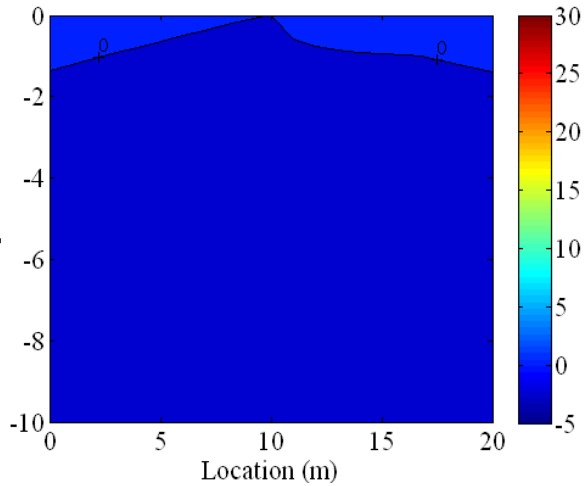
Figure 7.13 shows the soil temperature variations in Section D. Soil temperature variations at the original slope surface and one foot below follow the pattern as for Sections A through C except that the soil temperature response is damped by overlying rock blanket. At 3, 6, 10, and 20 feet below the slope surface, temperatures slightly increased throughout the measurement period. Figure 7.13 indicates that soil 10 feet or more below the original slope surface remained frozen throughout the monitoring period reported here. Sensors installed above the 10 foot depth in Section D indicated thawing with time.

Besides the temperature variations with time at individual slope locations, temperature contours at different times in degree Celsius for four sections were presented in Figures 7.14 to 7.17. Each plot provides soil temperature contours for a specific date, interpreted from the temperature sensor data recorded on that date. Each plot provides a “map” of isothermal contours of soil temperatures at various depths from the bottom of the slope (left side of plot) to the top of the slope (right side of plot) for the indicated date. For Section A shown in Figure 7.14, the isotherms were approximately parallel to the slope surface right after the construction on April 30th, 2013. Also, the temperature gradient was almost evenly distributed with depth. However, after construction, the temperature varied dramatically within 1 to 2 ft below the slope surface. The maximum temperature variation was found to be at the top of the section. The possible

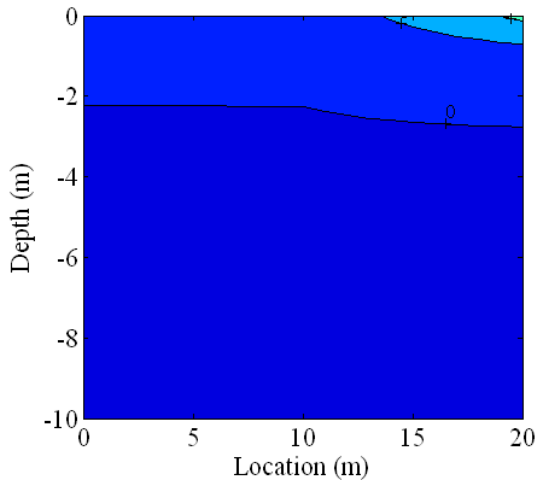
reason was discussed previously, i.e., the wood chip thickness was greater at the bottom than at the top of the slope. In Section B, as shown in Figure 7.15, one finds that the temperature varied dramatically within 3 to 4 ft of the slope surface. A comparison of Figures 7.14 and 7.15 strikingly illustrates the fact that the single-layer coconut blanket provided essentially no thermal protection for the frozen cut slope soils compared with one foot of wood chips. Basically, the isothermal lines more or less parallel the slope face at the different times plotted. In Section C, as shown in Figure 7.16, isothermal lines were at an angle to the slope surface which is different from the other sections. The bottom of the slope within Section C, the Tecco-mesh section, was warming much faster than at the top of the slope for reasons that are as yet unknown. Due to construction for the Section C slope protection replacement on June 17th, temperature sensors at the bottom of the slope unfortunately stopped working. Thus, after that date, temperature information for defining a 3-point isotherm was not available and Figures 7.16 e and f only presented half of the isotherm lines. Soil temperatures for Section D are presented in Figure 7.17. Until late May, the bottom of the slope was experiencing more rapid warming than upper portions of the slope. This accentuated warming at the bottom of the slope was similar to but not as severe as in Section C. Penetration of the thaw front within this section appears to have been somewhat slowed by the additional rock placed in Section D during the Section C repairs.



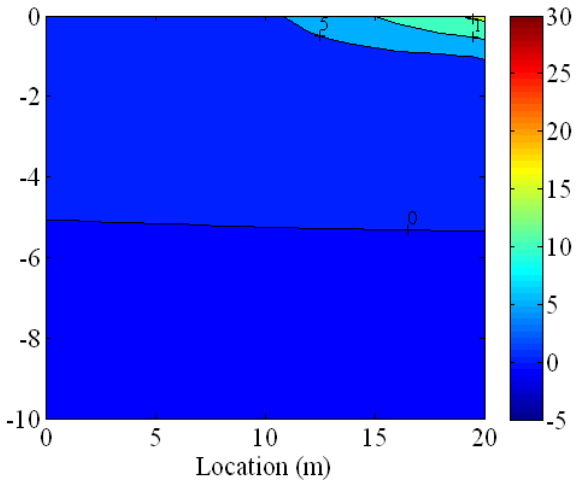
(a) At 7:00 pm on April 30th, 2013



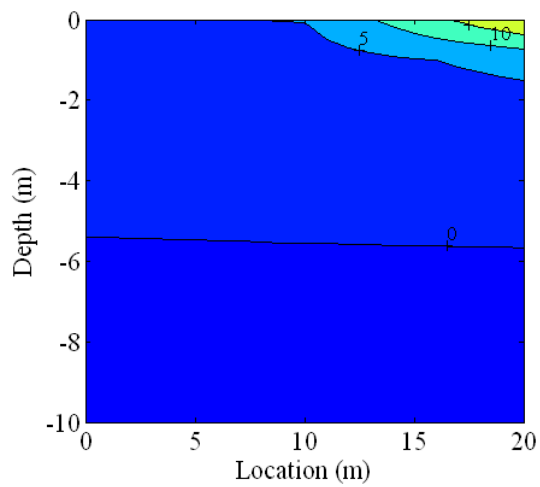
(b) At 7:00 pm on May 8th, 2013



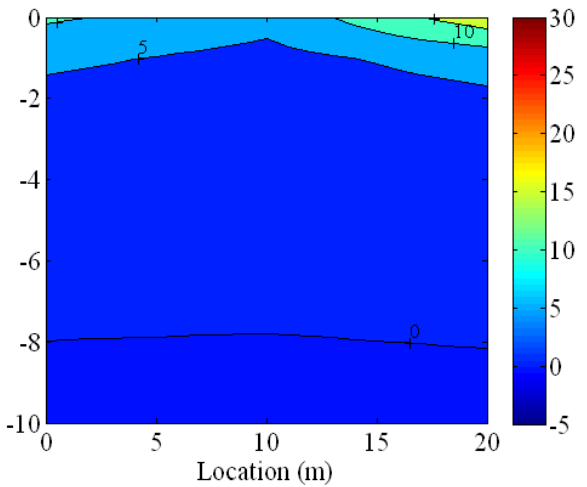
(c) At 7:00 pm on May 23th, 2013



(d) At 7:00 pm on June 13th, 2013



(e) At 7:00 pm on June 17th, 2013



(f) At 7:00 pm on July 14th, 2013

Figure 7.14 Temperature contours at different times in Section A

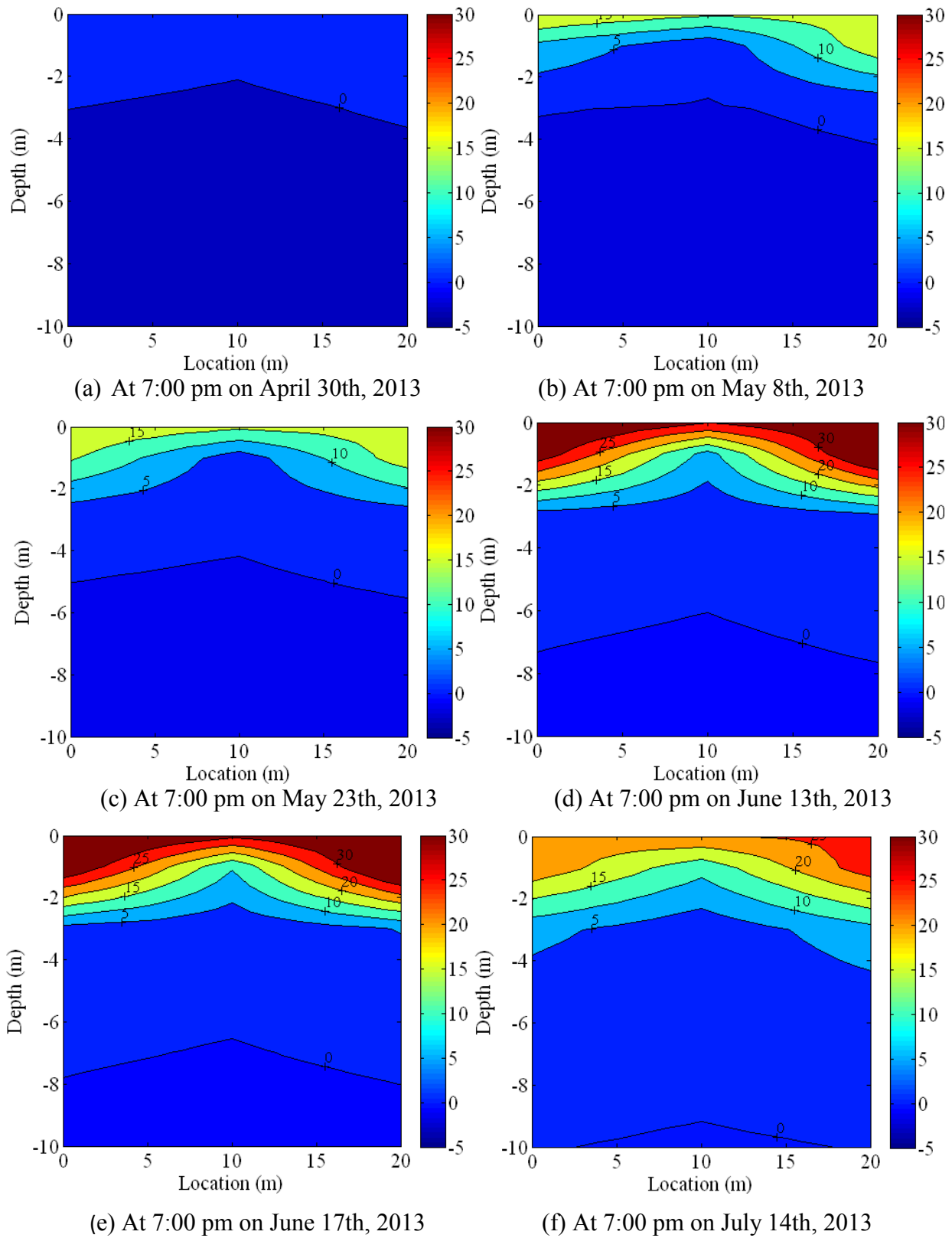
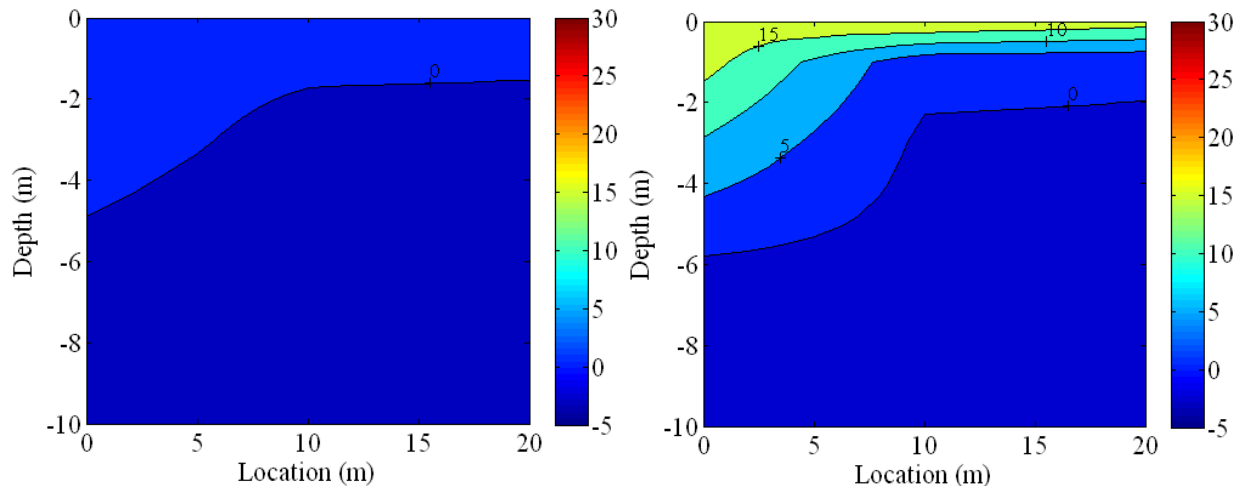
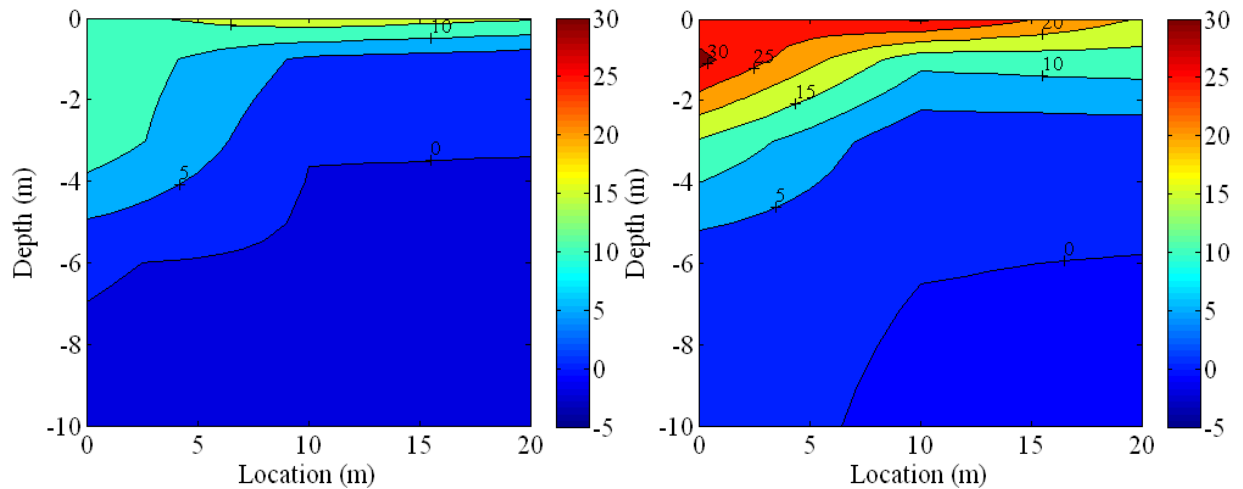


Figure 7.15 Temperature contour at different times in Section B



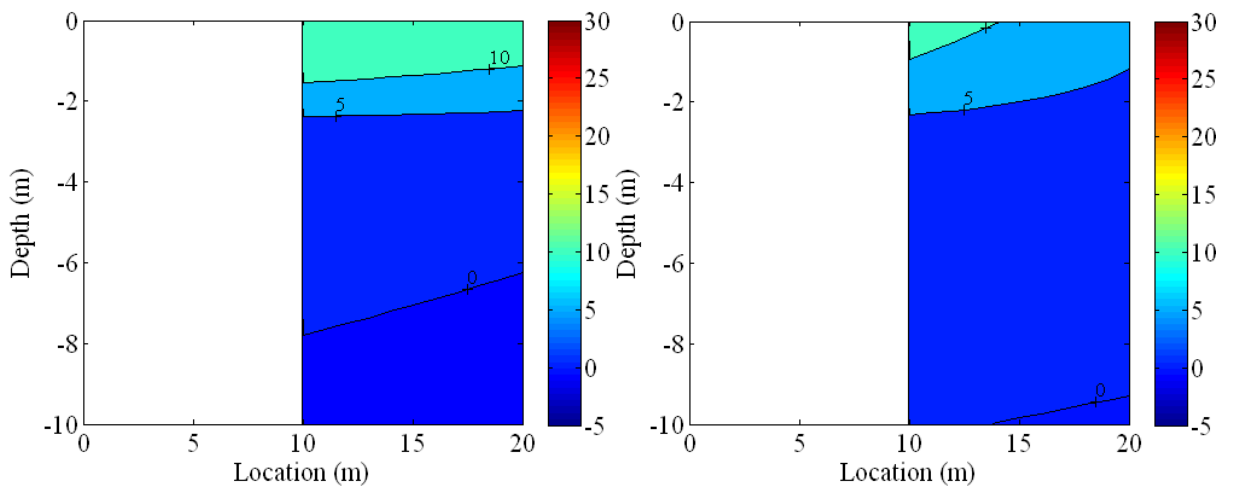
(a) At 7:00 pm on April 30th, 2013

(b) At 7:00 pm on May 8th, 2013



(c) At 7:00 pm on May 23th, 2013

(d) At 7:00 pm on June 13th, 2013



(e) At 7:00 pm on June 17th, 2013

(f) At 7:00 pm on July 14th, 2013

Figure 7.16 Temperature contour at different times in Section C

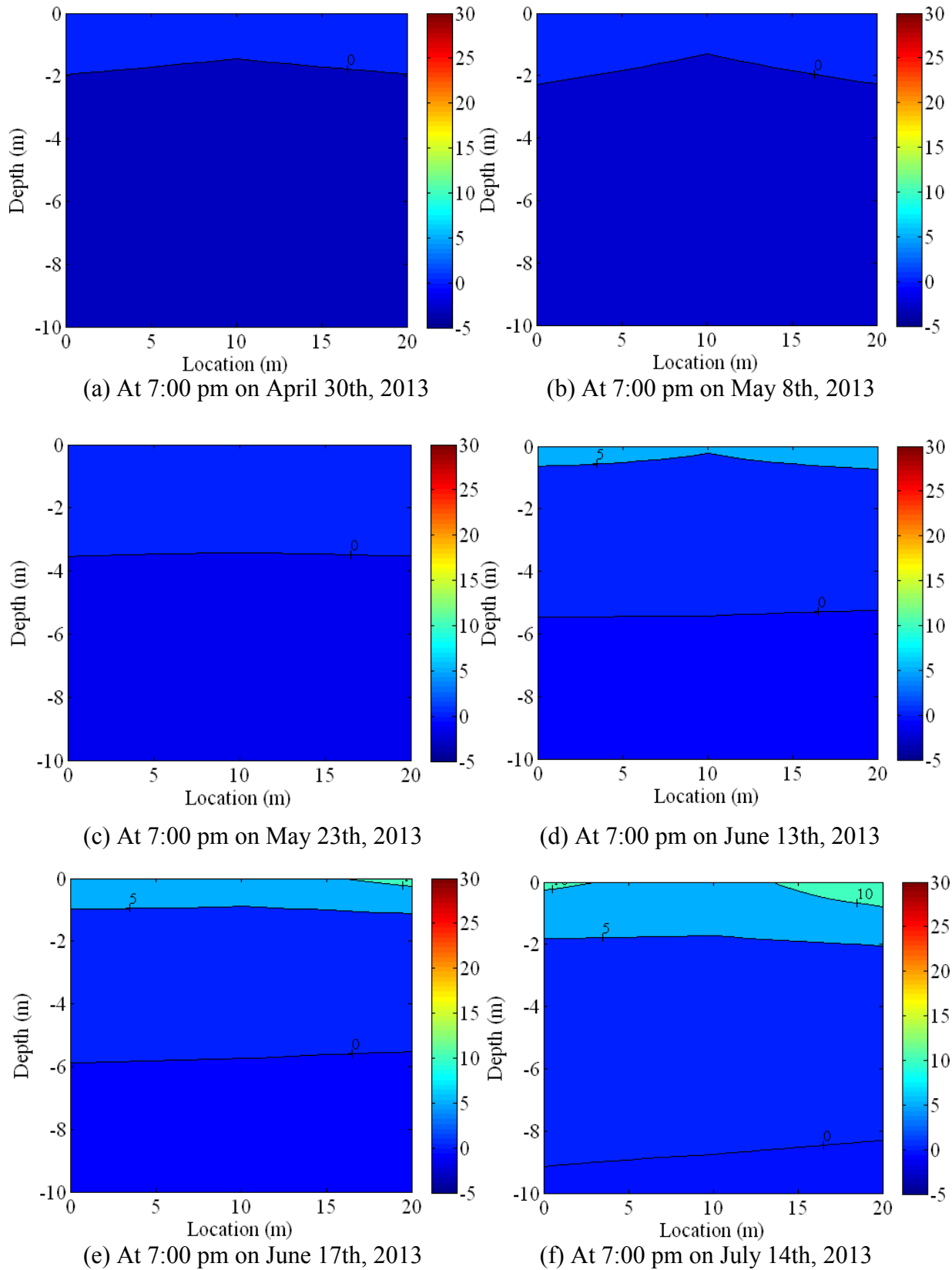


Figure 7.17 Temperature contour at different times in Section D

Moisture Changes in the Test Section

In this project, all volumetric moisture content sensors (TDR) were placed at the slope surface. Moisture content variations throughout the measurement period were recorded and presented in Figures 7.18 to 7.21. Figure 7.18 shows the volumetric moisture content changes for the TDR sensors at the slope surface in Section A (wood chips) which is located at the left side of the cut slope. Only one of the three sensors in Section A was functional throughout the measurement period. Shortly after construction the volumetric moisture content decreased slightly and then stabilized for about two weeks. This minor desiccation was probably associated with the exposure of the slope face to air circulation during construction, for a period of time before the wood chips were placed. Beginning in late May, the moisture content gradually increased from approximately 10% to 18% percent due to the air temperature increase which resulted in melting of ice in the slope. The volumetric moisture content continued to increase during the period of data acquisition. For sections B and C, volumetric moisture contents continually increased to 20% to 50% on May 25th, 2013, after which it became fairly stable. The stabilized volumetric moisture contents at the lower part of the cut slope were higher than at the upper part, likely due to drainage of water down the slope face. For Section D (crushed rock) the volumetric moisture contents stabilized at approximately 50% at the beginning of June which is one to two weeks later than in Sections B and C. Even though only one data point is available for Section A, it appears that the longer moisture stabilization times for Sections A and D may be supporting the temperature-based observation that the wood chips and rock blanket are thermally superior to the treatments used in Sections B and C. Along the same line of thought, Section A's wood chip treatment would appear to provide better thermal protection than Section D's rock blanket during the mid-months of summer 2013.

Before leaving this subject it is necessary to comment briefly on a very positive characteristic of certain rock blankets. The authors do realize and acknowledge that a rock blanket of sufficient thickness and permeability has the potential to significantly cool underlying soils during the winter season via convective heat transport. If properly designed, such a rock blanket can more than compensate for its lack of summertime insulation value by its considerable wintertime heat extraction.

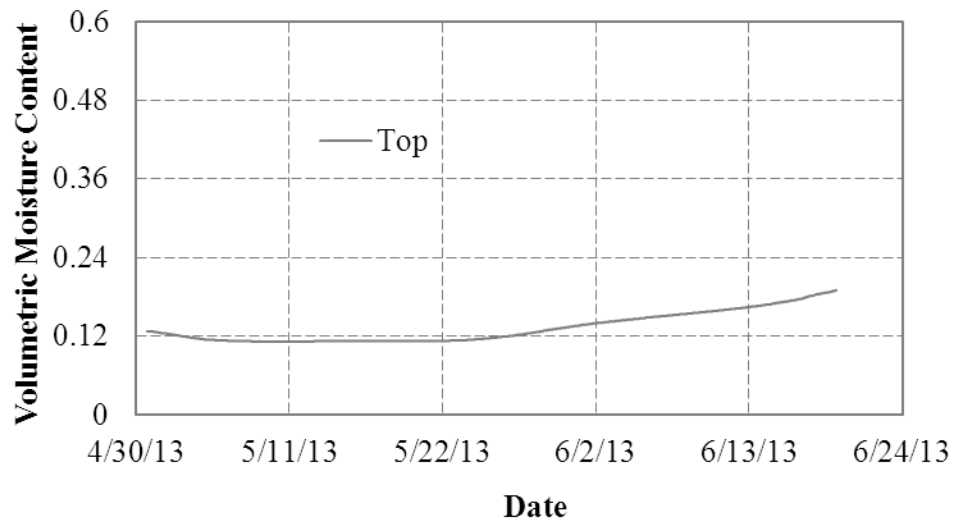


Figure 7.18 Volumetric moisture content variations in Section A

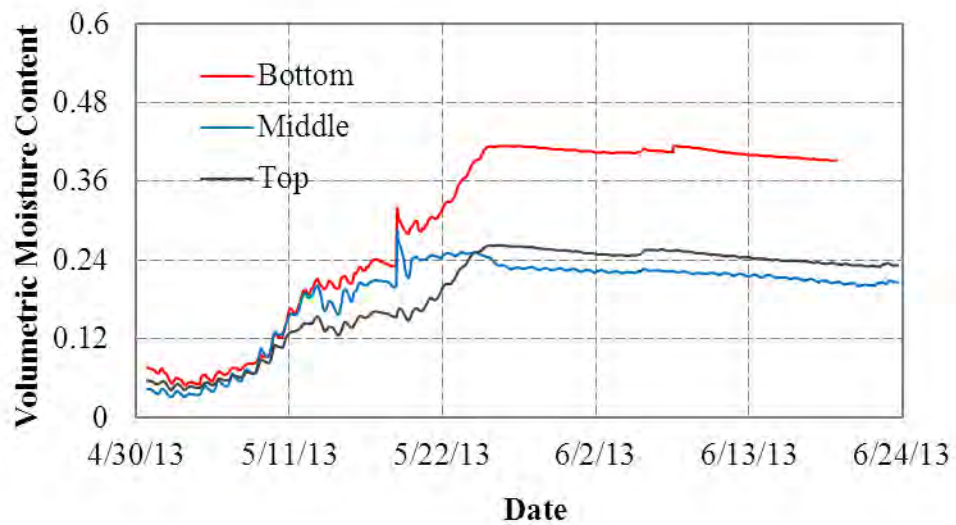


Figure 7.19 Volumetric moisture content variations in Section B

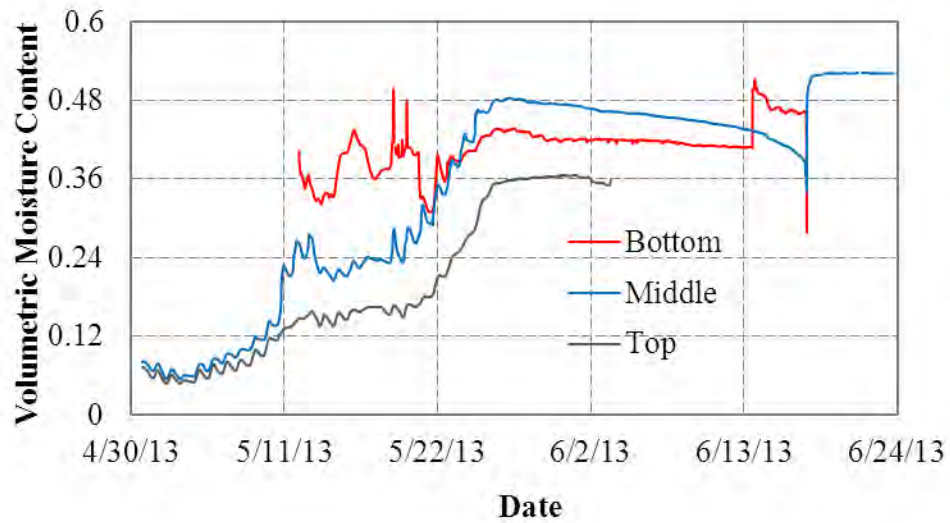


Figure 7.20 Volumetric moisture content variations in Section C

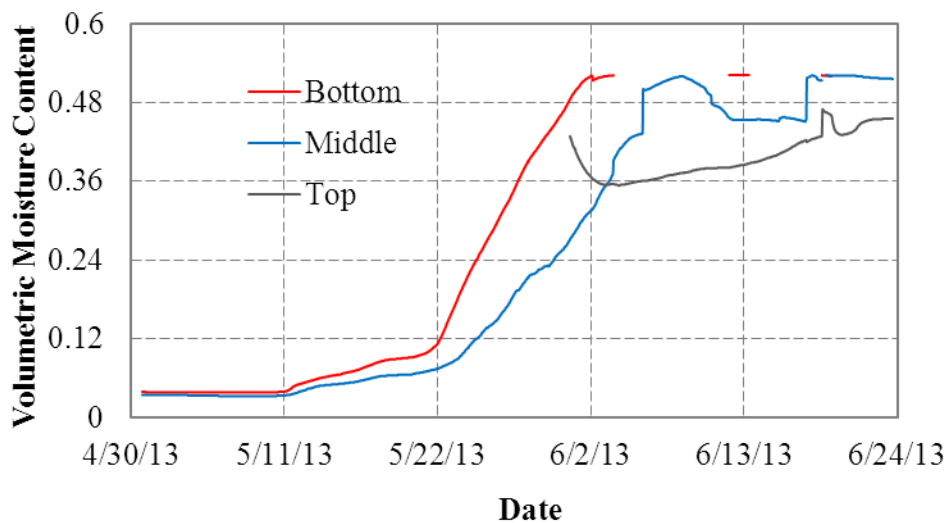


Figure 7.21 Volumetric moisture content variations in Section D

Photogrammetric Erosion Monitoring

Nowadays, rapid developments in digital camera technology and low-budget photogrammetric software products mean that standard, consumer-grade cameras may be a viable option for photogrammetric measurements. To perform the erosion measurement using photogrammetric methods, a digital camera was required to obtain the photos. To reach a high level of accuracy, a digital single-lens reflex camera with a fixed focal length lens was needed. Before being used for

erosion measurement, the used camera was required to be calibrated. For a single measurement, several images of the cut slope were captured for photogrammetric analysis. Then, a 3D point cloud, which indicated the 3D position of the slope surface, was generated. Based upon the movement of the slope surface, the erosion could be calculated. Principle of photogrammetry and detailed information on erosion measurement are presented in Appendix A.

On April 26th, after construction on the Section A slope, the volume of this section, above the reference x-y plane, was measured using the photogrammetric method previous explained. The difference between the volume measured on April 26th and volumes measured on subsequent dates indicates the cumulative volume gains or losses along the face of Section A with time. Volume losses were interpreted as a loss of material through surface erosion or thaw-settlement. Volume gains were interpreted as an increase in surface cover whether by vegetation of other materials.

A record of the cumulative surface volume changes for Section A between April 26th and September 27th, 2013 is shown in Figure 7.22. In Figure 7.22, volume changes are indicated on various dates between April 26th and September 27th, 2013. A volume increase relative to the slope face condition on April 26th is shown as a positive value in the figure. A volume decrease relative to April 26th would be shown as a negative value in the Figure 7.22. Figures 7.23 and 7.24 are photos of Section A on April 26th and April 30th, respectively. Figure 7.22 indicates that the volume along the Section A slope face actually increased (varying between 8 and 12 m³) during this period. Part of the increase is because additional wood chips were applied over Section A after April 26th. Another reason is the light snow cover on Section A that was added between April 26th and 30th. After April 30th, there were small fluctuations in the volume of material added to the surface of Section A. These fluctuations are attributed to animal activity on the slope. Observation of this section identified no significant erosion throughout the 2013 monitoring period. This is indicated by the excellent condition of the slope on September 27th indicated in the Figure 7.25 photo.

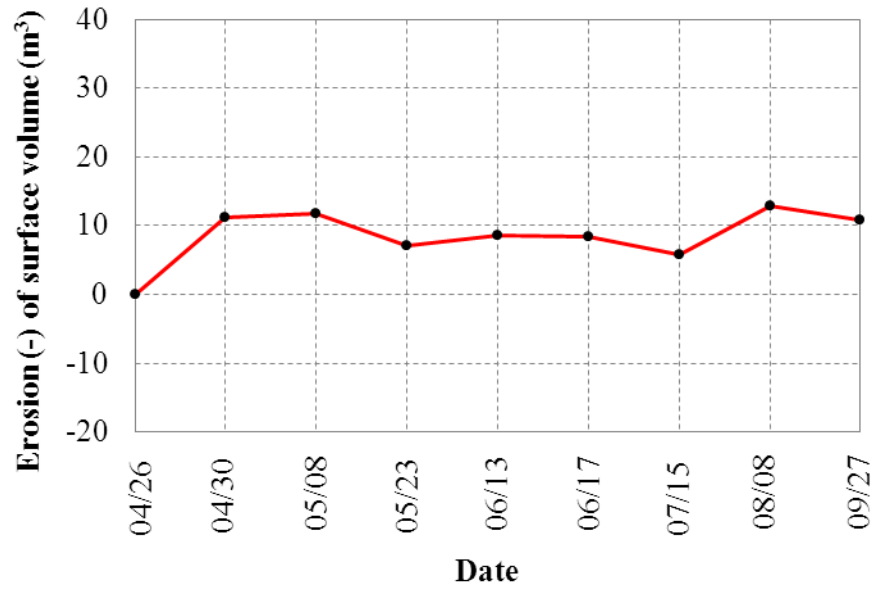


Figure 7.22 Erosion on Section A



Figure 7.23 Section A after construction on April 26th, 2013



Figure 7.24 Section A with more wood chips on April 30th, 2013



Figure 7.25 Section A with more wood chips on September 27th, 2013

Similar to Section A, no erosion on Section B (the coconut blanket section) was observed which is consistent with the photogrammetric erosion measurement results shown in Figure 7.26. Before June 17th, the volume change on the surface of Section B was not significant. Figure 7.27 presents a picture of this section on June 17th prior to the rapid growth of grass on the slope surface. However, after June 17th, significant grass growth on this section was observed. This is

shown in Figures 7.28 and 7.29 which are photos of this section captured on July 15th and August 8th respectively. Figure 7.30 is a photo showing the surface of Section B on September 27th. This fall-time photo shows that the grass has wilted. This wilting process was detected as a surface volume loss during the fall season and is shown in Figure 7.30.

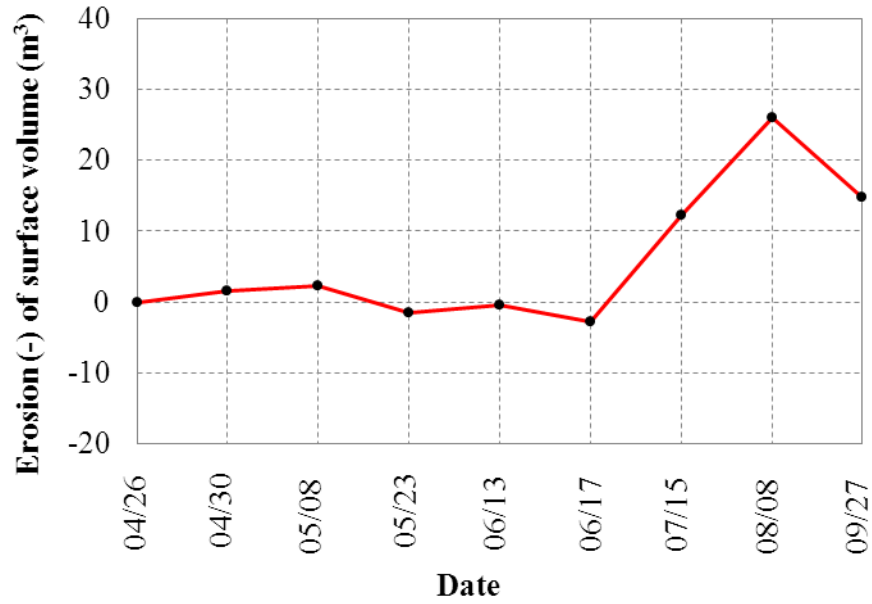


Figure 7.26 Erosion on Section B



Figure 7.27 Section B on June 17th, 2013



Figure 7.28 Section B on July 15th, 2013



Figure 7.29 Section B on August 8th, 2013



Figure 7.30 Section B on September 27th, 2013

As discussed previously, massive ground ice was found in Sections C and D. Erosion within these two sections was much greater than anything observed in Sections A and B. Figure 7.31 provides a very misleading record of the total surface volume changes for Section C (Tecco-mesh + coconut blanket) because the photogrammetric process was only able to discern changes at the surface of the Tecco-mesh instead of the underlying soil surface. At the beginning of the

photogrammetric record, April 26th, measurements indicated a small surface volume increase due to the snow cover shown in Figure 7.32. During the period between about April 30th and June 13th a rather large volume of icy soil (and massive ice) materials, originally located beneath the Tecco-mesh slope cover, were lost to runoff and thaw-consolidation. Photogrammetric measurements, as indicated in Figure 7.31, keyed on the surface of the Tecco-mesh, and therefore provided no indication of the volume loss that was occurring under the Tecco-mesh. Figure 7.33 shows obvious signs of the actual condition of the cut slope face under the Tecco-mesh by June 13th. Obviously, the deterioration process of the cut slope face under the Tecco-mesh was not detected by the photogrammetric process! On June 17th, the Tecco-mesh and coconut blanket on this section were removed and replaced by crushed rock as shown in Figure 7.34. This significant slope surface volume change (due to the added crushed rock) was captured by the subsequent set of photogrammetric measurements, and is indicated on the right hand side of Figure 7.31. Figure 7.35 shows the appearance of Section C on September 27th, the end of the monitoring period for this report. Figure 7.31 indicates than an attenuation of thaw-related volume change was occurring in Section C prior to the September 27th date.

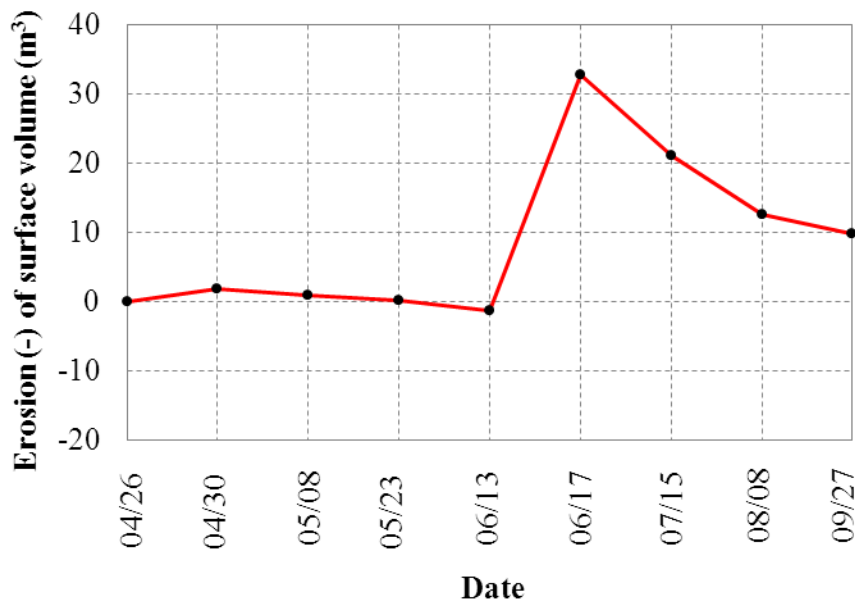


Figure 7.31 Erosion on Section C



Figure 7.32 Section C on April 30th, 2013



Figure 7.33 Section C on June 13th, 2013



Figure 7.34 Section C on June 17th, 2013



Figure 7.35 Section C on September 27th, 2013

Section D (originally constructed with a crushed rock blanket) serves as the control section for the Experimental Feature. Figure 7.36 indicates that a more or less continual loss of slope surface volume has occurred through September 27th. The initial small volume increase at the surface of Section D was because of the late April snowfall shown in the Figure 7.37 photo. Loss of surface

volume (through erosion and/or thaw-consolidation) continued through June 13th. Figure 7.38 shows the condition of the slope face on June 13th. Then, on June 17th, a volume of rock material was added to the surface of Section D during Section C repairs (also see the Figure 7.39 photo). The immediate surface volume increase due to this addition of material in Section D is plotted in Figure 7.36. After placement of additional crushed rock on June 17th, the loss of surface volume continued through the end of the monitoring period for this report on September 27th. The condition of the slope at that time is shown by the Figure 7.40 photo. Figure 7.36 indicates that the surface volume loss rate for Section D had not much attenuated prior to September 27th, 2013.

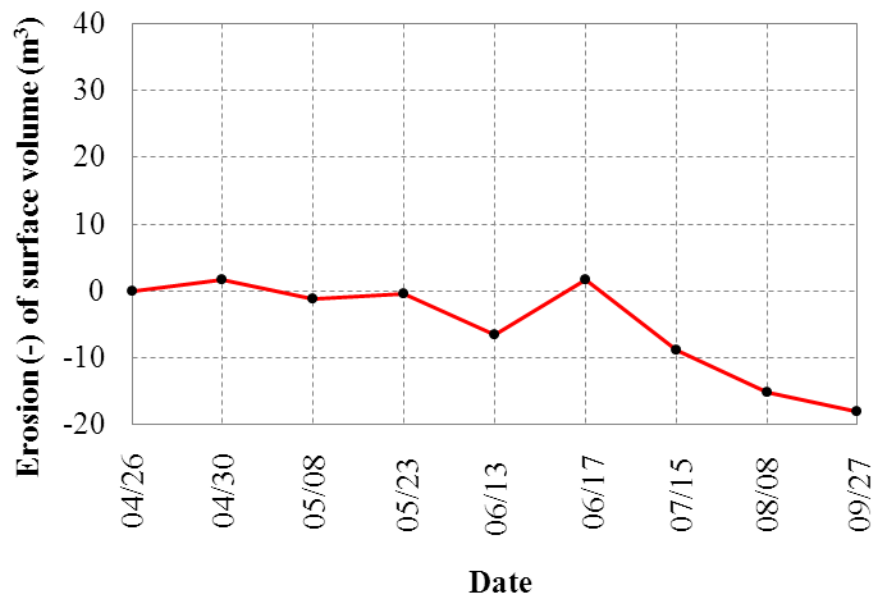


Figure 7.36 Erosion on Section D



Figure 7.37 Section D on April 30th, 2013



Figure 7.38 Section C on June 13th, 2013



Figure 7.39 Section C on June 17th, 2013



Figure 7.40 Section C on September 27th, 2013

CHAPTER 8. CONCLUSIONS AND RECOMMENDATIONS

This report focuses on the design, construction, and initial performance of an Experimental Feature located at approximately Mile Post 10 of Alaska's Dalton Highway. The Experimental Feature examines three methods for protecting a permafrost cut slope, exposed during a highway construction project, in an environmentally acceptable, permanent way. The Experimental Feature also incorporates a fourth slope protection design. This is a control section where the frozen cut slope surface is treated using the standard-design rock blanket intended for protecting permafrost cut slopes in all other areas of the construction project. The Experimental Feature project is introduced in Chapter 1. Chapter 2 reports on the review of pertinent literature conducted during an early phase of this study. The design and construction of the four slope treatments is discussed in Chapters 3 and 4 of this report. The four forms of slope treatment addressed in this report include:

Section A, incorporating a wood chip slope treatment,

Section B, incorporating standard-type coconut mat slope treatment,

Section C, incorporating a mechanically robust slope surface treatment of Tecco-mesh underlain by coconut matting, and

Section D, the control section, incorporating a rock blanket treatment on the cut slope.

Conclusions Specific to the Experimental Feature

The following points summarize some of the research findings to date. This incorporates recommendations regarding the ice-rich cut slope protection methods garnered from the research work thus far:

1. The performance of each slope protection method was heavily dependent on the ice content in area of the slope where that particular protection method was used. In Sections B and C, same coconut blanket was used to cover the slope surface. However, about one and a half months after the construction, Section C failed due to thermal erosion. No such erosion was found on Section B. The drastic difference in performance is considered mainly due to the presence of the massive ground ice in Section C. The construction

process exposed large areas where the presence of massive ice was obvious. And of course the exposed ice was immediately subjected to air and solar warming. Even though the coconut blanket and Tecco-mesh were soon placed on the thawing surface, these layers provided little thermal protection. It is assumed that air spaces that quickly developed between the Tecco-mesh and the soil surface retained pockets of still air warmed by solar heating of the overlying coconut blanket (a sort of “hot house” effect), thus adding more heat to the thawing soils. Another source of added heat is thought to have been the long steel anchor shafts which had been installed in the frozen soils. These shafts should have been excellent heat conductors.

2. The strong, anchored Tecco-mesh survived intact during the soil thawing process that was occurring beneath it. Just prior to removal, the Tecco-mesh was simply providing a strong tent covering for the degrading soil surface, and was at some spots seen to be suspended several feet above that surface. The Tecco-mesh did not protect the ice-rich slope that contained massive ice inclusions. Once the ice-rich permafrost in the slope thawed, a large quantity of the fully saturated silty soil behaved like mud and flowed out from under the very robust and intact tent of strongly suspended Tecco-mesh. The Tecco-mesh itself did not fail, but it did nothing to hold the saturated silty soil in place. **It is stressed here that there were absolutely no problems with the Tecco-mesh material itself per se. This was simply an experimental application of Tecco-mesh for which it was not suited.**
3. In Section D, crushed rock was used to protect the slope. Due to massive ground ice which was detected during construction, obvious thermal erosion was also found in this section even though 1 ft crushed rock was used. However, temperatures in this section were generally lower than that in Section C. Also, erosion in Section D was less compared with Section C and was not problematic—even though Section D also contained much massive ice. The crushed rock treatment worked much better than the Section C treatment.
4. Wood chips were used to protect Section A. No significant erosion was identified in this section until the end of September. The temperature in this section was lower than Sections B and C, which indicated that wood chips worked better than coconut blanket

5. Photogrammetry offered a cost-effective way to monitor the changing topography of the ice-rich cut slope. To apply this photogrammetric method for such a purpose, stable control points were required to build the coordinate system. By comparing the exact locations of the slope surface at different times within a given period, the total volume of the erosion or surface accumulation during that period could be measured. Results from this study were consistent with previous research-related observations indicating that the measurement results were reliable.
6. It is recommended that long-term performance monitoring at the Experimental Feature site continue as long as the sensors and recording devices at the site remain functional.

Some Generalized Thoughts and Conclusions Pertinent to the Experimental Feature

As of this reporting, it is appropriate to finally offer some *informed conjecture* regarding the Experimental Feature based on observations of the Experimental Feature test sections themselves as well as the research team's many years of combined permafrost-related experience. In considering various methods for protecting permafrost cut slopes, it appears absolutely necessary, for any specific location, to identify and consider the morphology of the soil's frozen moisture content in addition to simply quantifying the moisture content of the frozen soil. More specifically, the question is whether the frozen moisture in the soil is uniformly dispersed throughout the soil or segregated into massive ice features (a much worse case). A standard drilling program geared to highway route exploration in Alaska will likely not provide enough information, prior to construction, to make this determination for a specific cut slope.

The case without massive ice — For example, freshly exposed cut slope soils known to have an average volumetric frozen moisture content of, say, 40 percent or higher might be treated in an environmentally acceptable way using a combination of standard slope protection matting and the rapid establishment of a dense grass cover — IF — the frozen moisture is evenly distributed throughout the soil. Given this “desirable” frozen soil type, such treatments need not necessarily prevent the permafrost from thawing. The treatment function is to retard the thaw process by virtue of shading and evapotranspiration offered by the surface vegetation while

armoring the surface against external sources of erosion (spring runoff, etc.). The result is that the cut slope generally remains stable while clean water is slowly released to the ditch during the thaw-consolidation process. However, even if the frozen soils exposed in the cut slope are found to be the “desirable” form of permafrost (having uniform ice distribution), there are as yet unresolved design issues. At some high level of frozen moisture content, the previously described slope protection method will not work. At some, as yet unknown, high frozen moisture content—and considering the local air / soil temperature regime—the soil will not thaw-consolidate in a stable manor during the thaw process. Such problems may be countered by some combination of lowering the slope angle and/or increasing the strength of the stabilization matting and density of vegetative covering, but such variables have not been systematically studied in Alaska.

The case with massive ice — Exposure of massive ice in a new cut slope poses a real problem! To date, including consideration of the Experimental Feature subject of this report, there seem to be four ways of contending with this problem.

1. Reroute the road to avoid cutting into massive ice—often economically or geographically impossible
2. Remove the massive ice—expensive, many unknowns, almost never attempted
3. Keep the massive ice frozen—except perhaps in some of the coldest areas of Alaska, requires installation of expensive passive refrigeration system or an active system with perpetual power supply
4. Cover the slope with a thick blanket of free-draining material—the subject Experimental Feature now contains three such installations including Section A (wood chip blanket per original design), and Section C (crushed rock blanket repair expedient), and Section D (the control section w/crushed rock blanket per original design)

As of this reporting, the option 4 blanket appears to provide a reasonably practical form of slope treatment where massive ice is involved. Such a blanket, composed of individual pieces of aggregate, wood chips, etc., has several desirable characteristics. The blanket material is easily placed against the cut slope face and may be relatively inexpensive on some projects. More important: the loose blanket cover will settle and stay in intimate contact with the slope face as it undergoes significant changes in shape during the time that the massive ice features are thawing.

In both the above cases it is assumed that the thawing process does not continue unabated forever. Eventually, the combined thickness of slope protection material (including vegetative covering) and the accumulating under-layer of thawed material becomes great enough that a practical level of thermal equilibrium is reached and the mature slope becomes reasonably thaw-stable.

REFERENCES

- Alyeska Pipeline Service Company. (1974). "Report on Thermal Erosion Test Sites, Hess Creek, Alaska (Phase I - July-August, 1973)." *Report Number TE-005*.
- Alyeska Pipeline Service Company. (1975). "Hess Creek Thermal Erosion Site - 1974 Evaluation." *Report Number TE-006*.
- Berg, R, and Smith, M. (1976). "Observations Along the Pipeline Haul Road Between Livengood and the Yukon River." *US Army CRREL Special Report 76-11*. Oct. 1976.
- Mageau, D.W. and Rooney, J.W. (1984). "Thermal erosion of cut slopes in ice-rich soil." FHWA-AK-RD-85-02 Final Report. Alaska Department of Transportation and Public Facilities. http://www.dot.state.ak.us/stwddes/research/assets/pdf/fhwa_ak_rd_85_02.pdf
- McHattie, R.L., and Vinson, T.S., 2008. Managing ice-rich permafrost exposed during construction. *Proceedings of the 9th International Conference on Permafrost*. University of Alaska Fairbanks, Fairbanks, U.S.A., pp. 1167–1172.
- Naviq Consulting Inc. and AMEC Earth & Environmental (2007). Monograph on the Norman Wells Pipeline Geotechnical Design and Performance -2006 Update. Geological Survey of Canada Open File 5702. Natural Resources Canada, Ottawa, Ontario, 214 p.
- Oswell, J.M. and J.R. Everts. (2008). Field trials of surface insulation materials for permafrost protection. *Proceedings of the 9th International Conference on Permafrost*, Fairbanks, Alaska. Institute of Northern Engineering, University of Alaska Fairbanks.
- Vinson, T.S. and McHattie, R.L. (2009). "Documenting Best Management Practices for Cutslopes in Ice-rich Permafrost." FHWA-AK-RD-09-01 Final Report, Alaska Department of Transportation and Public Facilities Research Development, and Technology Transfer Library: http://www.dot.state.ak.us/stwddes/research/assets/pdf/fhwa_ak_rd_09_01.pdf

APPENDIX

Appendix A. PHOTOGRAMMETRIC METHOD FOR EROSION MONITORING

A Nikon D7000 (pixel resolution: 4928×3264) with a fixed focal length lens (AF-S NIKKOR 20 mm f/2.8D), as shown in Figure A.1, was used for erosion measurement.



Figure A.1 Camera and lens

Photogrammetry principles are illustrated in Figure A.2 using the ideal pinhole camera model. When a photograph of an object is taken, a two dimensional (2D) image is obtained and the depth of the object is lost. For the same object (Figure A.2a), 2D images taken from different positions differ due to the varying perspectives. These differences can be used to calculate the orientation of the camera for each image. Using a combination of images and known camera orientations, one can reconstruct the 3D geometry of the object. In Figure A.2a, perspective center (center of an ideal pinhole camera lens) of the left camera (S_1) is set as the origin of an arbitrary coordinate system. For the camera on the right (S_2), the three coordinates of the perspective center (X_s, Y_s, Z_s) and directional angles (κ, ω, ϕ) are unknown. Usually the distance between any two points can be used as a scale, which reduces the unknowns to five. In Figure A.2b, five equations can be generated by identifying five pairs of corresponding points on the two images and the second camera orientation can be solved. Since there are numerous pairs (far more than five) of corresponding points on the two images, the redundancy in information can be used to perform an optimization analysis to accurately determine the camera orientation so that the errors in measurement are minimized. In addition, multiple images can be taken from different orientations, and which, with sufficient overlap, can provide more redundant equations, to improve the accuracy of the camera orientation determination. Once camera orientations are

determined, a straight optical ray can be mathematically projected from the object (point) on the photograph through perspective center of each camera as shown in Figure A.2b (collinearity). The intersection of these rays for cameras at different orientations (triangulation) can then be used to determine the 3D coordinates of the point. As a noncontact 3D measurement technique, photogrammetry has proven to be highly accurate.

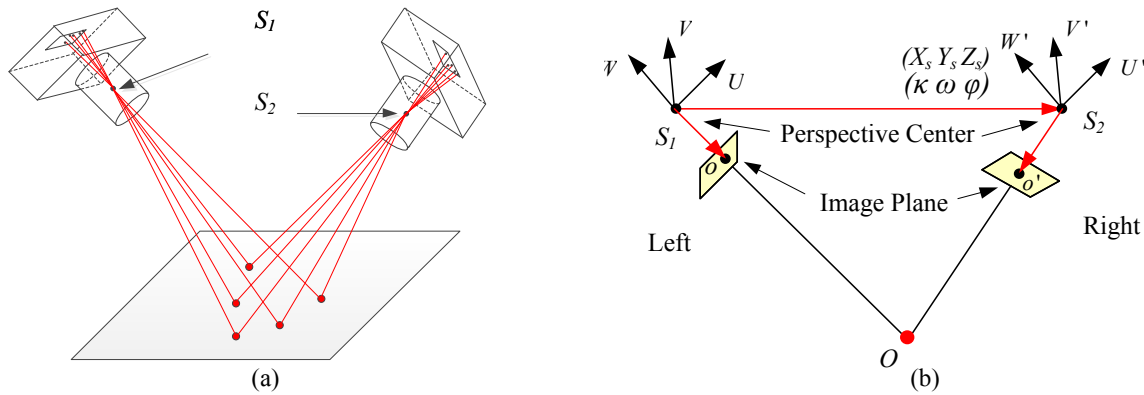


Figure A.2 Principle of Photogrammetry

For high-accuracy photogrammetric measurements, camera calibration is required. For the subject research, camera calibration was performed by capturing a group of images for a point grid from different orientations. After calibration, the image sensor format size (23.9974×15.8961 mm), principal point ($x = 12.0249$ mm, $y = 8.0434$ mm), focal length ($f = 20.9611$ mm) as well as some other distortion parameters were determined as tabulated in Table A.1. As can be seen in Table A.1, the actual focal length of the 20 mm fixed focal length lens is 20.9611 mm when the camera is treated as an ideal pinhole camera model. After slope construction, several images of the slope were captured. For such images, a small aperture size (f-stop number $> F10$) was used to ensure a longer depth of field for better image clarity. Also, image quality could be improved using the highest possible shutter speed permitted by the ambient or artificial light conditions, and further improved using a tripod-mounted camera.

Table A.1 Camera calibration parameters

$f (mm)$	20.9611
$M (pixel)$	4928
$N (pixel)$	3264
$F_x (mm)$	23.9974
$F_y (mm)$	15.8961
$P_x (mm)$	12.0249
$P_y (mm)$	8.0434
$K_1 (10^{-4})$	2.594
$K_2 (10^{-7})$	-4.081
$P_1 (10^{-6})$	-3.411
$P_2 (10^{-6})$	2.612

Figure A.3 is a typical picture of the ice-rich slope captured for erosion measurement. After obtaining photos along the slope, the images were processed to obtain orientations of camera stations by marking and referencing the targets in different images.



Figure A.3 Typical image captured for erosion monitoring

A coordinate system was defined as shown in Figure A.4. The origin was set to be at the lower left corner and the x and y axes were set to be parallel to the road and slope directions. For the precise measurements required in this study, stable reference points along the slope were necessary. These stable points were required as the basis for building a coordinate system from which relative movements of the surrounding slope face could be calculated. The long, grouted soil anchors installed in Section C, as part of the Tecco-mesh system, were considered reasonably stable, and were therefore used as the required reference points. The 3D coordinates for each of the reference points were photogrammetrically determined at a defined scale. For all subsequent photogrammetric measurements of slope face topography, the 3D coordinates of the reference points were set at the initially determined values. As the study progressed, changes in slope face topography could be determined at any time by obtaining a new set of photos and performing the necessary photogrammetric computations based on the initial 3D coordinates of the stable reference points.

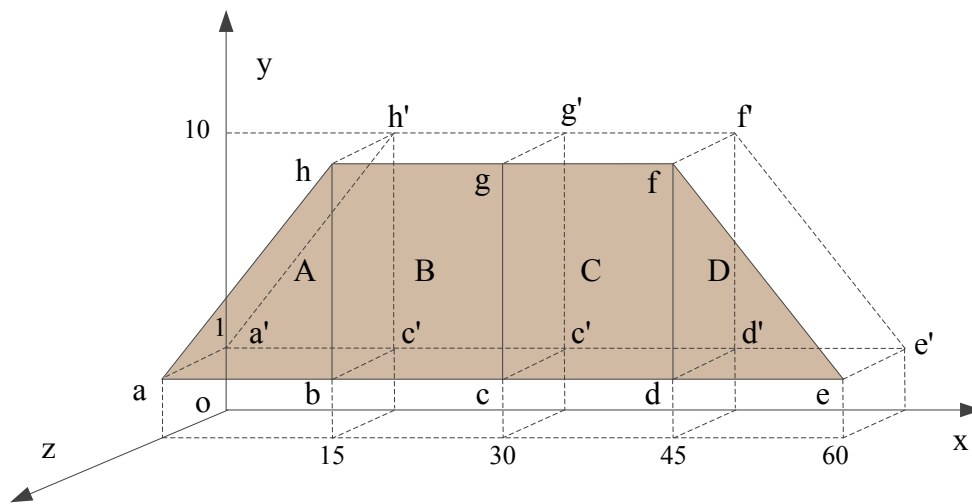


Figure A.4 Coordinate system for erosion measurement

As a result of photogrammetric analysis, point clouds representing the surface topography of the slope at specific times, can be generated as shown in Figure A.5 (the same point cloud view at different angles). Stations representing camera locations for the various images are illustrated in that figure. Typically, around 25 images were required to reconstruct the entire slope. Each point in the point cloud is defined by its x, y, and z coordinate. Taken together, the points represent a topographic surface above an x-y reference plane. Conceptually, given two such surfaces (each representing the topography of the cut slope surface at a different time) the volumetric difference, with respect to the reference plane, between the two surfaces represents the volume changes along the slope surface. And volume changes along the slope surface represent material actually lost through erosion or thaw consolidation. This process is further explained below.

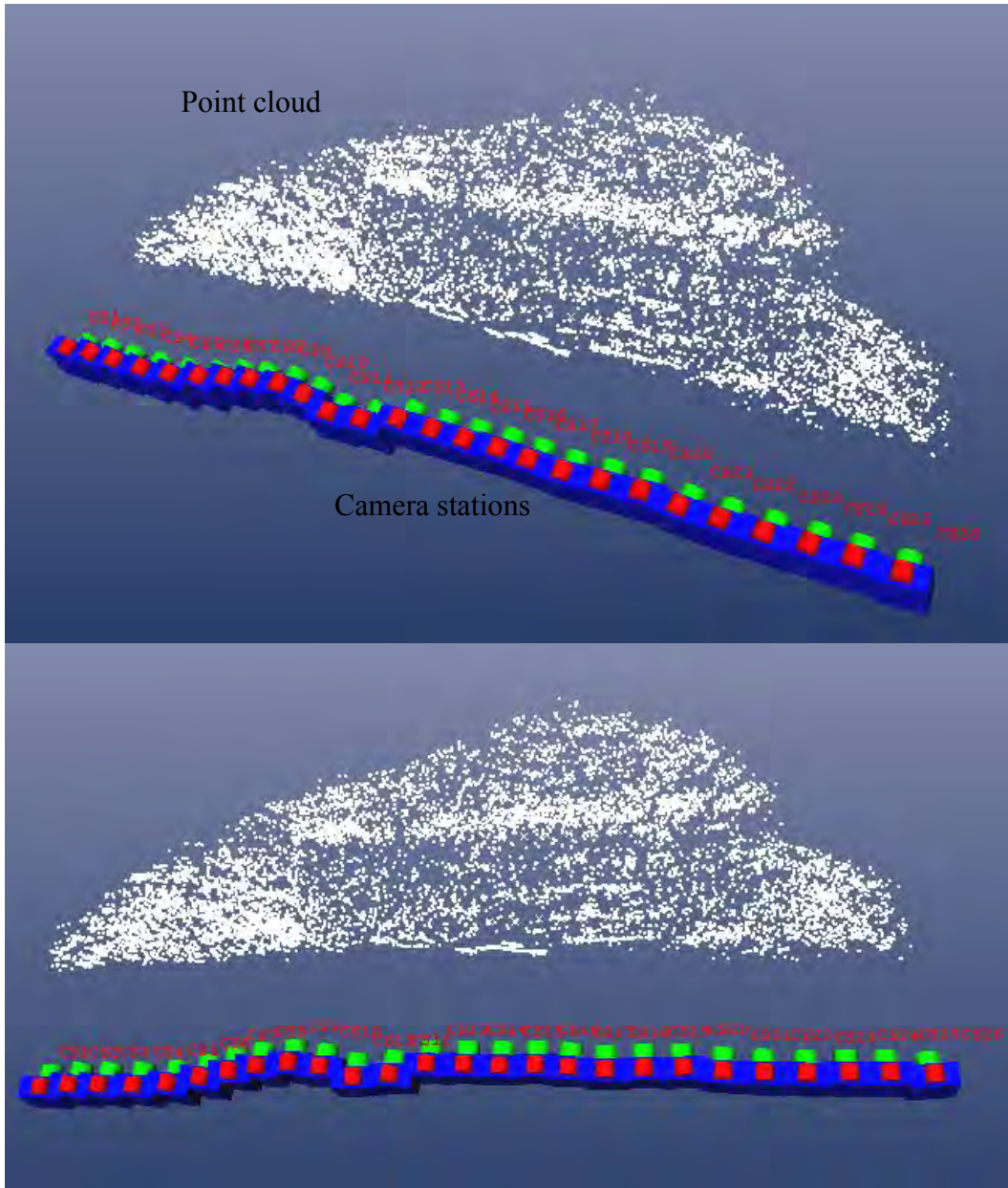


Figure A.5 Camera stations at different view angles

Figure A.6 shows a typical point cloud generated from one set of photos. Using the points lying within each of the four sections indicated in Figure A.4, a triangular mesh was generated for each section using MatLab function “DelaunayTri”. Triangular meshes for sections A, B, C, and D are shown in Figures A.7 to A.10. After mesh generation, the volume between each triangular mesh cell and its projected surface on the x-y reference plane can be calculated. The difference between this volume and the volume calculated for the same mesh cell at a later time represents

the loss or gain of soil material bounded by that mesh cell. The specific method used for calculating each mesh volume is explained in the following paragraph and illustrated in Figure A.11.



Figure A.6 Point cloud for erosion monitoring

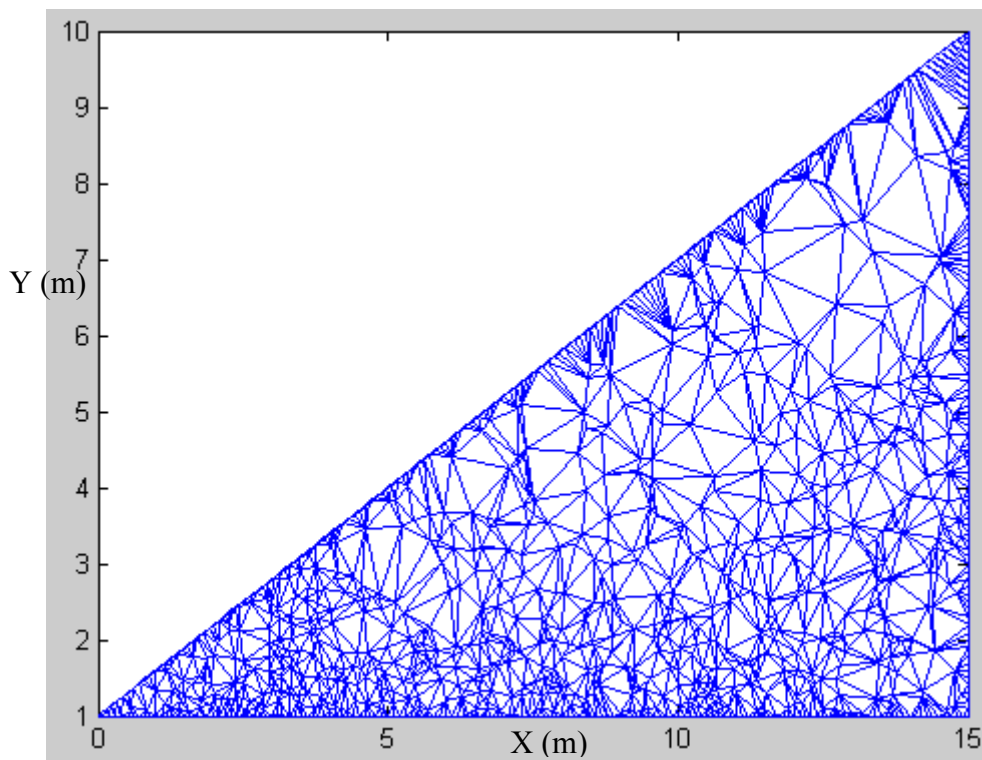


Figure A.7 Mesh generated for Section A for volume calculation

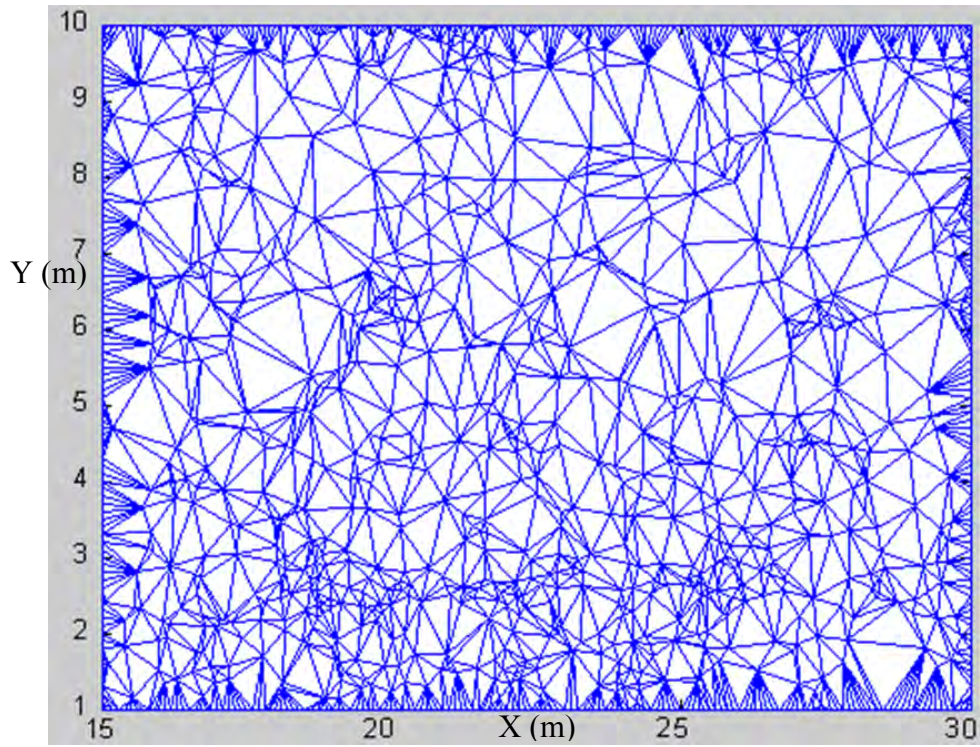


Figure A.8 Mesh generated for Section B

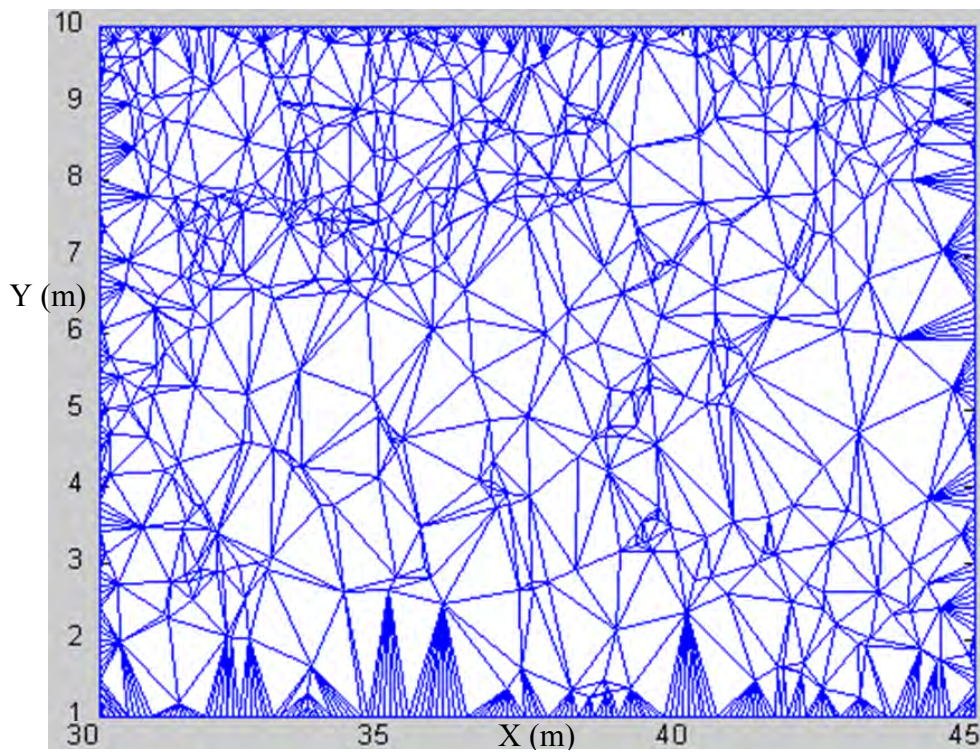


Figure A.9 Mesh generated for Section C

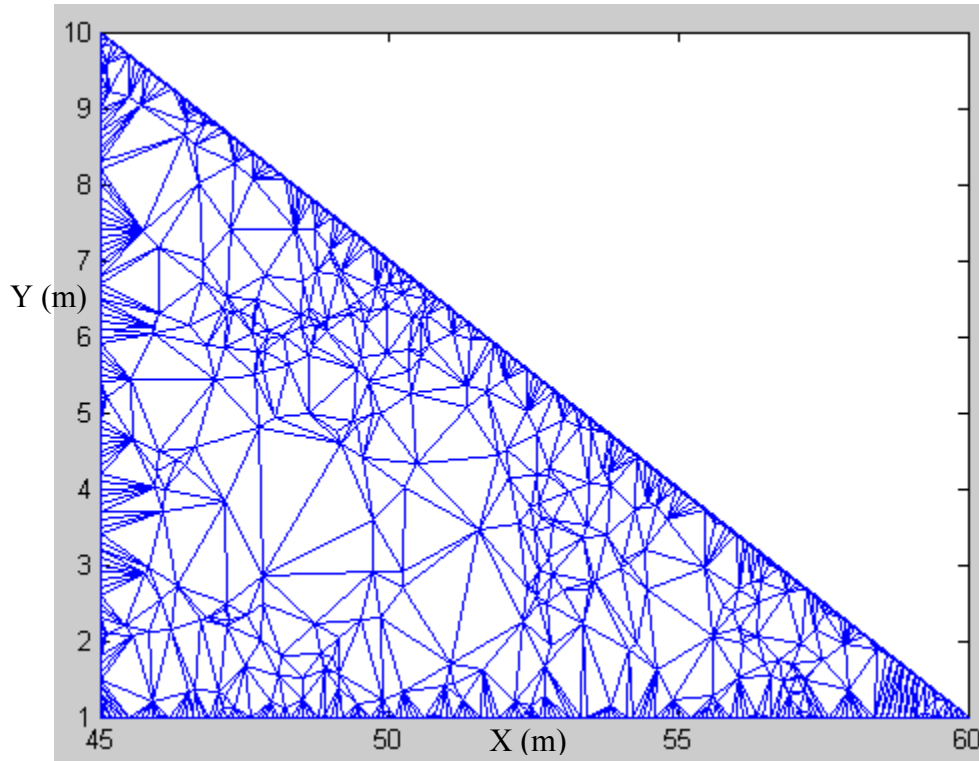


Figure A.10 Mesh generated for Section D

As an example of calculating a mesh cell volume, we begin with the mesh cell triangle ABC shown Figure A.11. A new triangle A'B'C' is formed by projecting points A, B, and C onto a plane parallel to the x-y reference plane and which passes through point C (point C being the closet of the A, B, and C points to the x-y reference plane). A'', B'', and C'' are the projections for A, B, and C onto the x-y reference plane. The volume between the A, B, C triangle area and its projection onto the x-y reference plane is equal to the summation of volumes for triangular prism ABCA''B''C'', tetrahedrons AA'B'C', and BB'AC. The total volume for each test section (using a single set of photos) can be calculated by summarizing volumes for all triangular cells within that test section. A new total volume for all triangular cells in the test section can be determined later based on a new set of photos, and the difference between the two volumes equals the loss or gain of material at the slope face for the time period between photo sets.

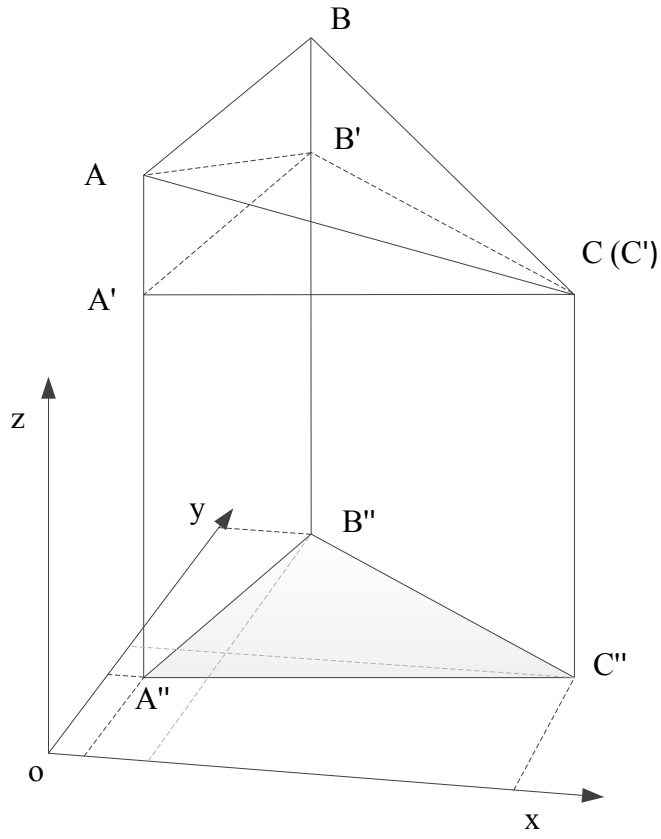


Figure A.11 Volume calculation for a single mesh cell

Appendix B. ALASKA DOT&PF CONSTRUCTION OBSERVATIONS & COMMENTS
(presented in a construction diary/timeline format)

Wednesday, April 17 to Tuesday, April 23

Drill subcontractor works on drilling the holes for the temperature sensors as well as the anchor bolts for test section C.

Friday, April 19

After concerns were voiced from Great Northwest's superintendent, it was decided to cover the back slope with concrete insulating blankets in an effort to keep the hillside frozen until the four treatments of slope protection were in place.

Wednesday, April 24

Anchor bolts were all installed in test section C today.

Thursday, April 25

1. Hand seeding of test sections B and C performed early in morning, while staging for other work on slope.
2. Most of day one was spent installing the treatment for Section C (Erosion Control Matting plus Tecco-mesh). After Great Northwest (referred to as GNI from here on) had the erosion control matting in place, they proceeded to use their CAT 330B L excavator to hoist the rolls of Tecco-mesh to the top of the test section. Crew members secured the top of each roll onto the slope and then proceeded to use the excavator bucket to help control the unrolling of the rest of the roll down the slope. The spike plates were put in place today, but wire rope was not installed.
3. After this section was mostly in place, most of GNI's crew went back to other activities, but three laborers were left behind to clamp Tecco-mesh overlaps together and then began work on pinning down erosion control matting for section B.
4. Borrow B slope protection Material placed on test section D. Approximately 212.45 tons per scale tickets.

Friday, April 26

1. Laborers continue with installation of erosion control matting on test section B. Progress is slow due to difficulty installing circle top wire pins. Two laborers securing rolls at a rate of approximately ½ a roll per hour.
2. First round of 4 side dumps loaded with woodchips arrive at approximately 10:15 am. Excavator starts placing wood chips along top “half” of slope, above test sections, starting at right end, working from section D toward section A. A CAT 966F loader was used to place woodchips on most of test section A. A Morooka MST-2200VD tracked end dump was used to transfer wood chips up to top surface of cut slope where excavator was used to place them on back slope.
3. Two rolls of erosion control (*matting*) remain to be pinned at end of work shift.

Saturday, April 27

Two laborers on site to pin remaining two rolls of erosion control matting, taking about 3 hours.

Tuesday, April 30

Two laborers spend approximately three hours tightening down spike plates and tensioning wire rope on test section C. Installation of slope treatments complete.

Summary of Problems & Thoughts Provided by Alaska DOT&PF Construction Personnel:

1. The drilling equipment being used by the subcontractor for drilling the holes for the anchor bolts was rather old. A newer piece of equipment with driers on the air compressor might have prevented some of the problems we observed.
2. The drilling equipment also used a certain proprietary drill steel, which was not readily available locally (in Alaska). In fact, replacement parts had to be acquired from Germany, which delayed progress by a couple days.
3. It seems to us like the anchor bolts for the Section C of the experiment (Tecco-mesh and Erosion Control Mat) might have acted as heat conductors once we got into the warmer months of summer. Heating up the frozen back slope enough that frozen areas of the slope melted.

4. The 1.5:1 slope that the experiment was installed on was at times difficult for the workers to work on; part of their effort is spent just on staying upright without falling down the slope.
5. The circle-top wire pins were not strong enough to be hammered into the slope by themselves. GNI laborers tried hammering pilot holes with nails, and then ended up settling on using some cordless drills with drill bits to pre-drill the hole for the pins. Using the drills occasionally resulted in matting getting tangle around drill bit. Different hardware for securing the matting to the slope would be worth researching for a future application like this.